SHEAR STRENGTH AND LIQUEFACTION RESISTANCE OF PARTICULATE RUBBER MIXED WITH SAND AND FLY ASH

A THESIS

submitted by

SENTHEN AMUTHAN M

for the award of the degree

of

MASTER OF SCIENCE

(By Research)

GEOTECHNICAL ENGINEERING DIVISION
DEPARTMENT OF CIVIL ENGINEERING
INDIAN INSTITUTE OF TECHNOLOGY MADRAS

JULY 2018

Our greatest weakness lies in giving up. The most certain way to succeed is always to try just one more time.

-Thomas Edision

This thesis is dedicated to my teachers, friends and family.

and

Also it is dedicated to all whom directly or indirectly motivating me in life to pursue towards the goals.

Certificate

This is to certify that the thesis entitled **Shear Strength and Liquefaction Resistance of Particulate Rubber Mixed with Sand and Fly Ash** submitted by **Senthen Amuthan M** to the Indian Institute of Technology, Madras for the award of the degree of Master of Science by Research is a bonafide record of research work carried out by him under our supervision. The contents of this thesis, in full or in parts, have not been submitted to any other Institute or University for the award of any degree or diploma.

Chennai 600 036	Research Guide	Research Co-guide
Date:		
	(Prof. A. Boominathan)	(Dr. Subhadeep Banerjee)

ACKNOWLEDGEMENT

I would like to express my sincere gratitude to **Prof. A. Boominathan and Dr. Subhadeep Banerjee**, my project guides, Indian Institute of Technology Madras, for their valuable guidance, ingenious suggestions and constant encouragement throughout the course of my project work. I sincerely thank them for their patience and constant help whenever needed, besides their heavy workload. The consideration extended by them is deeply acknowledged.

I thank **Prof. K. Ramamurthy**, Head of the Civil Engineering Department, and **Dr.Thyagaraj T.**, Head of Geotechnical Engineering Laboratory, for providing the necessary facilities for carrying out the project work. I wish to thank **Prof. K. Rajagopal, Prof.G. R. Dodagoudar, Prof. R. G. Robinson, Dr. Dali Naidu Arneppalli, and Dr. V. B. Maji** for their valuable suggestions and encouragement.

I extend my heartfelt gratitude to **the fellow scholars and friends** for immense help during the project. I also thank **lab assistants**, senior project technician and all the research scholars who had taken up their valuable time to help me and endowed me with a constructive suggestion for completion of my work.

I am grateful to my parents and my brother for the tremendous understanding, encouragement and adjustment they made for me to make my work here at IITM easier.

Finally, I would like to extend my deepest gratitude to my friends and family members for their unconditional love and moral support, which made my life here at IIT Madras a memorable one.

Above all, I thank God for providing me with good health and knowledge.

SENTHEN AMUTHAN M

ABSTRACT

KEYWORDS: rubber-sand mixture; rubber-fly ash mixture; shear strength; liquefaction; post-liquefaction; modeling.

Increase in the generation of scrap tires necessitates wide engineering applications to ease out the stockpiling. Researchers have examined the mixtures of shredded scrap tire mixed with sand for various engineering applications such as embankments, retaining wall backfill, buried pipe backfill, and base isolation. It is reported that the larger size of shredded scrap tire mixed with sand is prone to segregation. On the other hand, the mixtures of smaller size shredded scrap tire mixed with sand possess lower shear strength. Further, it is also evident that there is no proven study on the suitable method to determine the maximum density of the mixtures.

An alternative material for sand in the rubber-sand mixture is required considering the scarcity of sand and natural resource depletion required. In the present study fly ash is examined as an alternative material for sand. River sand and class F fly ash from Ennore thermal power plant Chennai are chosen for the present study. The shredded scrap tire rubber size less than 2mm, classified as particulate rubber, is mixed with sand and fly ash. The present study examines the pure rubber, sand and fly ash along with the two mixtures termed as rubber-sand mixtures and rubber-fly ash mixtures with 10%, 30% and 50% gravimetric proportion of rubber.

The maximum unit weight of the mixtures was determined using the vibratory table, Proctor compaction, and mini compaction method. The standard surcharge of 13.8kPa in vibratory table test is increased to examine the maximum unit weight changes. Two different tests such as standard and modified tests were carried out in Proctor compaction and mini compaction method. Further, the segregation resistance of the mixtures was examined using vibratory table tests without surcharge.

The shear strength of the rubber-sand mixture and rubber-fly ash mixture is determined using direct shear tests. The samples are prepared at a relative density of 85% and the normal pressures of 50, 100, and 150kPa were adopted for the tests. The tests results are shown that the rubber-fly ash mixtures possess higher shear strength than that of rubber-sand mixtures with the rubber content more than 10%. The increase in the shear strength is attributed to the increase in the inter-particulate contact between the fly ash and rubber. Further, the concrete and sand interface shear strength of the mixtures was examined using interface direct shear tests. The tests were carried out with the relative densities of 30, 60 and 85% and the effective normal pressure of 50, 100, and 150 kPa. It is found that both the interface shear strength rubber-fly ash mixtures are more than that of rubber-sand mixtures. The undrained shear strength of the mixtures was examined using consolidated undrained tests in triaxial apparatus (Make: VJ Tech, UK). The samples were prepared at the relative density of 50 and 75% and the confining pressure of 100kPa is adopted.

The liquefaction and post-liquefaction behaviour of the rubber-sand mixture and rubber-fly ash mixtures were examined using cyclic triaxial apparatus (Make: VJ Tech, UK). The samples were prepared for the relative density of 50 and 75% using Ladd's under compaction method. The confining pressure of 100kPa is used for the present study. The samples were subjected to stress controlled cyclic loading with the cyclic stress ratio (CSR = $\sigma_d/2\sigma_c$) of 0.1 to 0.23. Multi-stage cyclic triaxial tests were carried out to examine the liquefaction and post-liquefaction behaviour of the mixtures. The post-liquefaction behaviour is examined immediately after stress controlled cyclic loading by applying the undrained strain controlled static loading. It is observed that the excess pore water pressure of the mixtures is reduced with an increase in the rubber content. Further, the mixture does not show the initial liquefaction and the liquefaction failure occurs only by reaching the certain axial strain criterion. The rubber-sand mixtures with the rubber content between 10% and 50% do not liquefy with the CSR less than 0.2. The liquefaction strength of the rubber-sand mixtures with rubber content 10% to 50% is observed to be equal to sand. The post-liquefaction behaviour of the mixtures is identified as the elastic hardening. The elastic and hardening modulus is observed to decrease with increase in the rubber content. Further, the post-liquefaction strength of the rubber-fly ash mixture is observed to be more than that of rubber-sand mixtures with the rubber content more than 30% in the mixture.

The liquefaction behaviour of the mixture is modeled using the hyperbolic relation and the Masing's rule. The pore pressure development is indirectly modeled using degradation index. The model is validated using the experimental data reported in a literature. It is found that the model is capable of predicting the liquefaction behaviour of the mixtures with the rubber content between 10% and 50%.

TABLE OF CONTENTS

LIST OF TABLES

LIST OF FIGURES

ABBREVIATIONS AND NOTATIONS

ASTM	American Society for Testing and Materials
CSR	Cyclic Stress Ratio
CRR	Cyclic Resistance Ratio
CU	Consolidated Undrained
EDXA	Energy Dispersive X-ray Analysis
FOS	Factor of Safety
RD	Relative Density
SEM	Scanning Electron Micrograph
a_{max}	peak ground acceleration
c_r	correction factor for cyclic stress in cyclic triaxial testing
E_1	secant modulus of 1st cycle
g	acceleration due to gravity
M	Critical state parameter (function of friction angle)
N_L	number of cycles required to cause liquefaction failure
P’	Mean effective stress
q or q_r	deviator stress
q_{r1} and q_{r2}	deviator stress at the point of stress reversal
q_f	deviatoric stress at failure

R	modulus ratio
r	calibration parameter of the model
r_d	depth correction factor
r_u	excess pore water pressure ratio
u_n	excess pore water pressure ratio at nth cycle
e_{max}	maximum void ratio
e_s	sample void ratio
e_{cm}	void ratio obtained with compaction method
ε_{vol}	Volumetric strain
$\varepsilon_{vol, ul}$	Ultimate Volumetric strain
ε_r	axial strain
ε_{r1} and ε_{r2}	axial strain at the point of stress reversal
σ'	effective normal pressure
σ'_c	effective confining pressure
σ_n	effective normal pressure
σ_d	deviator stress
Δu	change in pore water pressure
$\Delta\sigma$	change in cell pressure
δ	degradation parameter
r_u	pore water pressure ratio

γ	density of the soil
τ	shear strength
$\tau_{M,\ ul}$	ultimate shear strength of PRSM, PRSFM, and PRFM
$\tau_{PRSM(50),\ ul}$	ultimate shear strength of PRSM50
τ_{cyc}	uniform cyclic shear stress amplitude
ϕ'_{p}	peak effective friction angle
ϕ'_{ul}	ultimate effective friction angle
$^\circ$	degree

CHAPTER 1

INTRODUCTION

1.1 GENERAL

Generation of scrap rubber tire is being increased worldwide which leads to stockpiling. The stockpiling of scrap tires is prone to fire hazard and it serves as the breeding place for rodent and mosquitoes which are often dangerous to human health. To reduce the stockpiling of the scrap tire, in the recent years, it is being utilized as various engineering resources, such as fuel in cement kilns, synthetic running track, and sound barrier. However, these applications are not adequate to utilize the large number of scrap tires. In the early 1990's researchers have examined the whole scrap tires and shredded scrap tires for the field applications such as embankments and retaining wall backfill to ensure the bulk usage of scrap tire in engineering applications and to ease out the stockpiling (e.g., Bosscher et al. 1992; Edil and Bosscher 1994; Garga and Shaughnessy 2000). It is found that the mixture of rubber and sand possess desirable properties such as high hydraulic conductivity, ductility, and light weight for the geotechnical engineering applications.

1.2 RUBBER-SAND MIXTURES

The field application of the scrap tire has been examined with whole tires and the shredded tire mixed with soil. Figure 1.1 shows the field applications of the whole tire and the rubber-soil mixtures. The pure rubber recycled from the scrap tire possesses ductility and lightweight. However, the stiffness and shear strength of the pure rubber is not adequate for engineering applications because of its significant settlement and larger rebound after the removal of the surcharge. Therefore sand has been identified as an additive material to rubber for improving the property such as stiffness, shear strength, and compressibility (Edil and Bosscher 1994; Masad et al. 1996). In the recent years, shredded scrap tire of different sizes mixed with sand has been examined to evaluate its properties such as shear strength, compressibility, stiffness, permeability, dynamic properties such as shear modulus and damping ratios and liquefaction potential (Anastasiadis 2011; Mashiri 2014). These properties were examined to assess the suitability of the mixtures for the applications such as embankments, retaining wall backfill, buried pipeline backfill, and base isolation (Bosscher et al. 1992; Hope 1998; Yoon et al. 2006; Indraratna et al. 2017; Meguid et al. 2018).

Figure 1.1: Field application of the scrap tire (a) rubber-sand mixtures (Yoon et al. 2006) (b) use of whole tire in embankment (Garga and Shaughnessy 2000)

In general, the larger size rubber (size > 20mm) mixed with sand increases the shear strength. However, the mixture of sand and larger size rubber is prone to segregation because of the incompatibility in the particle size. Conversely, the mixture of smaller size rubber and sand possess lower shear strength and it has segregation resistance. In addition, the mixtures associated with structures would have two interface behaviours such as mixture-concrete interface and mixture-soil interface.

1.3 LIQUEFACTION

Liquefaction is a phenomenon majorly occurs in saturated cohesionless soil subjected to random excitation. The increase in pore water pressure causes the reduction in the shear strength of the cohesionless soil. The complete loses of shear strength is known as liquefaction failure. The progressive liquefaction failure of the cohesionless soil is schematically shown in Figure 1.2. Eventually, the liquefaction will lead to the failure of structures which are associated to the cohesionless material. Therefore, it is important to analyze the liquefaction resistance of saturated cohesionless materials which would be used in earthquake-prone areas.

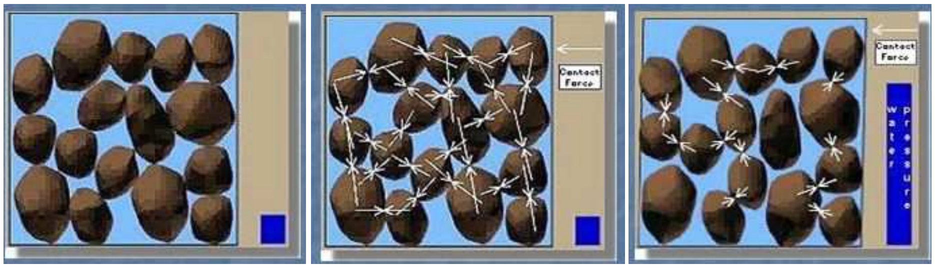

Figure 1.2: Schematic representation of the reduction in the contact force between particles due to liquefaction (Source: https://slideplayer.com/slide/4378090/)

1.3.1 Liquefaction Hazards and Mitigation

Liquefaction is a catastrophic phenomenon majorly occurs in cohesionless sandy soil subjected to random excitation. Figure 1.3 shows the failure of structures such as buildings, dams, and bridges due to the liquefaction in the past earthquakes.

The consequences of the liquefaction can be reduced by employing many techniques. The some of the available techniques to reduce the liquefaction resistance are: improving the soil by means of densification or stone column, building the liquefaction resistance structures, replacing the liquefaction susceptible soil, adding additives such as cement and fibers, and reinforcing the soil with help of geosynthetics.

1.3.2 Liquefaction Susceptibility of Rubber Mixed with Sand

The addition of shredded rubber to sand does not change its cohesionless characteristics since the rubber is a non-cohesive material. In addition, the stiffness of the sand reduces with the addition of the rubber. The reduction in the stiffness would cause the strain accumulation during the cyclic loading. In general, liquefaction failure is identified based on the two criteria: one is the excess pore water pressure reaching the effective confining pressure and the other is reaching of certain percentage of double amplitude axial strain, whichever occurs earlier. Since the rubber mixed with sand is cohesionless and possess stiffness less than sand, the liquefaction susceptibility of rubber-sand mixtures need to be evaluated considering both the pore pressure criterion and axial strain criterion.

Figure 1.3: Liquefaction failure of structures (a) apartments (Niigata, 1964) (b) bridge (Niigata, 1964) (c) bridge (Kobe, 1995) (d) dam (San Fernando 1971) [Sources: https://geomaps.wr.usgs.gov/sfgeo/liquefaction/image_pages/niigata_apts_bw.html, https://www.usgs.gov/science-explorer-results?es=liquefaction, and https://depts.washington.edu/liquefy/html/what/what1.html]

1.4 MOTIVATION

As mentioned earlier, the worn out vehicles tires are being stockpiled in huge quantities which are undesirable for a healthy environment. The available engineering solution to ease out the stockpiling of scrap tires is not enough for the bulk usage. The shredded scrap tire mixed with sand has been examined for many applications in the geotechnical engineering field. Utilization of scrap tires in geotechnical engineering field ensures the bulk and sustainable usage of the scrap tires. Many studies have been carried out on the mixture of different size shredded scrap tire and sand in the field and laboratory. In general it is found that the mixture of larger size rubber and sand is prone to segregation and the mixture of smaller size rubber and sand shows lower shear strength. Further, an alternative material needs to be studied for the potential use of rubber considering the scarcity of sand and natural resource depletion. In addition, the alternative material for sand should possess the tendency to increase the shear strength of mixtures with the smaller size rubber.

Fly ash is a by-product from the thermal power plant which is being utilized in many applications including embankments and retaining wall backfills. It possesses specific surface area higher than that of sand which is desirable to increase the shear strength of the smaller size rubber. The interaction between rubber and fly ash would be more than that of sand and fly ash. Also, usage of fly ash with shredded scrap rubber is a sustainable solution to reduce the bulk amount of stockpiling of both scrap tire and fly ash.

The mixtures of shredded scrap tire and sand or fly ash are cohesionless in nature which is prone to liquefaction. The liquefaction resistance not only depends on the development of pore pressure but also depends on the axial strain. In general, the stiffness of the mixtures decreases with increase in the rubber content since the stiffness of rubber is lower than that of sand. Therefore, the liquefaction potential of these mixtures needs to be evaluated considering pore pressure criterion and axial strain criterion for the safer design of the structures associated with these mixtures.

1.5 OBJECTIVES AND SCOPE OF THE PRESENT STUDY

The main objective of the present study is to find an alternative material for sand to mix with small size rubber (particulate rubber). The alternative material should improve the shear strength of the rubber and also possess adequate liquefaction resistance.

The specific objectives of the present study are given below:

- ✓ To assess the suitable methods to estimate the maximum density of particulate rubber-sand mixtures and particulate rubber-fly ash mixtures.
- ✓ To determine the shear strength and interface shear strength of the particulate rubber-sand mixtures and particulate rubber-fly ash mixtures.
- ✓ To determine the liquefaction resistance and post-liquefaction behaviour of particulate rubber-sand mixtures and particulate rubber-fly ash mixtures.
- ✓ To develop a semi-empirical constitutive model for the liquefaction behaviour of the mixtures.

The scopes for the objectives are as follows:

- ✓ Carrying out the vibratory table method and compaction methods to assess its suitability for the the mixtures.
- ✓ Carrying out consolidated undrained (CU) triaxial and direct shear tests to evaluate the shear strength of particulate rubber-sand mixtures and particulate rubber-fly ash mixtures.
- ✓ Carrying out CU cyclic triaxial tests to determine the liquefaction resistance and post-liquefaction behaviour of particulate rubber-sand mixtures and particulate rubber-fly ash mixtures.

- ✓ Formulation of a semi-empirical constitutive model for the liquefaction behaviour of the mixtures and validating the model using an experimental study in literature.

1.6 ORGANIZATION OF THE THESIS

Chapter 1 gives the brief about the waste tire and the problems associated with it. Further, the need for utilization of scrap tire in the geotechnical engineering field is discussed. It is followed by the motivation, objectives, and scope of the present study.

Chapter 2 presents the various literature related to density, shear strength, interface shear strength, liquefaction resistance and modeling the mixture behaviour. Based on the comprehensive literature review, the research gaps for the present study are identified.

Chapter 3 discusses characterization of the mixtures. In this the materials used in the present study and its index properties are presented. Further, it presents the maximum density of the mixtures determined using three different technique such as vibratory table method, Proctor compaction method and mini compaction method. In this chapter the suitable method to determine the density of the mixtures are also presented. Segregation is possible to occur when two different materials mixed together. Further, it is also evident from the literature that the large size rubber mixed with sand is prone to segregation. Therefore, the segregation resistance of the mixtures is examined in this chapter using the vibratory table without placing the surcharge.

Chapter 4 deals with the static and engineering properties of the mixtures. The shear strength of the particulate rubber-sand mixtures and particulate rubber-fly ash mixtures are examined using direct shear tests. The test results are substantiated with the micro structural study using scanning electron microscope. The undrained behaviour of the mixtures using the triaxial tests is reported. Further, the influence of the partial replacement of sand with fly ash on the shear strength is also presented in this chapter. The interface behaviour of the mixtures determined using interface direct shear tests are also presented.

Chapter 5 discusses the liquefaction and post liquefaction behaviour of the mixtures. The multi-stage cyclic triaxial tests results for the particulate rubber-sand mixtures and particulate rubber fly ash mixtures are discussed. The pore pressure response, axial strain response and the stress path of the different mixtures are presented. The liquefaction strength curve of the particulate rubber-sand mixture and particulate rubber-fly ash mixture considering pore pressure criterion and axial strain criterion is presented. The post-liquefaction behaviour of the mixtures is also presented in this chapter. Further, the post-liquefaction modulus of the mixtures is compared with the static modulus. In addition, a semi-empirical model based on the hyperbolic relation and Masing's rule is proposed for the mixtures.

Chapter 6 summarizes the experimental tests conducted in the present study. Further, the summary of the findings and the major conclusions drawn from the present study are also discussed. In addition, the limitations, major contributions and the future scope of the present study are presented at the end of this chapter.

CHAPTER 2

LITERATURE REVIEW

2.1 INTRODUCTION

Since the early 1990's the shredded scrap tire mixed with sand has been used in geotechnical engineering applications. The previous studies were carried out to mainly examine the shear strength, compressibility, permeability, dynamic soil properties such as shear modulus and damping ratios. However, limited studies have been reported on the determination of the density of the mixtures while the most of the previous studies have mainly concentrated on the engineering properties. Furthermore, the liquefaction resistance of the mixtures, which is crucial phenomenon majorly occurs in saturated cohesionless materials, are limited in the literature. In the present chapter, the literature mainly focuses on the density, shear strength, liquefaction resistance and modeling the mixture behaviour are discussed.

122 STUDIES ON THE CHARACTERIZATION OF RUBBER-SAND MIXTURES

2.2.1 Density

The maximum density of the mixtures is determined widely using vibratory table method. It is found that the density of the different size of rubber mixed with sand is decreased with increase in the rubber content (Bali Reddy et al. 2015; Mashiri 2014). Ahmed and Lovell (1993) is reported that the vibratory table method [ASTM D4253 (ASTM 2016a)] is suitable to determine the density of the rubber-sand mixtures while Proctor compaction method [ASTM D698 (ASTM 2012a) and ASTM D1557 (ASTM 2012b)] is suitable for the rubber mixed with cohesive soil. Conversely, Edil and Bosscher (1994) reported that the vibratory table method is not suitable for rubber-sand mixtures because of the vibration absorbent nature of the rubber. In spite of that claim by Edil and Bosscher (1994), many researchers have been used the vibratory table method to determine the maximum density of the mixtures. Others have used different approaches to represent the density of the mixtures since there is a lack of studies on a suitable method to determine the density of the mixtures. The different methods used in the literature to represent the density and their difficulties are given in Table 2.1.

The influence of water content on the density of the rubber-sand mixture is reported as difficult to determine. It is observed that the oozing of liquid from the mixtures when it was kept in the oven temperature greater than 40°C (Hyodo et al. 2007; Kawata et al. 2007; Hong et al. 2015).

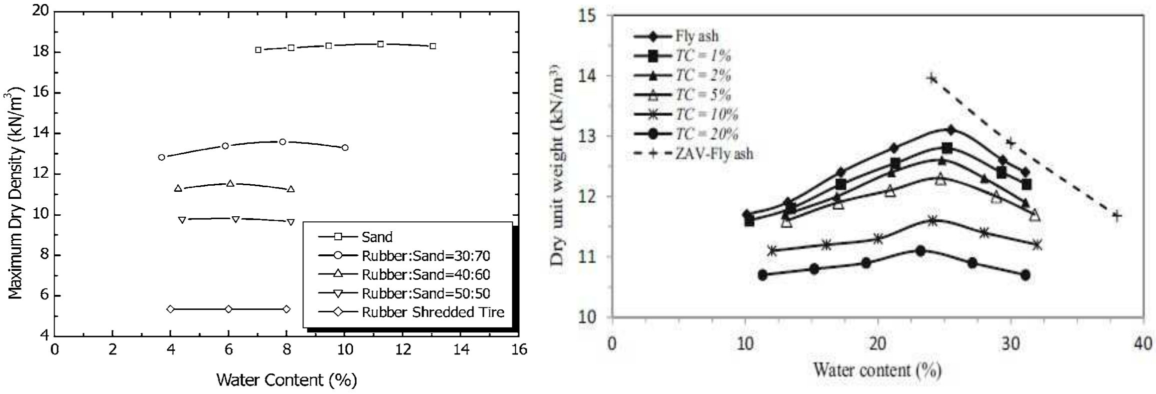

Figure 2.1: Influence of water content on the density of (a) rubber-sand mixtures (Youwai et al. 2004) (b) rubber-fly ash mixtures (Priyadarshee et al. 2015)

In addition, it is evident from Figure 2.1a that the density of the rubber-sand mixtures does not show any peak with increase in water content rather it is a flat curve (Youwai et al. 2004; Uchimura et al. 2007). It shows that the density of the mixtures is independent of the water content. Further, it is evident from Figure 2.1b that the density of the rubber-fly ash mixture is also independent of water content when the rubber content is more than 5% by weight (Priyadarshee et al. 2015)

Table 2.1: Different methods in the literature to represent the unit weight of the mixtures

Methods in the literature	Description of the method	Difficulties in adopting the method	References
Sand matrix unit weight	It is the unit weight of the sand present in the matrix.	It is not the intrinsic unit weight of the mixtures. In addition, it is difficult to measure and maintain the sand matrix unit weight in site execution.	Foose et al. 1996; Zornberg et al. 2004; Ghazavi and Sakhi 2005.
Relative densities based on the index density methods	Material density is described as a percentage based on minimum and maximum density.	The maximum density is determined using vibratory table method as per ASTM D4253 (ASTM 2016a). Because the rubber particle present in the mixture offers energy absorption, the measured maximum dry unit weight is not a true maximum dry unit weight.	Sheikh et al. 2013; Mashiri et al. 2015; Noorzad and Ravesshi 2017.
Wet and dry tamping	Applying equal energy to the sample of different rubber content mixtures by hand compaction.	Applying same energy to the different mixtures results in the different degree of compaction or it gives the degree of compaction in the wide range instead of the exact value. In addition, measuring the energy imparted to the sample by the hand compaction is difficult. Even if the energy is calculated, it is not the real energy imparted to the sample.	Feng and Sutter 2000; Youwai and Bergado 2003; Ghazavi 2004; Hyodo et al. 2007; Anastasiadis et al. 2011; Senetakis et al. 2012; Kaneko et al. 2013; Hong et al. 2015; Fuchiyama et al. 2015; Li et al. 2016; Bali Reddy et al. 2016.

2.2.2 Segregation

The shredded scrap tires are classified based on the size as per ASTM D6270 (ASTM 2012). The terminology used for the classifications are tire shreds (50 mm to 305 mm), tire chips (12 mm to 50 mm), granulated rubber or particulate rubber (0.425 mm to 12 mm), ground rubber or particulate rubber (0.425 mm to 2 mm) and powdered rubber (< 0.425mm). The different size of the rubber derived from scrap tire is shown in Figure 2.2. Though all these varieties have certain benefits, past studies revealed that there is a chance of segregation of the mixtures when the large portion (> 30% by weight) of tire chips or tire shreds were added to the sand (Edil and Bosscher 1992; Edil and Bosscher 1994; Kim and Santamarina 2008; Umashankar 2009; Anastasiadis 2011; Mashiri 2014; Umashankar et al. 2014). The segregation of tire chips-sand mixtures reported in the literature during the cyclic triaxial test is shown in Figure 2.3. The segregation of mixtures would result in the formation of the sand layer at the bottom and rubber layer at the top of the sample. The formation of the sand layer at the bottom is because of the higher specific gravity of sand than that of rubber chips.

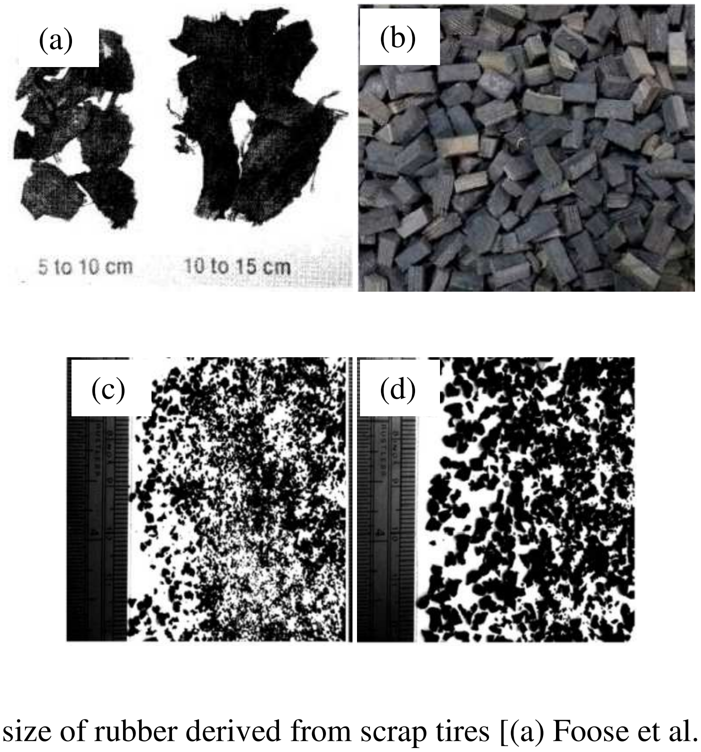

Figure 2.2: Different size of rubber derived from scrap tires [(a) Foose et al. 2016 (b) Bali Reddy et al. 2016 (c and d) Neaz Sheikh et al. 2013]

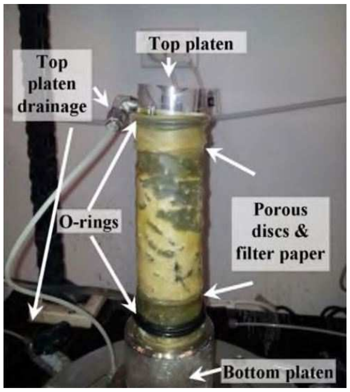

Figure 2.3: Segregation of tire chips-sand mixtures when rubber content is more than 30% (Mashiri 2014)

The rubber-sand mixtures no longer behave as a mixture matrix due to the segregation. The segregation results in the decrease in the shear strength and increases in the settlement of the mixtures. The liquefaction resistance of layered material with sand and rubber is studied with different configuration by Kaneko et al. (2013). It is observed from the study that the lower liquefaction resistance is shown for the configuration of rubber overlying the sand. The segregation also would result in rubber overlying sand configuration which eventually leads to reduction in the liquefaction resistance of mixture matrix. In general, segregation of the mixtures results to the higher settlement, reduction in shear strength and liquefaction resistance.

2.3 SHEAR STRENGTH AND VOLUMETRIC CHARACTERISTICS OF THE MIXTURES

The shear strength of the mixtures is widely examined using direct shear tests and triaxial tests. The shear strength of the rubber-sand mixtures is reported to show a clear peak followed by a reduction (e.g., Youwai and Bergado 2003; Zornberg et al. 2004; Mashiri et al. 2015). Conversely, it is also reported that the shear strength increases with increase in the axial strain without showing any peak (e.g., Neaz Sheikh et al. 2013). Further, the axial strain at which the peak shear strength occurs is increased with increase in the rubber content (Mashiri et al. 2015). In general, the shear strength of the mixtures increases with increase in the axial strain without showing any peak when the rubber content is more than 20% by weight in the mixture (e.g., Youwai and Bergado 2003; Zornberg et al. 2004). It is also apparent that, irrespective of rubber size, the mixture behaves like ductile material when the rubber content is more than 20% by weight.

The friction angle reported for the different size of rubber mixed with sand is given in Figure 2.4. The friction angle of larger size rubber mixed with sand is increased with increase in the rubber content of up to 50% by weight in the mixtures. Most of the previous studies have examined the mixtures of sand and larger size rubber (tire shreds (TS) and tire chips (TCh)) with the maximum rubber content of 50% by weight. The friction angle would decreases when the larger size rubber is more than 50% by weight in the mixture. Conversely, the friction angle of the mixtures with smaller size rubber (particulate rubber (PR) and tire crumb (TC)) is reduced with the increase in the rubber content. The lower bound in the figure is corresponding to the lower relative density while the upper bound is for higher relative density of the mixtures. In addition, the friction angle is observed to increase with an increase in the relative density of the mixtures with different size of rubber.

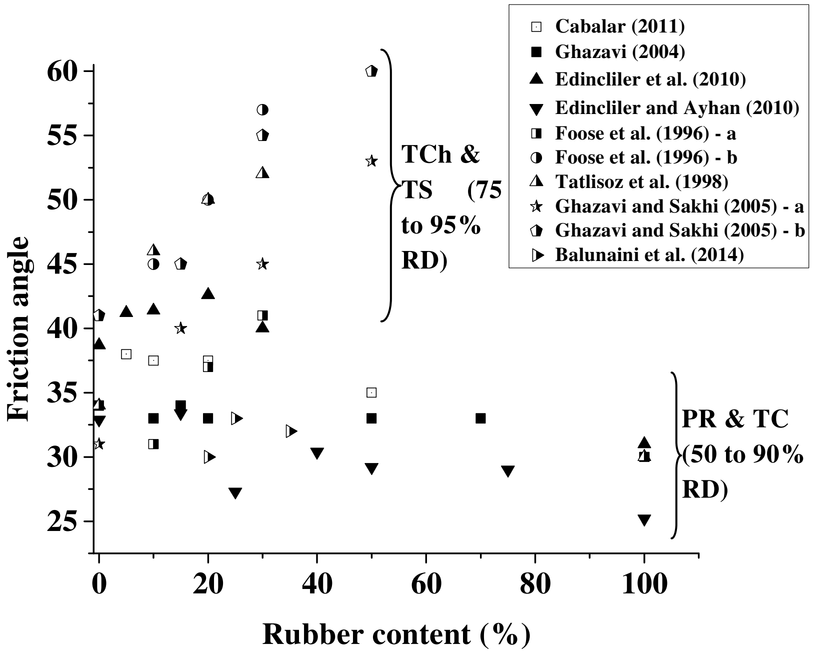

Figure 2.4: Friction angle of rubber-sand mixtures

The volumetric behaviour of the rubber-sand mixtures is initially reported to be contractive followed by dilative for the mixtures having larger size rubber. The axial strain corresponding to the change from contractive to dilative is increased with increase in the rubber content (Mashiri et al. 2015). However, the smaller size rubber mixed with sand shows dilative as like as larger size rubber-sand mixtures when the rubber content is less than 30% by weight (Youwai and Bergado 2003; Mashiri et al. 2015). The dilative behaviour of the smaller size rubber-sand mixtures is changed to fully compressive when the rubber content is more than 30% by weight.

2.3.1 Effect of Rubber Content

Two different behaviours are observed in the literature because of the increase in the rubber content of the mixtures. The first one is that the shear strength of the mixtures is increased with increase in the rubber content and the other is that the shear strength decreases with increase in the rubber content. The larger size rubber mixed with sand shows increasing shear strength (Zornberg et al. 2004; Mashiri et al. 2015) while the smaller size rubber shows decreasing shear strength (Youwai and Bergado 2003; Neaz Sheikh et al. 2013). Further, the increase in the rubber content decreases the dilation of larger size rubber mixed with sand while the smaller size rubber mixed with sand increases the compressibility with an increase in the rubber content (Masad et al. 1996; Youwai and Bergado 2003; Mashiri et al. 2015).

The initial tangent modulus and the secant modulus of the rubber-sand mixtures is observed to be decreased with increase in the rubber content even though the shear strength of the larger size rubber-sand mixtures increases with increase in the rubber content (Rao and dutta2006; Mashiri et al. 2015). The modulus of the material mainly depends on the stiffness. The addition of rubber, irrespective of size, reduces the stiffness of the matrix which leads to the reason for the reduction in the modulus of the matrix.

2.3.2 Effect of Initial Relative Density

The shear strength of the mixtures reported is being increased with increase in the initial relative density of the mixtures (Zornberg et al. 2004; Ghazavi and Sakhi 2005). The increase in the shear strength is less significant with an increase in the initial relative density when the rubber content increases in the mixture (Ghazavi and Sakhi 2005). The dilation of the larger size rubber-sand mixtures is reported to be increased with the increase in the initial relative density of the mixtures (Mashiri et al. 2015).

2.3.3 Effect of Confining Pressure

The shear strength of the rubber-sand mixtures is increased with increase in the confining pressure (Mashiri et al. 2015). It is due to the increase in the stiffness of the sample which attributed to the increase in the shear strength. The increase in shear strength with increase in confining pressure is less significant when the rubber content increases in the mixture. It is observed that for pure rubber, the increase in the shear strength with increase in confining pressure is less than that of the other mixtures (Masad et al. 1996). In addition, the dilative behaviour of the mixtures is observed to be decreased with increase in the confining pressure. Further, the strain at which the transition occurs from contractive to dilative is also increased with increase in the confining pressure (Masad et al. 1996; Mashiri et al. 2015).

2.3.4 Effect of Addition of Other Materials

In addition to the sand; steel furnace slag, coal wash, and recycled glass have also been examined with small size shredded rubber for the applications such as subballast and lightweight embankment (Disfani et al. 2017; Indraratna et al. 2017). These mixtures show the reduction in the shear strength and increase in the compressibility with an increase in the rubber content of the mixtures. However, the shear strength is observed to be more than that of the rubber-sand mixtures. It is also reported by Indraratna et al. (2017) that the mixture of steel slag, coal washes, and rubber possess the optimum mix ratio of 6.3:2.7:1 for the application of subballast.

2.3.5 Interface Shear Strength

In general, there exist two different interface behaviours when the rubber mixtures are used in the embankment, retaining wall and as buried pipes backfill: the first one between the structure and the mixture and the other is between the mixture and the prepared ground. However, the studies on the interface behaviour of the recycled rubber mixtures are limited in the literature.

The available limited studies were only concentrated the interface behaviour between pure tire shreds or tire chips (larger particles of size varies from 50 mm to 300 mm) and concrete or sand using direct shear tests. It is noted from the previous studies that the interface shear strength of pure rubber with the sand interface is observed to be more than that of the concrete interface (Bernal et al. 1997; Gebhardt 1997; Reddy et al. 2010; Xiao et al. 2015; Ghaaowd et al. 2017).

2.4 LIQUEFACTION

Liquefaction is a phenomenon majorly occurs in the cohesionless saturated material subjected to dynamic loading. The contact force between the particles reduces with the increase in the pore water pressure during the dynamic loading. Eventually all the contact force between the particles would be lost when the pore pressure reaches the effective overburden pressure and at that point, the cohesionless material would lose its full shear strength. This phenomenon is called as the onset of liquefaction. The liquefaction resistance of a material has been evaluated using cyclic stress approach (Seed and Lee 1966), effective stress approach (Fin 1981), cyclic strain approach (Dobry et al. 1982), energy-based approach (Davis and Berrill 1982), and critical state approach (Been and Jefferies 1985). However, the liquefaction behaviour of soil is widely studied using the cyclic stress approach since the cyclic strain approach is only capable of predicting the initial liquefaction.

2.4.1 Cyclic Stress Approach

Cyclic stress approach is introduced by Seed and Lee (1966). Based on this approach, the liquefaction potential of a soil is characterized by the shear stress induced during the earthquake loading and the shear strength of the soil under the dynamic loading.

The shear stress induced during the earthquake loading at the various depth of soil is given in equation 1 (Seed and Idriss 1971).

$$\tau_{avg} = 0.65 \frac{a_{max}}{g} \gamma h r_d \tag{2.1}$$

Where, τ_{cyc} is uniform cyclic shear stress amplitude, a_{max} is the peak ground acceleration, g is acceleration due to gravity, γ is the density of the soil, h is the depth of soil at which the cyclic shear stress would be calculated and r_d is the depth correction factor.

The cyclic shear stress induced during the earthquake loading can be normalized with the effective overburden stress and it is termed as cyclic stress ratio (CSR = τ_{avg}/σ'_v)

The cyclic shear strength of the material can be calculated in laboratory testing using either cyclic triaxial apparatus or cyclic simple shear apparatus or cyclic tensional shear apparatus. The loading would be applied in terms of cyclic deviatory stress in the case of cyclic triaxial testing while it is the cyclic shear stress in the case of cyclic simple shear testing. The cyclic shear stress applied to the sample in the case of cyclic triaxial testing is the half of the deviatory stress ($\sigma_d/2$). The loading nature in cyclic triaxial and cyclic simple shear stress is different, therefore, a correction factor is proposed for the cyclic shear stress applied in cyclic triaxial. Further, Seed et al. (1975) reported that the cyclic shear stress would be required to reach the initial liquefaction in the field is 10% less than that of required in the laboratory. The corrected cyclic shear stress for the cyclic triaxial test is given in equation 2.

$$(\tau_{cyc})_{field} = 0.9c_r(\tau_{cyc})_{tx} \tag{2.2}$$

where, c_r is the correction factor for cyclic stress in cyclic triaxial testing

It is customary to plot the cyclic strength of the material in terms of cyclic shear strength with respect to the number of cycles required to cause liquefaction failure (N_L). The number of cycles required to cause liquefaction failure depends on pore pressure criterion and axial strain criterion. The pore pressure criterion is the number of cycles required to reach the excess pore water pressure to the effective confining pressure (i.e., the point of initial liquefaction). The axial strain criterion is the number of cycles required for the axial strain to reach certain double amplitude axial strain. In general loose sandy soils shows initial liquefaction while dense sandy soil shows liquefaction failure by reaching 5% of double amplitude axial strain (Kramer1996). It is very important to consider the liquefaction failure by reaching 5% double amplitude axial strain for rubber-sand mixtures due to the reduced stiffness of the mixture matrix. The cyclic strength of the material is also can be normalized with the effective confining pressure and it is termed as cyclic resistance ratio (CRR). The factor of safety against liquefaction can be calculated using equation 3. The material is termed as non liquefiable if the factor of safety is observed to be less than one.

$$Factor\ of\ safety\ (FOS) againstliquefaction = \frac{CRR}{CSR} \tag{2.3}$$

2.5 LIQUEFACTION RESISTANCE AND POST LIQUEFACTION BEHAVIOUR OF SAND

The liquefaction resistance of well-graded sand is reported to be higher than that of the poorly graded sand (e.g., Kramer 1996; Rouholamin et al. 2017). Further two different observations have been reported in the literature for the effect of fines in the sandy soil: the first one is that the increase in the fines content increases the liquefaction resistance (Seed and Idriss 1979; Yasuda et al. 1994) and other is the liquefaction resistance decreases with increase in the fines content (Vaid 1994; Lade and Yamamuro 1997).

In addition to the evaluation of the liquefaction strength of the sandy soil, fewer studies have been reported the behaviour of sand during the post cyclic monotonic loading (e.g., Vaid and Thomas 1995; Rouholamin et al. 2017). These behaviours were studied to examine the foundation settlement, lateral spreading, and to develop load-displacement curves for soil-structure interaction analysis (Rouholamin et al. 2017). Figure 2.5 shows the post cyclic stress-strain behaviour and the excess pore water pressure behaviour of sandy soil. The post cyclic shear strength of sand is observed to be zero up to a post-dilation shear strain [the strain at which the sand starts taking axial load after liquefaction (Rouholamin et al. 2017)] followed by a rapid increase in the shear strength. It is also noted that the post dilation shear strain increases with increase in the density of the sand. Further, the excess pore water pressure which is equal to the effective confining pressure at the liquefied state is reported to maintain up to the post-dilation shear strain followed by a reduction. The reduction in excess pore water pressure is owing to the development of negative pore water pressure which in turn due to the dilatancy of sand during the post-cyclic loading.

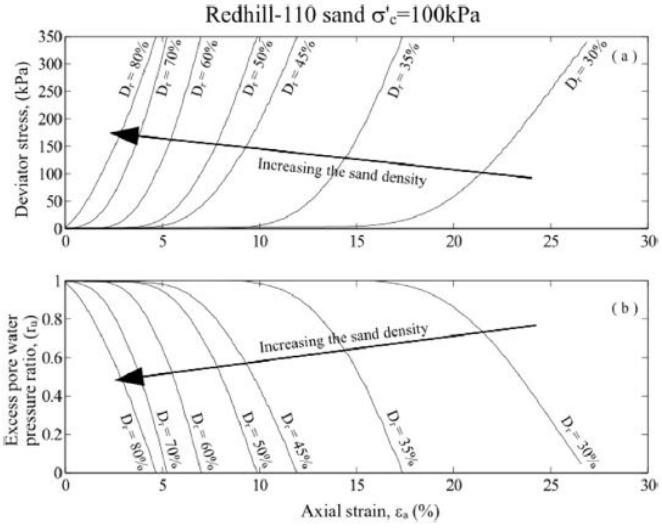

Figure 2.5: Post-liquefaction behaviour of sand (Rouholamin et al. 2017)

The liquefaction resistance of pure fly ash has been reported in fewer studies (Zand et al. 2008; Jakka et al. 2010). The limited literature shows that the excess pore water pressure of fly ash is observed to be increased rapidly. Further, Zand et al. (2008) reported that the axial strain accumulation is mainly during the compressive cycles while Jakka et al. (2010) observed that the axial strain is distributed both in compression and tension. In addition, it is observed that the fly ash (Badarpur) possess higher liquefaction resistance than that of sand (Yamuna) in the dense state (Zand et al. 2008). Phenomenologically, the liquefaction resistance of sand mixed with fly ash is reported by Keramatikerman et al. 2017. The fly ash content of up to 6% is examined in that study. It is reported that the liquefaction resistance of sand is increased with increase in the fly ash content and the addition of 6% fly ash shows higher liquefaction resistance.

2.6 LIQUEFACTION BEHAVIOUR OF THE RUBBER-SAND MIXTURES

The mixtures of rubber and sand behave like cohesionless material because both the materials do not show any cohesion. The applications of mixtures in earthquake prone area require the detailed examination of its liquefaction resistance. Since the inception of the studies on the mixtures of rubber and sand, researchers mainly concentrated the static and dynamic properties of the mixtures. The evaluation of liquefaction resistance is only initiated in the later 2000. The most of the previous studies were examined the liquefaction behaviour of the mixtures using cyclic triaxial tests. The studies which have been reported for the liquefaction behaviour of the rubber-sand mixtures are consolidated in Table 2.2.

2.6.1 Excess Pore Pressure and Axial Strain Response

The maximum excess pore water pressure ratio of the mixtures observed by Hyodo et al. 2008 with different rubber content is shown in Figure 2.6a. The excess pore water pressure ratio is observed to decrease with increase in the rubber content. The minimum excess pore water pressure ratio is observed for pure rubber samples (Hydo et al. 2008; Mashiri et al. 2016). It is also evident from the figure that the maximum pore water pressure ratio is shown insignificant change up to the rubber content of 30% by volume. However, the rapid decrease in the maximum pore water pressure ratio is reported when the rubber content is added more than 30% by volume. It is evident from Figure 2.6b that the development of axial strain depends on the amount of rubber content present in the mixture. For all the mixtures, the axial strain is rapidly developed at the initial number of cycles. However, the rapidly developed axial strain attains a saturated value less than 5% when the rubber content is between 30% and 70% by volume (Hydo et al. 2008).

Further, the mixtures possessing lower rubber content [i.e., less than 30% by volume (sand-like behaviour)] and higher rubber content [i.e., more than 70% by volume (rubbe-like behaviour)] reported to show higher axial strain than that of sand. The development higher excess pore water pressure and the reduction in the stiffness is the reason for the development of higher axial strain in low rubber content and higher rubber content mixtures respectively (Hydo et al. 2008; Mashiri et al. 2016).

Table 2.2: Studies on the liquefaction resistance of the rubber-sand mixtures

Literature	Size of rubber (mm)	Rubber content	Confining pressure (kPa)	Relative density (%)	CSR	Apparatus / testing
Promputthangkoon and Hyde (2008)	0.4 to 2	0 to 15% by volume	100	-	0.15	Cyclic triaxial
Hyodo et al. (2008)	0.1 to 1	0 to 100% by volume	100	-	0.15 to 0.3	Cyclic triaxial
Hazarika et al. (2008)	0.1 to 1	pure rubber	-	-	-	Shake table
Kaneko et al. (2013)	0.1 to 1	0 to 50% by volume	-	-	-	Simple shear
Hong et al. (2015)	0.06 to 3	pure rubber	100	-	0.15 to 0.2	Cyclic triaxial
Mashiri et al. (2016)	Tire chips of size 20mm	0 to 40% by weight	69	50	-	Cyclic triaxial (strain controlled)
Li et al. (2016)	D_{50} = 0.2 and 0.8	0 to 20% by volume	50, 100, 200	-	0.15 to 0.3	Cyclic triaxial
Otsubo et al. (2016)	Tire chips (2 to 20mm	-	-	-	-	Shake table

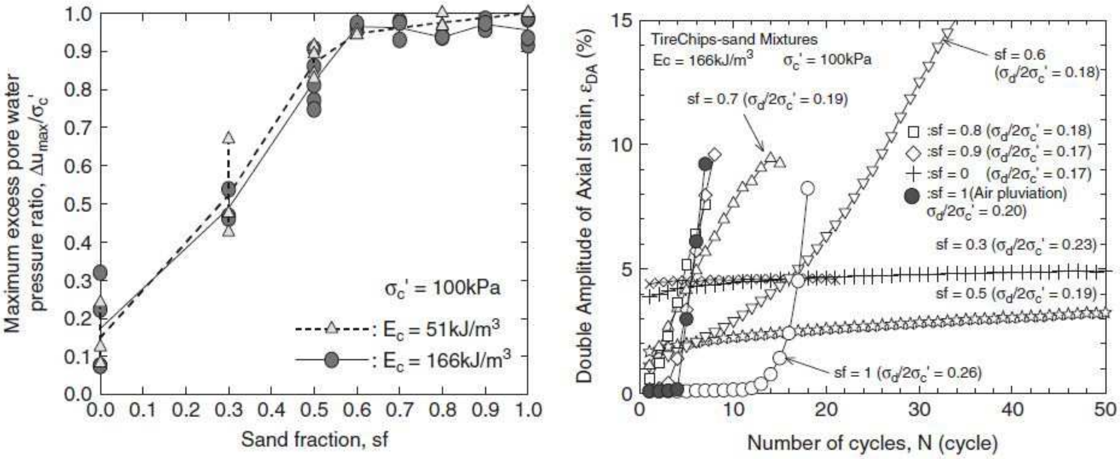

Figure 2.6: Variation in (a) maximum excess pore water pressure ratio (b) double amplitude axial strain (Hyodo et al. 2008)

2.6.2 Liquefaction Resistance of the Rubber-Sand Mixtures

The liquefaction resistance is observed to decrease with increase in the rubber content for the maximum rubber content of 15% by volume (Promputthangkoon and Hyde 2008). In addition, the liquefaction resistance is increased with increase in the rubber content for the rubber content in the range of 0 to 100% (Hydo et al. 2008). Further, it is also reported that the liquefaction resistance increases with increase in the rubber content up to30% by weight followed by a decrease (refer Figure 2.7a). The liquefaction resistance of rubber-sand mixtures mainly depends on the number of cycles required for reaching 5% axial strain rather than the initial liquefaction. It is observed from the literature that the excess pore water pressure rapidly increases for lower rubber content mixed with sand. Further, the presence of rubber reduces the stiffness of the mixture matrix. The reduction in the liquefaction resistance of lower rubber content mixed with sand is attributed to the increase in the excess pore water pressure and the reduction in the stiffness. The lower liquefaction resistance of the mixture having higher rubber content is mainly attributed to the lower stiffness of the matrix.

The liquefaction resistance of tire chips mixed with sand is reported to decrease for the rubber content more than 30% by weight. It is claimed that the reduction in the liquefaction resistance is attributed to the increase in the void ratio of the mixtures having tire chips more than 40% by weight (Mashiri et al. 2016). The larger size rubber mixed with sand is also reported to possess lower segregation resistance when the rubber content is more than 30% by weight (refer Figure 2.3). It is evident from Figure 2.3 that the segregation of the mixtures causes the formation of the sand layer at the bottom and the rubber layer at the top. The first reason for the decrease in the liquefaction resistance could be the measurement of pore water pressure at the bottom. The excess pore pressure measurement is the representative of pore pressure developed in the sand due to the settlement of sand at the bottom of the sample. The other reason could be that the formation of sand and rubber layer due to the segregation. Kaneko et al. (2013) reported that the liquefaction resistance of sand layer overlaid by rubber layer posses lower liquefaction resistance than any other configurations (Figure 2.7b).

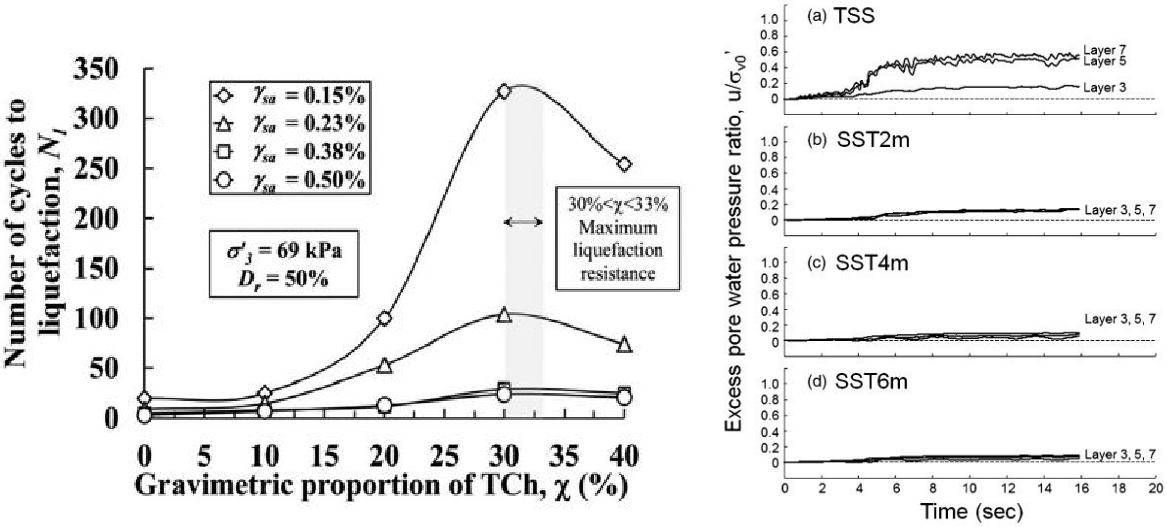

Figure 2.7. Liquefaction resistance of (a) tire chips mixtures (Mashiri et al. 2016) (b) sand and rubber layers (Kaneko et al. 2013)

Besides the rubber content, fewer studies were reported the effect of rubber size on the liquefaction resistance of the rubber-sand mixtures. Li et al. (2016) examined the liquefaction resistance of mixtures having the different size of the rubber (i.e., D_{50} = 0.2 and 0.8 mm). The liquefaction resistance of mixtures having larger size rubber is observed to be more than that of smaller size rubber. Further, the effect of confining pressure is also reported in the literature (Li et al. 2016). It is observed that the liquefaction resistance of the mixtures increases with increase in the confining pressure. The stiffness of the mixture increases with increase in the confining pressure which results in offering the higher liquefaction resistance.

2.6.3 Model Study on the Liquefaction Resistance of the Rubber-Sand Mixtures

In addition to the element tests, few researchers were attempted to examine the liquefaction behaviour of the rubber-sand mixtures using shake table tests. Hazarika et al. (2008) examined the pure rubber as a cushion material for quay wall in shake table tests. Figure 2.8 shows the typical quay wall with rubber cushion used in shake table testing. It is reported that the presence of tire chips cushion has reduced the generation of excess pore water pressure in the sand backfill.

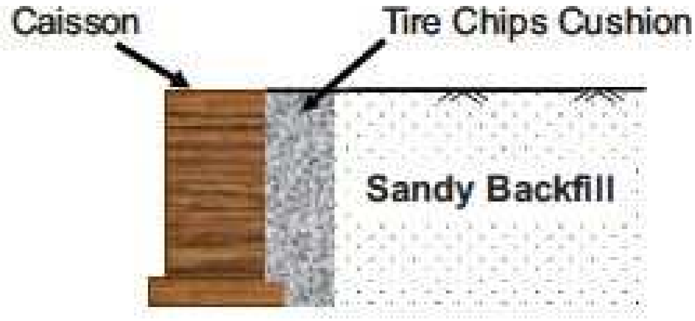

Figure 2.8: Tire chips as a cushion material for quay wall (Hazarika et al. 2008)

The rubber-sand mixture is also examined as a buried pipeline backfill material using shake table tests (Otsubo et al. 2016). The uplift of the rubber-sand mixture is compared with different backfill material at different surrounding subsoil. The rubber-sand mixture is reported to show the lowest uplift of the buried pipeline than that of the other backfill materials examined in that study for the liquefiable subsoil (Figure 2.9b). However, when the subsoil is unliquefiable, the uplift of the buried pipeline for mixture backfill is less than that of pure sand and more than that of crushed concrete and crushed glass (Figure 2.9a).

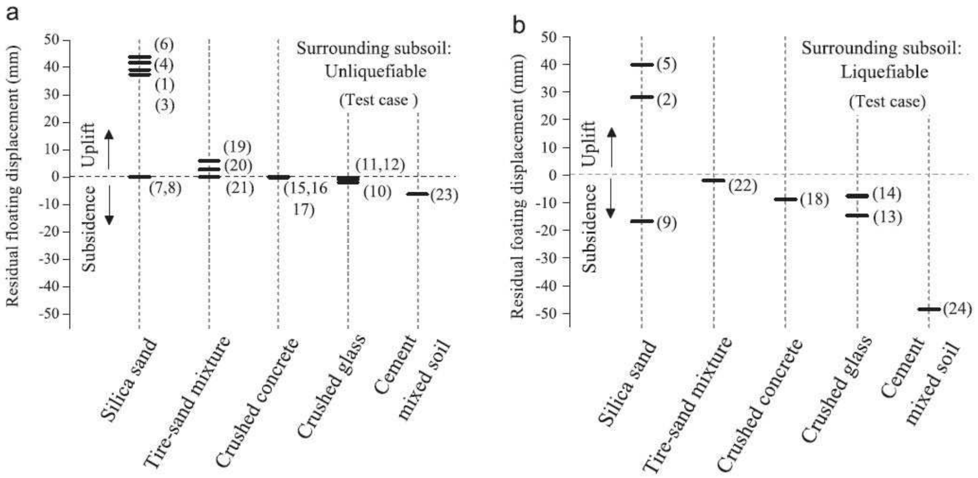

Figure 2.9: Uplifting of buried pipelinewith different backfill materials (a) unliquefiable surrounding subsoil (b) liquefiable surrounding subsoil (Otsubo et al. 2016)

2.7 CONSTITUTIVE FRAMEWORK FOR RUBBER-SAND MIXTURES

The static behaviour of the mixtures was modeled using hyperbolic relationship (Lee et al. 1999). The hyperbolic models are only capable of predicting the strain hardening behaviour. However, the mixture shows clear peak followed by strain softening when the rubber content is less than30% by weight or the mixture of tire chips and sand (Youwai and Bergado 2003; Zornberg et al. 2004; Mashiri 2014; Mashiri et al. 2015). Hence, the hyperbolic model is not capable of predicting the post-peak drop, plastic strains, and dilation of the mixtures (Mashiri et al. 2015b).

Further in the literature, hypoplasticity model based on critical state framework is developed to overcome the inadequacy of hyperbolic model (Youwai and Bergado 2004; Mashiri et al. 2015b). The hypoplasticity model can be explained using Figure 2.10 where the different surfaces of rubber-sand mixtures such as dilatancy, bounding, and critical state surfaces are shown in stress path space. As per the hypoplasticity model, the dilatancy of the mixtures will be accounted when the stress path touches the dilatancy surface. Further, the load increment would be continued up to only the stress path touches the bounding surface followed by the strain softening will be considered. Then the strain softening of the mixtures would be calculated till it reaches the critical state surface.

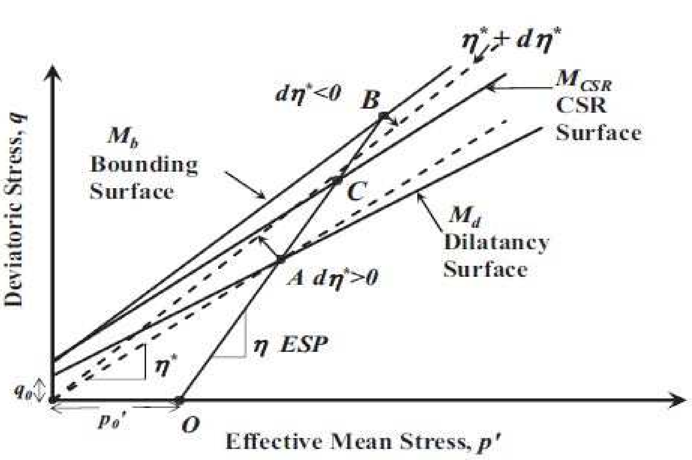

Figure 2.10. Different surfaces of the tire-chips mixture in stress path space (Mashiri et al. 2015b)

2.8 CRITICAL APPRAISAL

Since the inception of the usage of recycle rubber from scrap tire mixed with sand in geotechnical engineering field, researchers primarily followed two different methods to find the density or unit weight of the mixtures, namely index density method (Sheikh et al. 2013; Mashiri et al. 2015; Noorzad and Ravesshi 2017) and compaction method (Edil and Bosscher 1994). Ahmed and Lovell (1993) found that the vibratory table method is suitable for rubber-sand mixtures and Proctor compaction is suitable for pure rubber and rubber mixed with fine-grained soils. On the other hand, Edil and Bosscher (1994) reported that the determination of maximum index density of the tire chips-sand mixtures using the vibratory table method as per ASTM D4253 (ASTM 2016a) may not be appropriate to study the packing and compaction characteristics. Hence it is evident that there is no conclusive study reported in the literature to identify a suitable method to determine the maximum dry unit weight of the rubber-sand mixtures. Furthermore, Table 1 describes different approaches to obtain the unit weight or density of the mixture's samples along with their respective difficulties in adopting for practical applications.

It is also noted that the shear strength of the mixtures generally increases with the increase in tire shreds (e.g., Foose et al. 1996; Ghazavi and Sakhi 2005) and tire chips (e.g., Mashiri et al.

2015; Reddy et al. 2016) up to a certain content. Reddy et al. (2016) reported that up to a maximum addition of 30 to 40% of tire chips by weight increases the shear strength. However, the shear strength and friction angle of tire crumbs (e.g., Ghazavi 2004; Edincliler et al. 2010) and particulate rubber (e.g, Cabalar 2011; Sheikh et al. 2013; Anbazhagan et al. 2016) mixed with sand reduces with an increase in rubber content. Moreover, beyond 20% rubber content by volume (i.e., 10% by weight), the particulate rubber sand mixtures show a reduction in shear strength (e.g., Anbazhagan et al. 2016). These observations show that the larger size rubber (tire shreds and tire chips) mixed with sand increases the shear strength and the smaller size rubber (tire crumbs and particulate rubber) decreases the shear strength with an increase in the rubber content. In addition, it is evident from the literature that the dilation trend of tire chips, tire crumb, and particulate rubber mixed with sand decreases with increase in the rubber content (e.g., Youwai and Bergado 2003; Ghazavi 2004; Mashiri et al. 2015; Anbazhagan et al. 2016). However, tire shred-sand mixtures show increasing dilation with increasing the tire shred content in the mixture (e.g., Foose et al. 1996; Ghazavi and Sakhi 2005). It shows that the dilation trend of the mixtures changes to compression due to the reduction in the size of rubber.

Though the mixture of small size rubber and sand gains importance in the geotechnical engineering applications (e.g., Hazarika et al. 2008; Hazarika et al. 2012; Sheikh et al. 2013), till now there is no single study has been performed on the interface behaviour of the mixtures posses small size rubber. In addition, it is reported in various literature that the tire shreds and tire chips mixed with sand is susceptible to segregation when the rubber content in the mixture is more than about 30% (Edil and Bosscher 1992; Edil and Bosscher 1994; Kim and Santamarina 2008; Umashankar 2009; Anastasiadis 2011; Mashiri 2014; Umashankar et al. 2014). It is also observed that the mixture of particulate rubber (size 0.425mm to 2mm) and sand does not segregate due to the size compatibility between the two materials. Further, the particulate rubber mixed with sand posses lower shear strength. To increase the shear strength of the particulate rubber mixture, fly ash is proposed as a replacement for sand in the mixture.

Applications of rubber mixed with sand have been examined as embankment material, lightweight retaining wall backfill, buried pipe backfill, and base isolation. The static and dynamic properties of these mixtures are extensively examined in earlier studies (Anastasiadis

2011; Mashiri 2014). However, it is important to examine the liquefaction potential of the mixtures to avoid the damages to the overlying structures. Though the mixture, in general, is believed to possess satisfactory resistance against liquefaction (Hydo et al. 2008; Mashiri et al. 2016), there is no exclusive study on the liquefaction behaviour of the mixtures considering the initial liquefaction as well as liquefaction due to the attainment of certain double amplitude axial strain.

Cyclic behaviour of recycled rubber obtained from scrap tire mixed with sand has been studied by various researchers. Though the mixture behaves like cohesionless material when the rubber is added to sand, limited studies were carried out on the liquefaction resistance of the mixture (Li et al. 2016; Mashiri et al. 2016; Kaneko et al. 2013; Hazarika et al. 2010). The available limited liquefaction studies have only concentrated the effect of CSR and energy for preparing the samples. However, the post cyclic strength, effect of confining pressure, density and a rubber content above which the mixture does not liquefy is not discussed in the available literature. In addition, there is no single study in the literature on the modeling of the cyclic behaviour of the rubber sand mixtures.

In general, it is found that the liquefaction resistance of tire chips (size 20mm to 50mm) increases with increase in the rubber content up to 30% rubber content followed by reduction (Mashiri et al. 2016). It is also evident from Mashiri 2014 that the tire chips content more than 30% is prone to segregation. The segregation results in the formation of the sand layer at the bottom and the tire chips layer at the top. It is also evident from the literature that the sample having sand layer at the bottom and tire chips layer at the top posses lower liquefaction strength than that of the mixtures (Kaneko et al. 2013). It shows that the reduction in the liquefaction resistance is attributed to the segregation of tire chips-sand mixture. Further, it concludes that the usage of large size rubber in sand is prone to segregation which in turn increase the liquefaction potential of the mixture. The studies on the liquefaction resistance of sand mixed with particulate rubber (size 0.45 to 2 mm) show that the increases in resistance with an increase in the rubber content (Hazarika et al. 2010). In addition, it is noted that the pure rubber does not liquefy. It is due to the compressibility nature of rubber particles present in the sample which suppresses the accumulation of excess pore water pressure while the sand particles in the pure sand specimen do not compresses resulting which the development of excess pore water pressure. It is evident that regardless of the size of the rubber, the liquefaction resistance increases with increase in the rubber content.

The liquefaction resistance of the mixtures increases with the increase in the rubber particle size in the mixture, especially at lower rubber content subjected to lower confining pressure (Li et al. 2016). However, it can also be inferred that the liquefaction resistance of tire chips (size 20mm to 50mm) mixture (Mashiri et al. 2016) is less than that of the particulate rubber (size 0.425mm to 2mm) mixture (Hazarika et al. 2010). It is also to be noted that to achieve the given load, the samples deforms more in tension than that in compression for the mixtures with rubber content less than 10% by weight (Li et al. 2016).

the axial strain of the mixture increases with the increase in the number of loading cycle even though there is insignificant increase in excess pore water pressure (Hydo et al. 2008). It is attributed to the reduction in the stiffness of matrix due to the addition of rubber particles. Therefore, initial liquefaction may not occur in the mixtures. However, there is a chance of liquefaction failure of the sample by achieving a stipulated double amplitude axial strain (for e.g., 5% as per Kramer 1996). As can be seen, most of the previous studies mainly concentrated on the initial liquefaction of the mixture (Promputthangkoon and Hyde 2008; Hong et al. 2015; Mashiri et al. 2016). On many surmise that it is important to study the liquefaction resistance considering both initial liquefaction and failure by achieving certain double amplitude axial strain.

Furthermore, researchers in past attempted to model, mostly semi-empirical, the static behaviour of mixtures (Lee at al. 1999; Youwai and Bergado 2003; Mashiri et al. 2015b). These frameworks include several notable features such as deviator stress-strain behaviour, post-peak shear strength, dilatancy, etc. However, there is a need for modeling the cyclic behaviour of the mixtures to study the applications of mixtures in seismically active region. It is also evident from the various literature on the cyclic behaviour of recycled rubber mixed with sand that the liquefaction resistance, post cyclic monotonic behaviour and the modeling of the cyclic behaviour of sand-rubber mixtures need to be studied in detail for the effective application of these mixtures in the field.

2.9 RESEARCH GAPS

The literature review suggests that there is an ambiguity in the determination of the maximum dry unit weight of the mixtures. In addition, the shear strength of the particulate rubber-sand mixtures decreases with increase in the rubber content. It should be noted that the segregation resistance of the mixtures are needed to be studied since two different particulate materials are used in the mixture.

Further, the shear strength of rubber-sand mixtures having smaller size rubber needs to be improved with an alternative material for sand. In addition, the different (i.e., concrete and soil) interface behaviours of the smaller size rubber mixed with sand or fly ash, which can be used in various engineering applications, need to be studied. It is also noted form the literature that the sample preparation technique for the interface behaviour between mixtures and sand is not clear. The influence of the initial relative density on the interface shear strength and the interface coefficient is also not reported in the literature.

The liquefaction resistance and the post cyclic monotonic behaviour of the recycled rubber mixed with sand are limited in the literature. Further, there is no single study on the modeling of the liquefaction behaviour of rubber-sand mixtures.

2.10 SUMMARY

In this chapter, the various literatures on the density, shear strength, interface shear strength, liquefaction resistance and modeling the rubber-sand mixtures behaviour are discussed in detail. The literature review on these topics of rubber-sand mixtures gives insight to the extent at which the past studies have been carried out. From the detail discussion a collection of research gap are identified, a few of which would form the major contribution of the present study.

CHAPTER 3

CHARACTERIZATION OF THE MIXTURES

3.1 INTRODUCTION

The density of the rubber-sand mixtures is one of the important properties which require careful observation. The past studies were used different terminology to represent the state of the sample since there is no study on the suitable technique to determine the maximum density of the rubber-sand mixtures. Therefore in the present study different techniques such as vibratory table method, Proctor compaction methods and mini compaction methods are chosen to examine a suitable method to determine the maximum density of the mixtures. Further, segregation is one of the major problems in the mixture matrix which needs to be studied. The mixture of sand and tire chips (larger size rubber) with the rubber content more than 30% by weight was found to show segregation in the literature. Therefore, a higher rubber content mixture with sand and particulate rubber (small size rubber) is examined for the segregation problem using vibratory table method without surcharge.

3.2 MATERIALS

The shredded scrap tire, river sand and fly ash of class F are used in the present study. The scrap tire is grinded after removing the steel reinforcement in the workshop. The shredded tire rubber is sieved through 2mm sieve which is then classified as particulate rubber (0.425 mm to 2 mm) as per ASTM D6270 (ASTM 2012c). Prior to mixing with the particulate rubber, the river sand is also sieved through 2 mm sieve to have the uniform particle size in the mixture. The fly ash of Class F used in the present is collected from Ennore thermal power station, Chennai. The grain size distribution of particulate rubber, sand, and fly ash is shown in Figure 3.1.

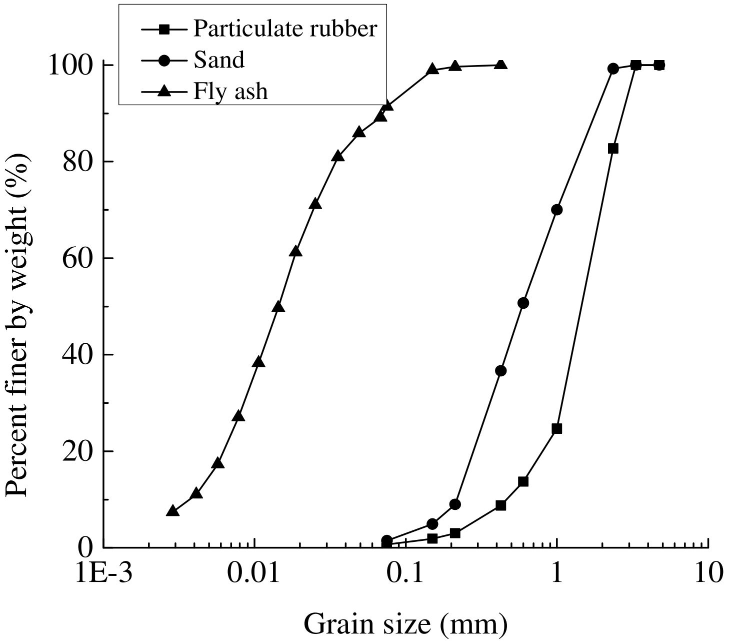

Figure 3.1: Particle size distribution of particulate rubber, sand, and fly ash

The rubber of gravimetric percentage of 10, 30 and 50% is mixed with sand and fly ash for the different tests in the present study. These mixtures are termed in the present study as particulate rubber-sand mixtures and particulate rubber-fly ash mixtures. The typical images of the mixtures are shown in Figure 3.2. The specific gravity of all the materials and mixtures are presented in Table 3.1. It is evident from the table that the specific gravity of the mixtures decreases with increase in the rubber content. Moreover, it should also be noted that the specific gravity of particulate rubber used in the present study shows marginally higher range than that reported by different researchers for recycled rubber from scrap tire in general (e.g., Edil and Bosscher 1994; Ngo and Valdes 2007; Sheikh et al. 2013). Energy dispersive X-ray analysis (EDXA) is carried out to examine the reason for the higher specific gravity of particulate rubber. EDAX results for pure rubber are shown in Figure 3.3. It is observed from EDXA that the pure rubber possess the elements of C = 62.06% (% by weight), O = 19.94%, Al = 7.37%, Ca = 1.18%, Ti = 0.84%, Fe = 3.51%, Zn = 3.99% and Sr = 1.12%. Hence, rubber specific gravity of 1.45 is attributed to the presence of higher amount of carbon (C).

Table 3.1: Specific gravity of materials and mixtures

	Particulate rubber-sand mixtures					Particulate rubber-fly ash mixtures				
	Sand	10%R	30%R	50%R	Rubber	Fly ash	10%R	30%R	50%R	Rubber
Specific Gravity	2.66	2.39	2.1	1.93	1.45	2.29	2.1	1.92	1.82	1.45

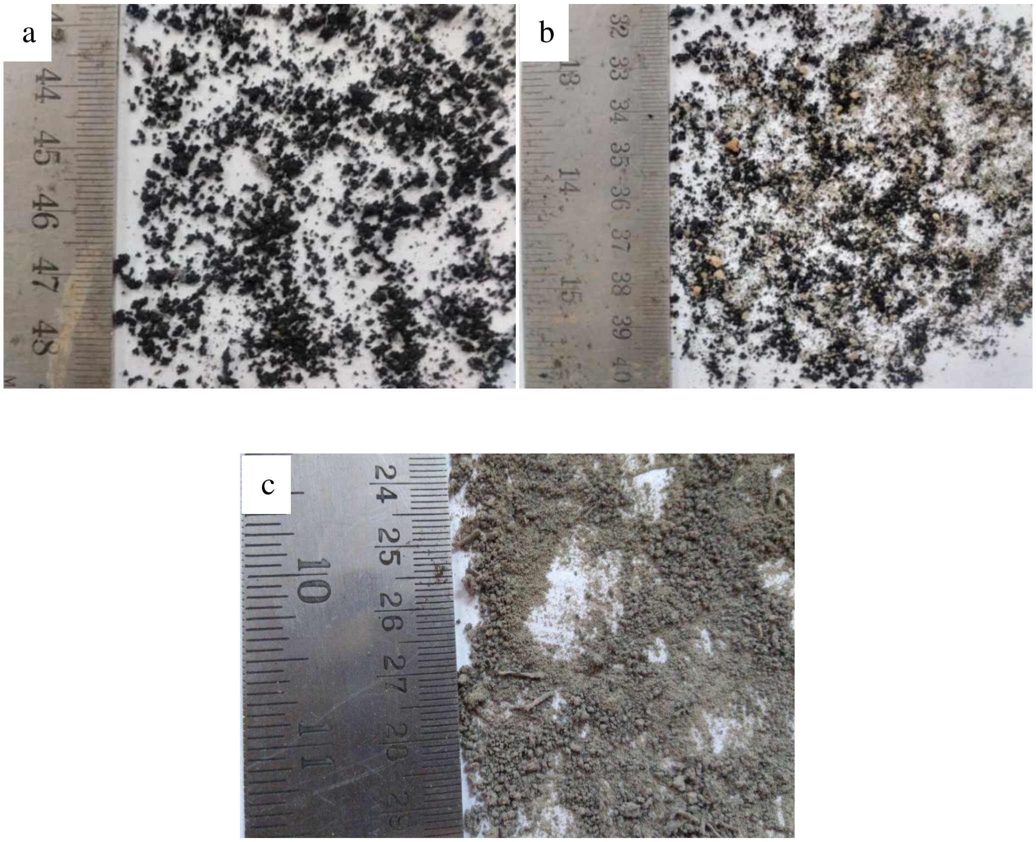

Figure 3.2: Typical sample of (a) particulate rubber, (b) particulate rubber-sand mixture, and (c) particulate rubber-fly ash mixture

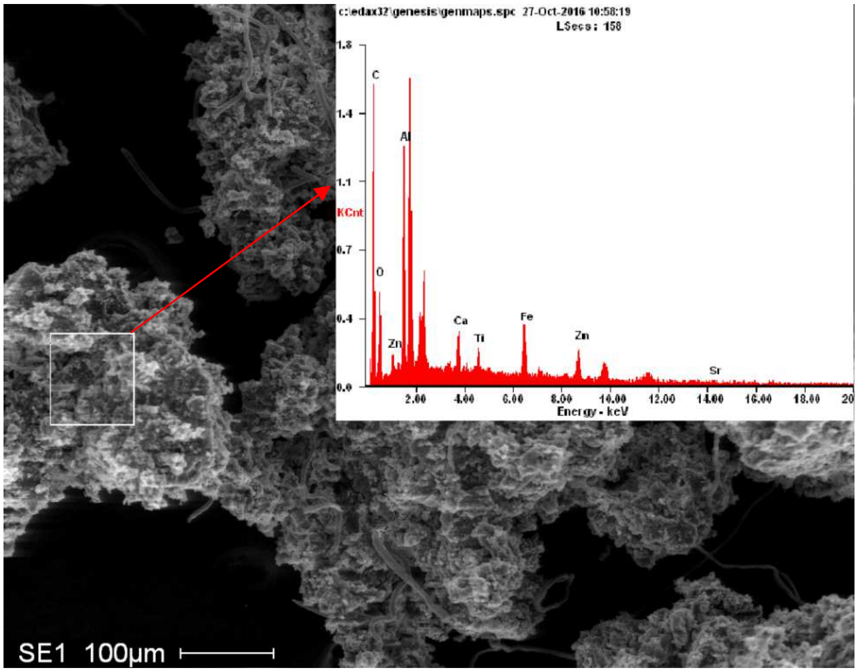

Figure 3.3: EDAX results of pure particulate rubber

3.3 DENSITY

The particulate rubber used in the present study is a particulate material which possesses little or no plasticity, with high compressibility, and energy absorption characteristics. Hence, in the following sections, different methods are evaluated to find the maximum dry unit weight of particulate rubber mixed with sand and fly ash.

3.3.1 Vibratory Table Method

The maximum dry unit weight of particulate rubber-sand mixtures and particulate rubber-fly ash mixtures is obtained using vibratory table method as per ASTM D4253 (ASTM 2016a). The standard surcharge of 13.8 ± 0.1 kPa as per ASTM D4253 (ASTM 2016a) is progressively increased (as shown in Figure 3.4) to observe the change in maximum dry unit weight of the mixtures. The surcharge is maximum increased to 23.3 kPa with 4 or 5 equal increments. After the vibratory table test, the settlements of the mixtures are measured before and after removal of the surcharge. Usually, the material filled in the vibratory table mould settles in the process of densification. The difference in both the settlement is termed as rebound height.

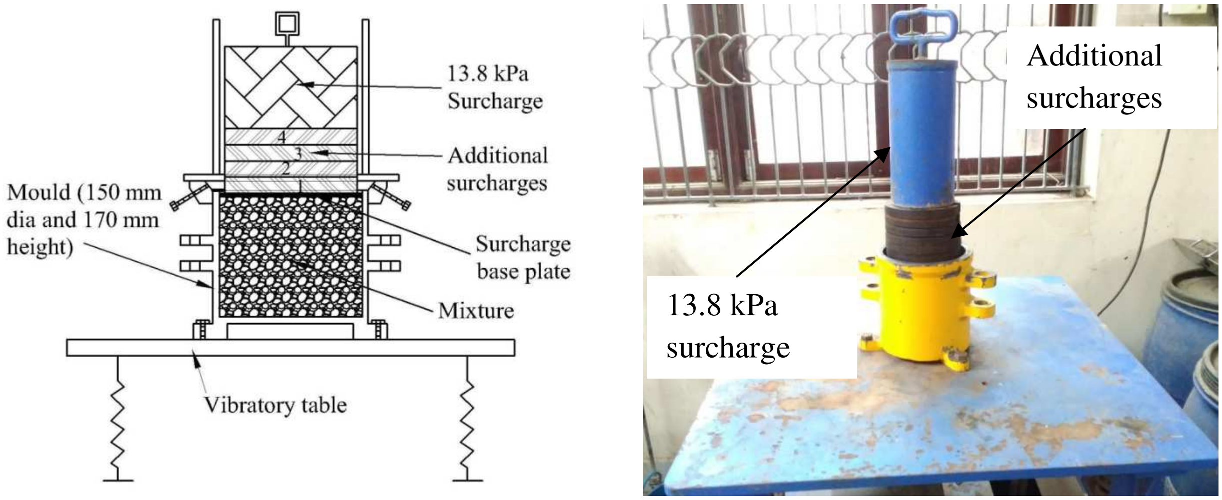

(a) **(b)**

Figure 3.4: Vibratory table with additional surcharges (a) schematic representation and (b) view of sample set for test

The percentage variation of maximum dry unit weight with the increase in surcharge is shown in Figure 3.5. The percentage variation of maximum dry unit weight is calculated with respect to the standard surcharge (i.e., 13.8kPa). The maximum dry unit weight of pure sand obtained with the surcharge of 13.8 kPa [standard surcharge as per ASTM D4253 (ASTM 2016a)] and 23.3 kPa are 17.66 kN/m^3 and 17.70 kN/m^3, respectively. Hence for an increase in surcharge by 68.5%, the unit weight is marginally increased by 0.2%. The particle breakage of test material due to the increase in standard surcharge is examined with the gradation analysis of the material before and after the vibratory table test. The gradation analysis of the rubber and mixtures is shown in Figure 3.6. It is noted from the gradation analysis that due to the increase in surcharge, there is no significant change in the gradation of sand before and after the test in the vibratory table, which in turn shows that there is no particle breakage. Further, it can also be found that there is a negligible increase in rebound height (~0.4 mm) for the increase in the surcharge by 68.5% (refer Figure 3.7). In summary, the vibratory table test results show that there is no significant change in the maximum dry unit weight and the rebound height due to the increase in surcharge for sand. It can be further concluded that the surcharge of 13.8 ± 0.1 kPa as per ASTM D4253 (ASTM 2016a) is adequate to obtain the maximum dry unit weight of sand.

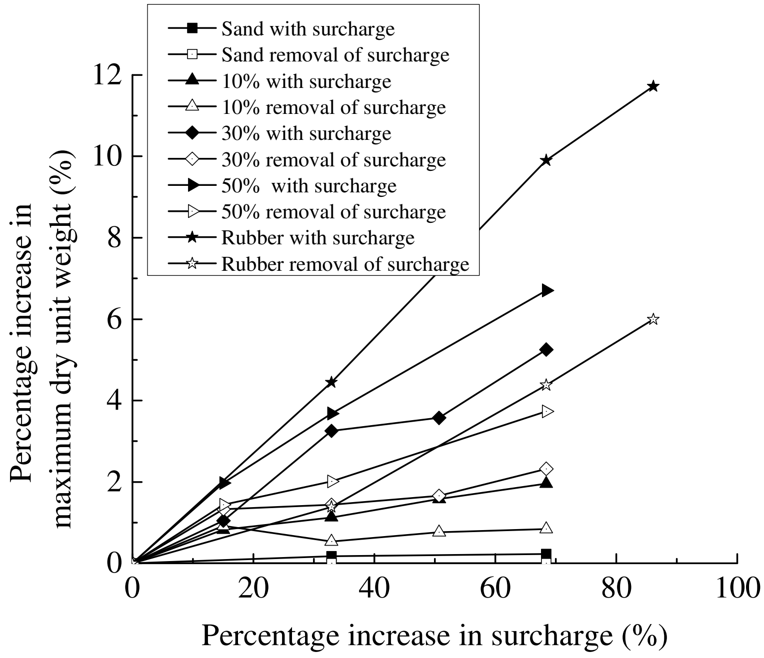

Figure 3.5: Influence of surcharge on the maximum dry unit weight of rubber-sand mixture

In the case of mixtures, two maximum dry unit weights are observed for a particular surcharge because of the significant rebound height. These two maximum dry unit weights are presented in terms of percentage increase in maximum dry unit weight with the percentage increase in the standard surcharge, as shown in Figure 3.5. The percentage increase in maximum dry unit weight is calculated based on the maximum dry unit weight obtained with the standard surcharge. It is evident from Figure 3.5 that the maximum dry unit weight of particulate rubber-sand mixture increase with an increase in the surcharge. Unlike sand, it can be clearly seen from Figure 3.5 that the maximum dry unit weight of pure rubber significantly increases by 11.7% for the increase in the standard surcharge by 86.2%. However, the typical gradation analysis of particulate rubber-sand mixture with 50% rubber and pure rubber before and after the test confirms that there is no significant change in the gradation of particulate rubber-sand mixture due to the increase in the surcharge (refer Figure 3.6). Therefore the increase in maximum dry unit weight due to the increase in standard surcharge is attributed to the denser arrangement of particles.

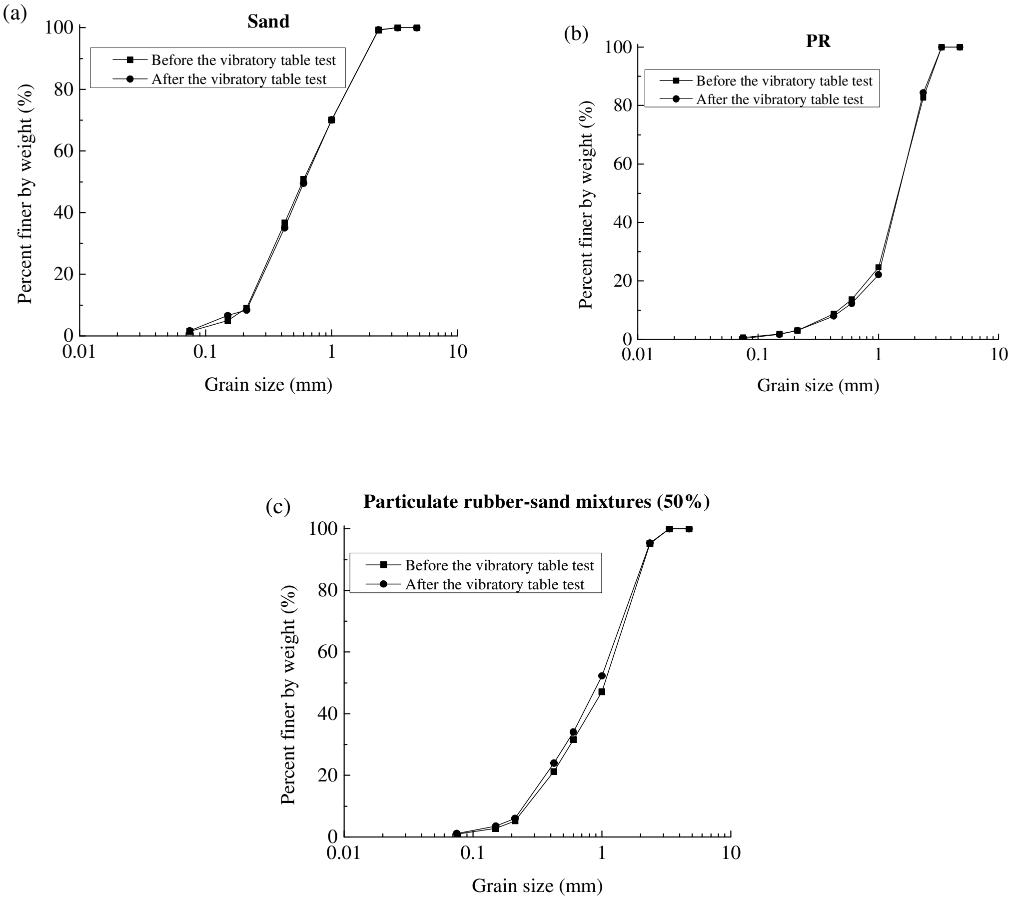

Figure 3.6: Influence of increased surcharge on the gradation of (a) sand, (b) particulate rubber, and (c) particulate rubber-sand mixture with 50% rubber

The change in rebound height of particulate rubber-sand mixture with the increase in standard surcharge is presented in Figure 3.7. The figure shows that the measured rebound height for particulate rubber-sand mixture increases with an increase in the standard surcharge which is due to the elastic nature of rubber present in the mixture. As a result of rebound, the maximum dry unit weight of the mixtures after removal of surcharge is lower than that measured with the surcharge as it is evident from Figure 3.5. As per ASTM D4253 (ASTM 2016a), the maximum dry unit weight or density should be measured after removal of surcharge for soil since there is no difference in unit weight before and after removal of the surcharge. However, for particulate rubber-sand mixture, the maximum dry unit weight decreases due to the removal of the surcharge, indicating that the energy imparted to the material during vibratory process under the particular surcharge is getting released which in turn disturbs the denser arrangement of the particles. Though the maximum unit weight of the mixtures with the presence of surcharge is observed to be higher, the maximum unit weight should be measured after removal of the surcharge considering the site applications of the mixtures.

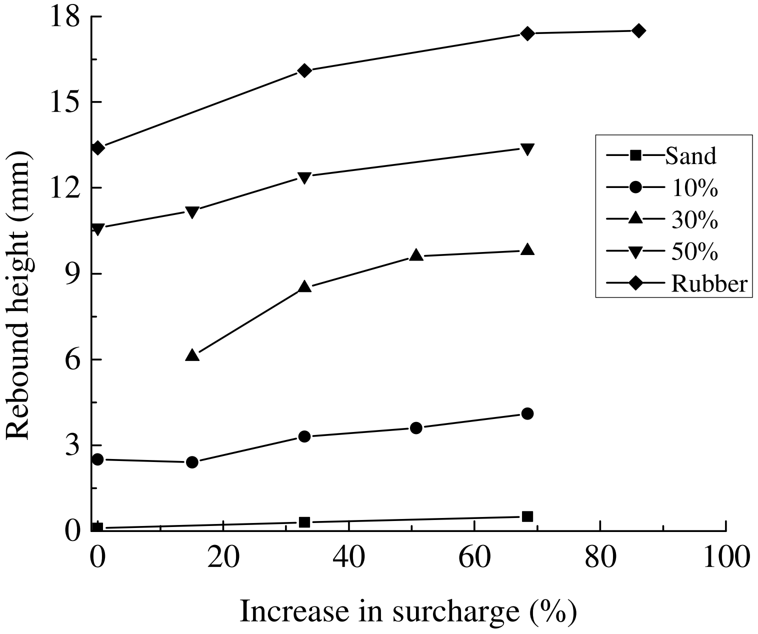

Figure 3.7: Influence of surcharge on the rebound height of rubber-sand mixture

An attempt also has been made to find the maximum dry unit weight of particulate rubber-fly ash mixture using vibratory table method. However, it is observed that the fly ash is ejected through the small gaps between the mould and the surcharge base plate. Hence, this method is not appropriate to determine the maximum dry unit weight of particulate rubber-fly ash mixture.

3.3.2 Compaction Methods

The maximum dry unit weight of particulate rubber-sand mixtures and particulate rubber-fly ash mixtures is also obtained by Standard and Modified Proctor compaction test as per ASTM D698 (ASTM 2012a) and ASTM D1557 (ASTM 2012b), respectively. While doing the test, it was observed that the hammer rebounds on the material due to the elastic nature of rubber in the mixture. To maintain the constant energy, care has been taken to avoid the multiple impacts on pure rubber and its mixtures during the single blow. Mini compaction technique (Sridharan and Sivapullaiah 2005), generally suitable for the particles size lesser than 2 mm, is also used to determine the maximum dry unit weight of pure particulate rubber and its mixtures. The mould of size 38.1 mm diameter and 100 mm height is used in this method. Thus the compaction is achieved with two parts, first from the energy transferring foot which is of 36.5 mm diameter and 125 mm height and the other from the hammer which gives impacts to the energy transferring foot, which in turn compact the material. In mini compaction, hammers of 9.8 N (1 kg) and 24.5 N (2.5 kg) with a height of fall of 160 mm are used for standard and modified tests, respectively. Therefore, the energies generated in standard and modified tests are 1419 kN-m/m^3 (for 3 layers and 36 blows per layer) and 3548 kN-m/m^3 (for 3 layers and 36 blows per layer), respectively. The part of the applied energy in mini compaction technique is lost due to the impact of the hammer on the energy transferring foot. Hence the energy adopted in mini compaction technique is more than that of Proctor compaction technique (Sridharan and Sivapullaiah 2005). The rebounding of the hammer is minimized in mini compaction technique compared to Proctor compaction technique by avoiding the direct contact of the hammer to the material.

The dry unit weight obtained using the compaction methods without adding water is taken as the maximum dry unit weight. This is because, as per ASTM D6270 (ASTM 2012c), the influence of water on the unit weight of tire chips mixture is not significant and the same is considered as applicable for particulate rubber mixtures. A similar observation is also reported by Uchimura et al. (2007). It is also observed that the water content does not have significant effect on the maximum dry unit weight of rubber-fly ash mixture when the rubber content in the mixture is more than 5% by weight (Priyadarshee et al. 2015). Moreover, previous studies reveal that the determination of water content of the sample is difficult due to the oozing of liquid from the rubber particles when it is kept in the oven at a temperature greater than 40°C (Hyodo et al. 2007; Kawata et al. 2007; Hong et al. 2015).

The maximum dry unit weight of the materials and mixtures obtained using the different method is given in Table 3.2. The table shows that the maximum dry unit weight of sand, determined from the standard and modified compaction tests, do not differ significantly from that obtained using the vibratory table method. However, the maximum dry unit weight of particulate rubber-sand mixture, possessing different rubber content, obtained from conventional Proctor compaction methods is 13 to 46% more than that obtained from vibratory table method. As in the case of vibrating table tests, it is observed that the portion of fly ash spills out of the mould during conventional Proctor compaction methods. Hence, the Proctor compaction method is not appropriate to determine the maximum dry unit weight of particulate rubber-fly ash mixtures in dry state.

The percentage increase in the maximum dry unit weight of particulate rubber-sand mixture using different technique is shown in Figure 3.8. As mentioned earlier, the percentage increase is calculated based on the maximum unit weight of the mixtures obtained using the vibratory table method with standard surcharge. It is evident from the figure that the maximum dry unit weight of particulate rubber-sand mixture obtained using the modified test of mini compaction method matches reasonably well with that determined from standard Proctor compaction method. It shows that the energy adopted in the modified test of mini compaction method is equivalent to the energy (Sridharan and Sivapullaiah 2005) adopted to obtain the maximum dry unit weight of particulate rubber-sand mixture using the standard Proctor compaction method. The spillage of fly ash during the compaction of particulate rubber-fly ash mixture is reasonably controlled in mini compaction method because of the reduced size of the mould with the different mode of transferring the energy to the mixture. Hence, the maximum dry unit weight of particulate rubber-fly ash mixture obtained with this method is reasonably accurate in comparison with the other methods.

Table 3.2: Maximum dry unit weight of different mixtures obtained using different method

Sample	Maximum dry unit weight (kN/m^3)					
	Vibratory table		Proctor Compaction		Mini Compaction	
	Standard surcharge[a]	Maximum surcharge[a]	Std. Proctor	Mod. Proctor	Std. Proctor	Mod. Proctor
Sand	17.66	17.67	17.35	17.98	17.66	17.66
10%	13.07	13.18	14.81	15.28	14.45	14.95
30%	9.05	9.26	10.76	11.53	10.84	11.17
50%	6.97	7.23	9.23	9.57	8.05	9.12
Fly ash	FAS	FAS	FAS	FAS	11.58	12.24
10%	FAS	FAS	FAS	FAS	10.34	11.58
30%	FAS	FAS	FAS	FAS	10.27	10.68
50%	FAS	FAS	FAS	FAS	9.03	9.69
rubber	4.34	4.6	6.01	6.34	5.42	5.99

Note: FAS = fly ash spilling.

[a] measured after removal of surcharge.

In summary, it can be stated that the maximum dry unit weight of particulate rubber-sand mixture obtained with vibratory table method is significantly lower than that determined from the compaction methods. Secondly, the maximum dry unit weight of particulate rubber-sand mixture obtains with vibratory table method influenced by various factors such as the vibration absorbent nature of rubber, rebounding of mixtures after removal of surcharge, and inadequate surcharge. Similar observation of vibration absorbent nature of tire chips mixture is reported by Edil and Boscher (1994). On the other hand, Proctor compaction method though suitable for finding the maximum dry unit weight of particulate rubber-sand mixture, cannot be used for particulate rubber-fly ash mixture because of the spillage of fly ash from the mould. However, mini compaction is suitable for both particulate rubber-sand mixture and particulate rubber-fly ash mixture.

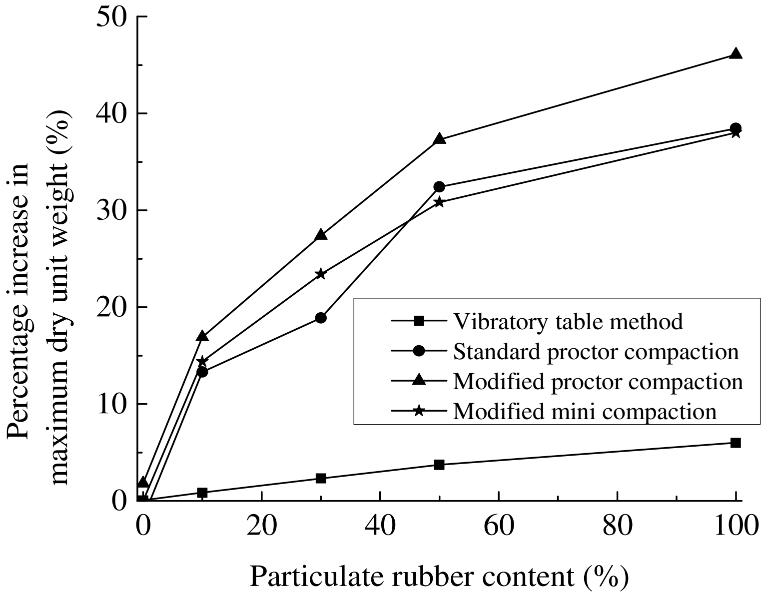

Figure 3.8: Increase in the maximum dry unit weight of particulate rubber-sand mixture using various methods

In the present study, the relative density of all particulate rubber mixtures is obtained using equation 4.1.

$$\mathrm{RD} = \frac{e_{max} - e_s}{e_{max} - e_{cm}} \times 100 \tag{3.1}$$

where, e_{max} = maximum void ratio, e_s = sample void ratio, and e_{cm} = void ratio obtained with compaction method.

The maximum void ratio of particulate rubber-sand mixtures and particulate rubber-fly ash mixtures is obtained in accordance with ASTM D4254 (ASTM 2016b). The standard Proctor compaction method or modified mini compaction method can be adopted to determine e_{cm} of particulate rubber-sand mixtures. However, modified mini compaction method (Sridharan and

Sivapullaiah 2005) can be adopted for particulate rubber-fly ash mixtures to control the fly ash spillage. In the present study, e_{cm} is obtained using modified mini compaction method for both particulate rubber-sand mixtures and particulate rubber-fly ash mixtures to have the consistency in the results.

The minimum and maximum dry unit weight of particulate rubber-sand mixtures and particulate rubber-fly ash mixtures used further in this study is given in Table 3.3. The minimum and the maximum dry unit weights of particulate rubber-sand mixture and particulate rubber-fly ash mixtures are determined as per ASTM D4254 (ASTM 2016b) and the modified mini compaction method (Sridharan and Sivapullaiah 2005) respectively. It is evident from Table 3.3 that the minimum and maximum dry unit weights decrease as the rubber content increase in both the mixtures. In addition, table also shows that the maximum dry unit weight of particulate rubber-fly ash mixtures is lower than particulate rubber-sand mixtures up to a rubber content of 30% followed by an increase. The increase in the unit weights of particulate rubber-fly ash mixtures, when rubber content more than 30%, is due to the filling of more voids present in the mixture matrix.

Table 3.3: Minimum and maximum dry unit weight of materials and mixtures

	Particulate rubber-sand mixtures					Particulate rubber-fly ash mixtures				
	Sand	10%R	30%R	50%R	Rubber	Fly ash	10%R	30%R	50%R	Rubber
Minimum (kN/m^3)	14.87	10.95	6.89	4.99	2.65	6.93	6.82	6.46	5.21	2.65
Maximum (kN/m^3)	17.66	14.95	11.17	9.12	5.99	12.24	11.58	10.68	9.69	5.99

3.4 SEGREGATION ANALYSIS

The segregation resistance of particulate rubber-sand mixtures is examined with the vibratory table, which is used to determine the maximum dry unit weight of granular materials as per ASTM D4253 (ASTM 2016a), without adopting the surcharge. It is reported in the literature that the rubber content more than 30% by weight is prone to segregation. Therefore in the present study, the segregation analysis is carried out on the mixture possessing 50% sand and particulet rubber. The mixture is thoroughly mixed and filled into the mould before placing the base plate on top of the mould (as shown in Figure 3.9a). The entire setup is fixed on the vibratory table to apply vibration for 8 minutes (as shown in Figure 3.9b). After the tests, the mixture is visually examined for any segregation.

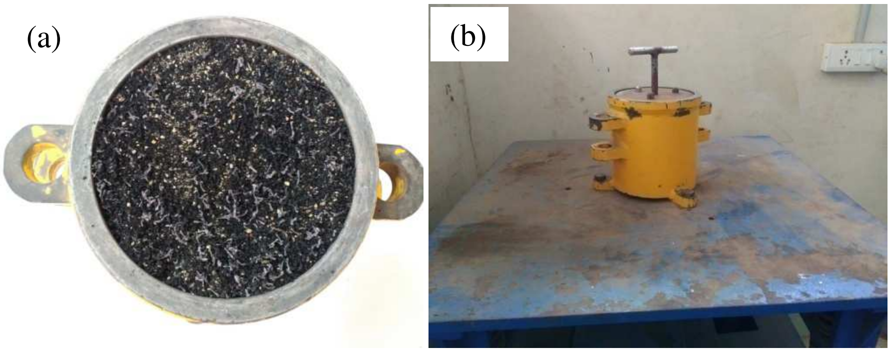

Figure 3.9: Segregation analysis: (a) and (b) sample before the test and

As per ASTM D 6270 (ASTM 2012), the rubber recycled from scrap tire can be classified as tire shred (50 mm to 305 mm), tire chips (12 mm to 50 mm), granulated rubber or particulate rubber (0.425 mm to 12 mm), ground rubber or particulate rubber (0.425 mm to 2 mm) and powdered rubber (< 0.425mm). Though all these varieties have certain benefits, past studies revealed that there is a chance of segregation of the mixtures when the large portion (> 30% by weight) of tire chips or tire shreds were added to the sand (Edil and Bosscher 1992; Edil and Bosscher 1994; Kim and Santamarina 2008; Umashankar 2009; Anastasiadis 2011; Mashiri 2014; Umashankar et al. 2014). In view of that, it is required to study the segregation resistance of mixtures having higher content particulate rubber. The segregation resistance of particulate rubber-sand mixture is examined with the vibratory table, which is used to determine the maximum dry unit weight of granular materials as per ASTM D4253 (ASTM 2016a), without adopting the surcharge. The mixture particulate rubber-sand mixture with 50% rubber is thoroughly mixed and filled into the mould before placing the base plate on top of the mould. The entire setup is fixed on the vibratory table to apply vibration for 8 minutes. The images of the sample after application of the vibration are shown in Figure 3.10. It is observed from the figure that the mixture is not segregated unlike reported in past studies with tire chips and tire shreds mixed with sand. This may be explained using maximum particle size ratio which is defined as the ratio of the maximum size of rubber to that of sand particles. It can be noted that the chances of segregation of mixtures increase with the increase in maximum particle size ratio (Kim and Santamarina 2008). For example the sand and rubber in the mixtures which has the maximum particle size ratio of unity. On the other hand the tire chips and tire shreds mixed with sand possess the size ratio in the range of 25 to 150.

Figure 3.10: Segregation analysis: sample after the test

3.5 SUMMARY

The most reliable technique to determine the maximum density of cohesionless material is vibratory table method. Many researchers have used this technique to determine the density of the rubber mixtures since the mixture does not show cohesion. However, the surcharge of 13.8kPa as per ASTM D4253 (ASTM 2016a) to be adopted for the test is only for the sandy soil. The surcharge of 13.8kPa may not be adequate for the particulate rubber mixed with sand. Further, the mixture matrix rebound to some level while the removal of surcharge. Hence, the vibratory table tests is decided to carried out with increase in surcharge and the maximum density is determined with and after removal of the surcharge. The density of the mixtures is also examined using Proctor and mini compaction to observe any difference of results from vibratory table method. It is found that the unit weight of particulate rubber-sand mixtures obtained from vibratory table method is influenced by various factors such as the vibration absorbent nature of rubber, rebounding of mixtures after removal of surcharge, and inadequate surcharge. Further, the vibratory table method is found non suitable for particulate rubber-fly ash mixtures due to the fly ash ejection through the gap between the mould and the surcharge base plate. The unit weight of the mixtures obtained with compaction method is observed to be more than that of the vibratory table method. Further, the segregation tests on mixture have shown that the particulate rubber-sand mixtures do not segregate unlike tire chips-sand mixtures with higher rubber content.

CHAPTER 4

SHEAR STRENGTH OF THE MIXTURES

4.1 INTRODUCTION

The present chapter discusses the static behaviour of the mixtures examined using direct shear tests and triaxial tests. The shear strength of the particulate rubber-sand mixtures and particulate rubber-fly ash mixtures is presented. The test results are supported with the micro-structural study. In addition, triaxial tests are carried out to examine the undrained behaviour of particulate rubber-sand mixtures and particulate rubber-fly ash mixtures. Further, the usage of mixtures in the field would experience two types of interfaces; one is between structures and the mixture and the other is between soil and the mixture. Therefore, the interface behaviour of mixtures with concrete and sand interface is examined using interface direct shear tests for different initial relative density. A new sample preparation technique for soil-mixture interface behaviour is also discussed.

4.2 SHEAR STRENGTH AND VOLUMETRIC BEHAVIOUR OF THE MIXTURES

Direct shear tests are carried out to examine the shear strength and volumetric behaviour of the mixtures. A certain quantity of each mixture is prepared by thoroughly mixing the materials based on their gravimetric proportions and then stored separately in an airtight bag for further tests. The samples are prepared using under-compaction method developed by Ladd (1978). The weight of the sample required for direct shear tests is calculated based on the required dry unit weight and the volume of the sample (60 mm X 60 mm X 30 mm) to be prepared. The particular mixture is then divided into five equal parts which are required to prepare the sample in five layers, each part is poured into the direct shear box from zero drop height and the desired dry unit weight is achieved with adequate tamping. The number of tamping given to each layer is increased in equal amount to achieve the uniform dry unit weight of the sample. Before placing another layer into the box, the top surface of the previous layers is scarified to have the better bonding between the subsequent layers.

The sample of size 60 mm X 60 mm X 30 mm and strain rate of 0.625 mm/min is adopted in the direct shear tests. The mixtures are examined with the initial relative density of 85%. The normal pressure of 50, 100, 150kPa is adopted for the tests. It is to be noted that the relative density adopted for the tests is initial relative density. However, the unit weight of the mixture samples increases due to the application of effective normal pressure which is the unit weight before shearing. The unit weight before shearing of the sample is also calculated by measuring the settlement of mixture due to the effective normal pressure.

The variation of stress ratio (τ/σ') with respect to the horizontal displacement of particulate rubber-sand mixtures and rubber-fly ash mixtures at 85% RD subjected to 100 kPa effective normal pressure is shown in Figure 4.1. The figure shows that the shear strength of pure sand and pure fly ash increases at low horizontal displacement followed by a reduction to ultimate shear strength, the behavior commonly termed as work-softening (Holtz et al. 2011). On the other hand, pure rubber in general exhibit work-hardening behavior where the shear strength increases with an increase in the horizontal displacement (Dixit and Dixit 2015). Hence it can be concluded that, as rubber content increases, the mixture transforms from a work-softening material towards work-hardening one. In addition, it is also noted that the horizontal displacement corresponds to the peak shear stress increase with the rubber content for both the mixtures. Mashiri et al. (2015) also reported similar behavior for tire chips-sand mixtures. Moreover, as in the case of particulate rubber-sand mixture, particulate rubber-fly ash mixture also behaves as ductile material when the rubber content is more than 30% with a little work-softening at large horizontal displacement. A similar observation is also noted for all the different effective normal pressures.

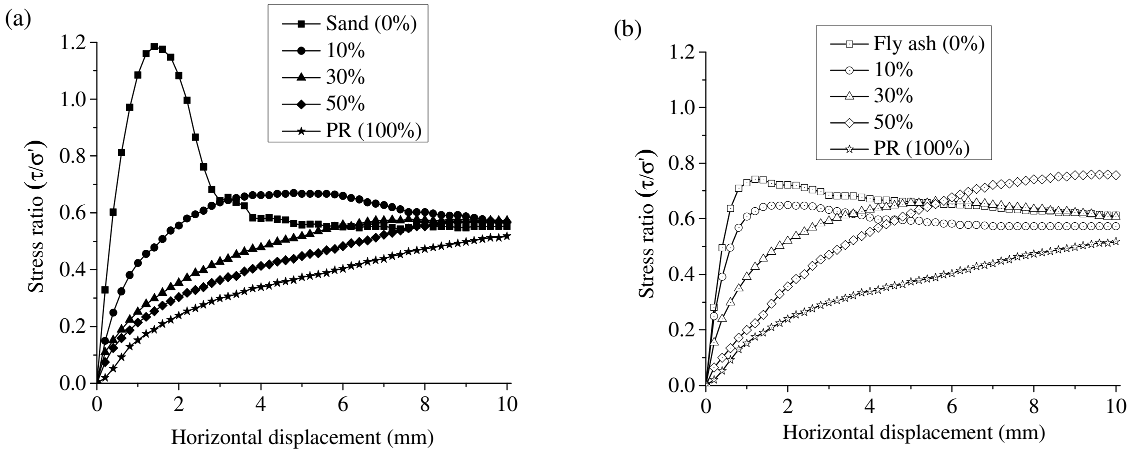

Figure 4.1: Stress-horizontal displacement variation of (a) particulate rubber-sand mixture and (b) particulate rubber-fly ash mixture at 85% RD subjected to σ' of 100kPa

Figure 4.2 plots the variation of the volumetric strain of particulate rubber-sand mixtures and particulate rubber-fly ash mixtures with horizontal displacement for the samples prepared at 85% RD subjected to 100 kPa effective normal pressure. The figure shows that the sand and the fly ash exhibit initial compression followed by dilation until it attains the constant volume. It is due to the denser arrangement of sand particles at which the particles roll over each other during the loading (Wood 2009). However, pure rubber shows entirely compressive nature during the loading.

It is further evident from Figure 4.2 that the increase in rubber content changes the behavior from dilative to a compressive one. Similar observations can be found in previously published literature on particulate rubber, tire crumb and tire chips mixed with sand (Rao and Dutta 2006; Youwai and Bergado 2003; Ghazavi 2004; Mashiri et al. 2015; Anbazhagan et al. 2016). As in the case of pure sand, figure shows that particulate rubber-sand mixture with 10% rubber exhibit dilation with increase in initial compression. However, other two mixtures, i.e., mixture having 30% and 50% rubber content, show complete compressive behavior. As observed in the case of particulate rubber-sand mixtures, addition of rubber to fly ash decreases the dilation intensity of fly ash. Unlike particulate rubber-sand mixtures, compressibility of particulate rubber-fly ash mixtures is constantly lower for all the three percentage of mixtures (i.e., 10, 30, and 50%). These three particulate rubber-fly ash mixtures show initially compression, as like as fly ash, followed by dilation. The initial compression of these mixtures increases with increase in the rubber content. In addition, the horizontal displacement at which the transition occurs, i.e., compression to dilation, increases with the increase in the rubber content. A similar observation is also noted for all the different effective normal pressures.

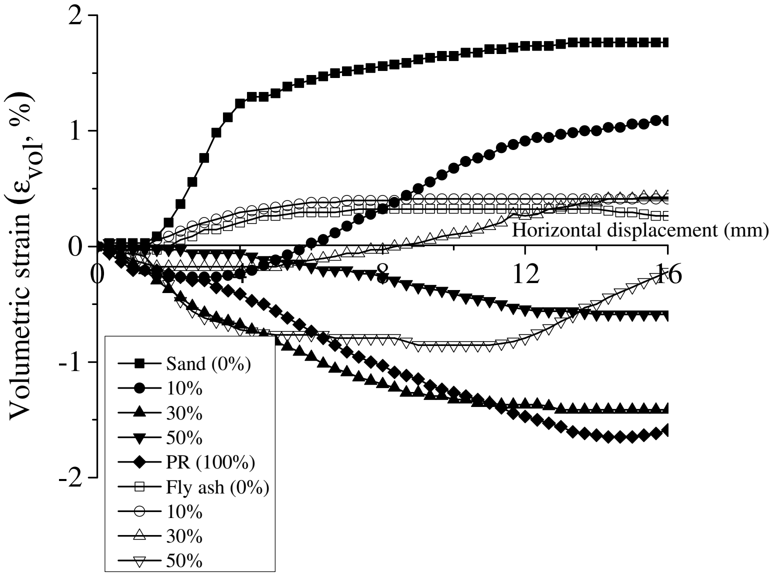

Figure 4.2: Volumetric strain variation of mixtures at 85% RD subjected to σ' of 100kPa

Figure 4.3a and 4.3b show the variation of peak shear stress and ultimate shear stress of particulate rubber-sand mixtures and particulate rubber-fly ash mixtures respectively with rubber content for the samples prepared at 85% RD, subjected to three different effective normal pressures. Figure 4.3a shows that the peak shear stress of both the mixtures is reduced with the increase in rubber content. Further, particulate rubber-fly ash mixtures possess the higher peak shear strength than rubber-sand mixtures when the rubber content is greater than 10% in the mixtures. In addition, it can be evident from Figure 4.3b that the ultimate shear strength of both particulate rubber-sand mixtures and particulate rubber-fly ash mixtures increases initially up to certain rubber content followed by a reduction. Further, the ultimate shear strength of particulate rubber-fly ash mixtures is observed to be more than particulate rubber-sand mixtures for all the rubber content. The average increase in peak and ultimate shear strength of particulate rubber-fly ash mixtures is observed to be 20% more than that of particulate rubber-sand mixtures for the effective normal pressures considered in this study.

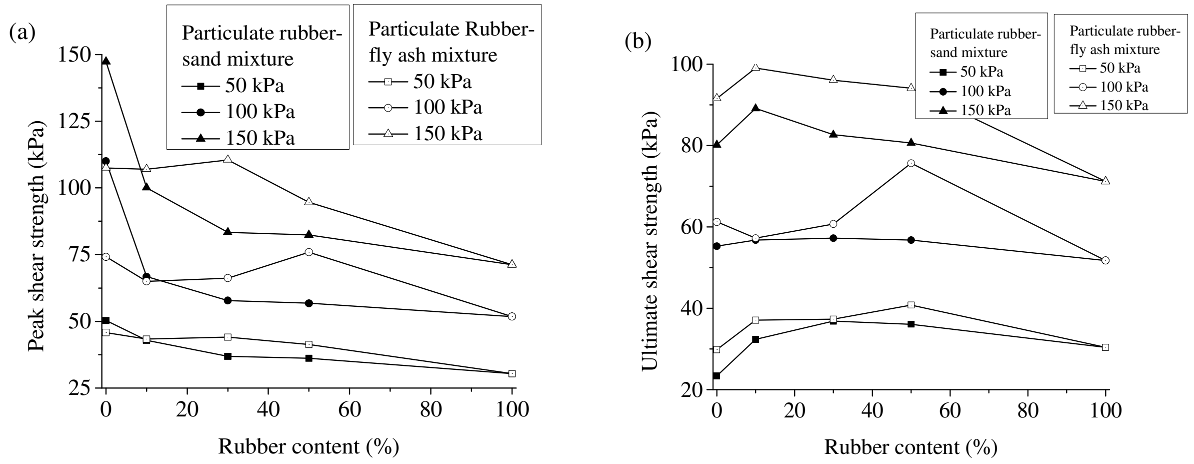

Figure 4.3: Variation of (a) peak and (b) ultimate shear strength of mixtures with rubber content at 85% RD

Figure 4.4 plots the variation of peak effective friction angle (ϕ'_p) and ultimate effective friction angle (ϕ'_{ul}) of particulate rubber-sand mixtures and particulate rubber-fly ash mixtures with rubber content for the samples prepared at 85% RD. It is apparent from the figure that the peak effective friction angle of particulate rubber-sand mixtures and particulate rubber-fly ash mixtures reduces as the rubber content increase in the mixtures. However, the ultimate effective friction angle of the particulate rubber-sand mixtures and particulate rubber-fly ash mixture increases with the addition of rubber content up to certain percentage followed by a reduction. Wood (2009) suggested that the ultimate effective friction angle has to be considered over peak effective friction angle for a reliable design strength parameter. In view of that, more emphasize is given on the ultimate shear strength and ultimate effective friction angle in the present study. The optimum rubber content at which the higher ultimate effective friction angle exists is in between 10% to 50% for both the mixtures. It is further noted that the ultimate effective friction angle of particulate rubber-fly ash mixtures is more than that of particulate rubber-sand mixtures. In addition, it can also be seen that the peak and ultimate effective friction angle of particulate rubber-sand mixtures and particulate rubber-fly ash mixtures matches when the rubber content is more than 30% and 50% respectively. It clearly shows that the dilation angle (Bolton 1986) of particulate rubber-sand mixtures and particulate rubber-fly ash mixtures is zero when rubber content is more than 30% and 50% respectively. Further, it is evident from the figure that the ultimate and peak effective friction angle of particulate rubber-fly ash mixtures is more than the peak effective friction angle of particulate rubber-sand mixtures when rubber content is more than 10%.

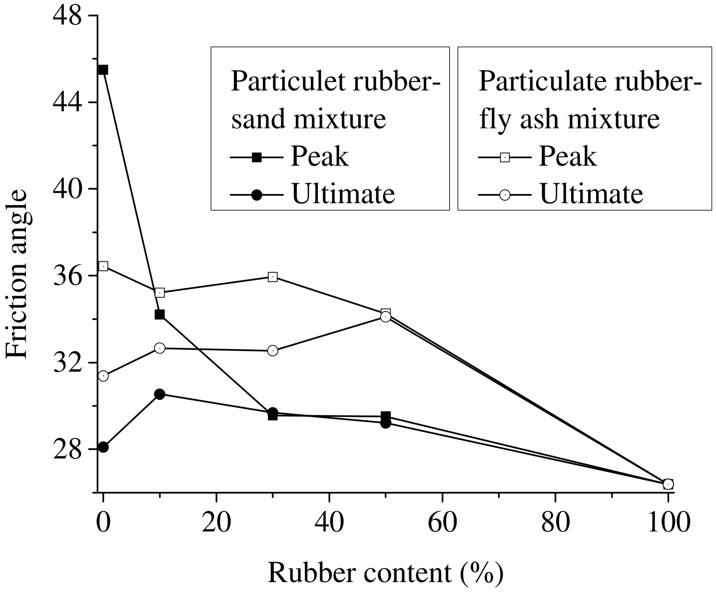

Figure 4.4: Variation of ϕ'_p and ϕ'_{ul} of mixtures with rubber content at 85% RD

The friction angle observed from the literature for Particulate Rubber (PR), Tire Crumb (TC), Tire Chips (TCh) and Tire Shreds (TS) mixed with sand is presented in Figure 4.5 along with the results of present study. Despite the variation of the unit weight of tested samples in different study, it is evident from the figure that the friction angle decreases with an increase in the rubber content for particulate rubber and tire crumbs. However, the friction angle of mixtures having tire chips and tire shreds is observed to be increased with an increase in rubber content. It is evident from the figure that the friction angles of particulate rubber-sand mixtures observed from Cabalar (2011) is higher than that of the present study. It is due to the unit weight of the mixture samples which is more than that of the present study.

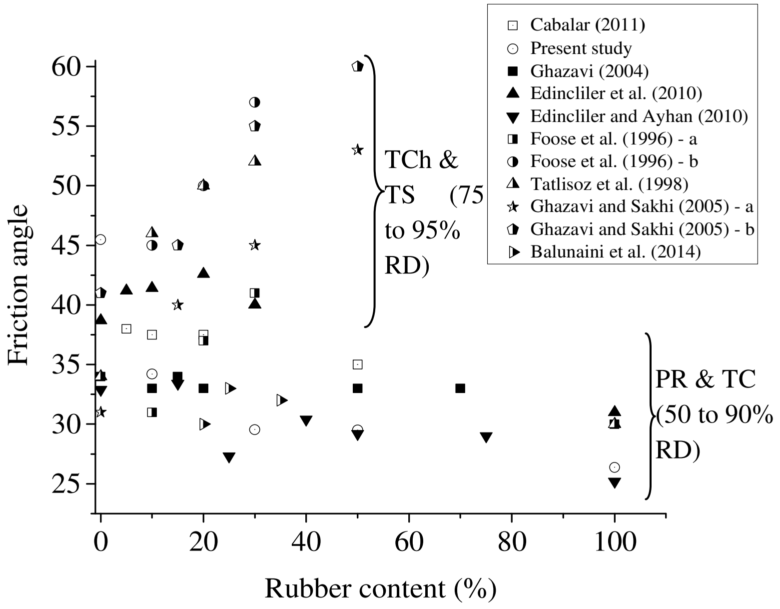

Figure 4.5: Variation of friction angle with rubber content

4.2.1 Shear Stiffness of the Mixtures

Initial and ultimate shear stiffness of particulate rubber-sand mixtures and particulate rubber-fly ash mixtures measured at 85% RD subjected to three different effective normal pressures are shown in Figure 4.6a and 4.6b respectively. The initial stiffness and ultimate stiffness of the mixtures are computed from the slopes of the initial portion and the line connecting the origin to the ultimate point of the stress-horizontal displacement plots respectively. Both the figures show that the stiffness decreases with an increase in rubber content in the mixtures. It can be evident from Figure 4.6a that the initial stiffness of particulate rubber-fly ash mixtures is more than that of particulate rubber-sand mixtures for the different effective normal pressure considered in this study. Further, it is noted from the figure 4.6b that the ultimate stiffness of particulate rubber-fly ash mixtures is more than that of particulate rubber-sand mixtures except for the rubber content is less than 30% in particulate rubber-sand mixtures subjected to higher effective normal pressure (i.e., σ' = 150 kPa). This can be explained with the compression of mixtures due to the application effective normal pressures. The vertical deformation of particulate rubber-sand mixtures with rubber content for the samples at 85% RD when subjected to different effective normal pressure is shown in Figure 4.7. Figure indicates that the deformation of mixtures increases with an increase in the effective normal pressure and it is higher for σ' = 150 kPa. Therefore, the compression of rubber in the mixtures at σ' = 150 kPa increases the contact between the sand grains resulting in the increase of stiffness. However, at higher rubber content (i.e., >30%), the contact between the sand is suppressed in rubber and hence the ultimate stiffness of particulate rubber-sand mixtures is observed to be lower than that of particulate rubber-fly ash mixtures.

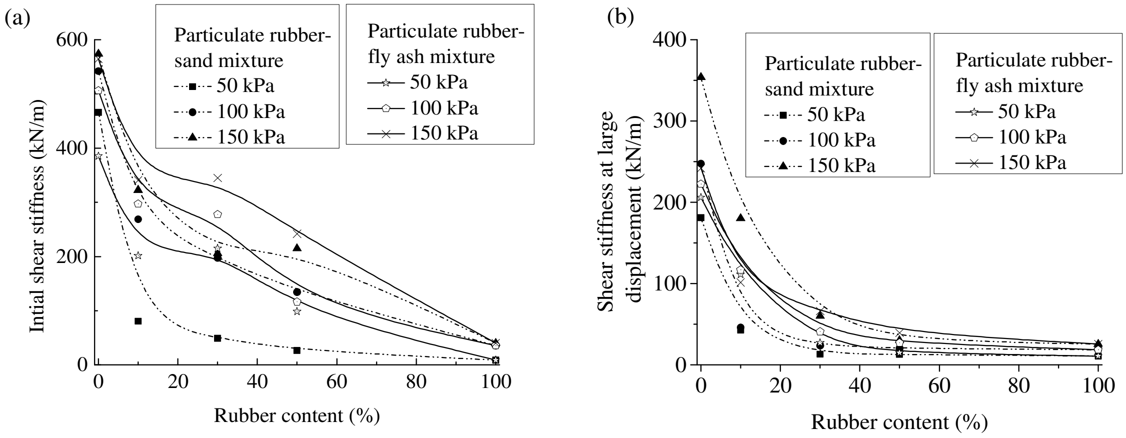

Figure 4.6: Variation of (a) initial shear stiffness and (b) ultimate shear stiffness of mixtures with rubber content at 85% RD

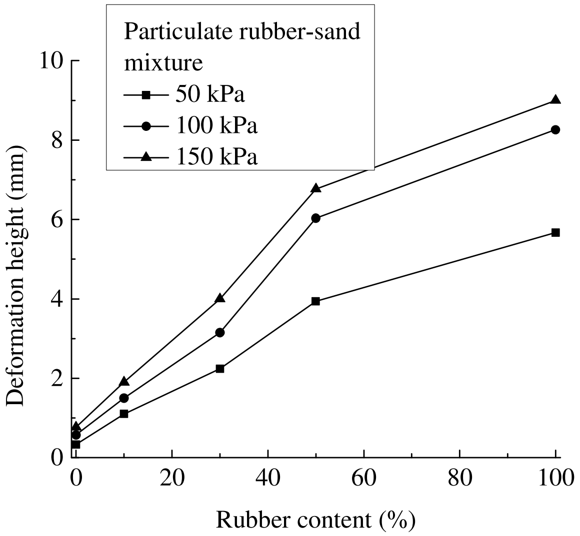

Figure 4.7: Influence of σ' on the deformation height of sample with rubber content at 85% RD

4.3 MICROSTRUCTURE STUDY

4.3.1 Scanning Electron Microscope (SEM)

The particulate form of the samples is used for the microstructure study of mixtures with the help of Quanta 400 available at scanning electron microscope laboratory of Indian Institute of Technology Madras. The samples are placed on the carbon tape which is pasted on the stub. The SEM sample prepared for the imaging is shown in Figure 4.8.

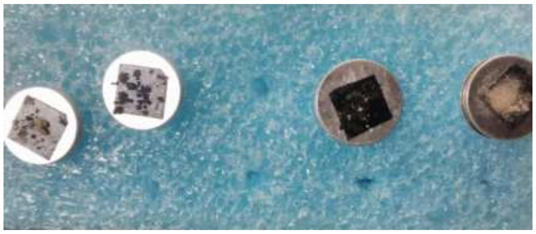

Figure 4.8: Prepared sample for SEM

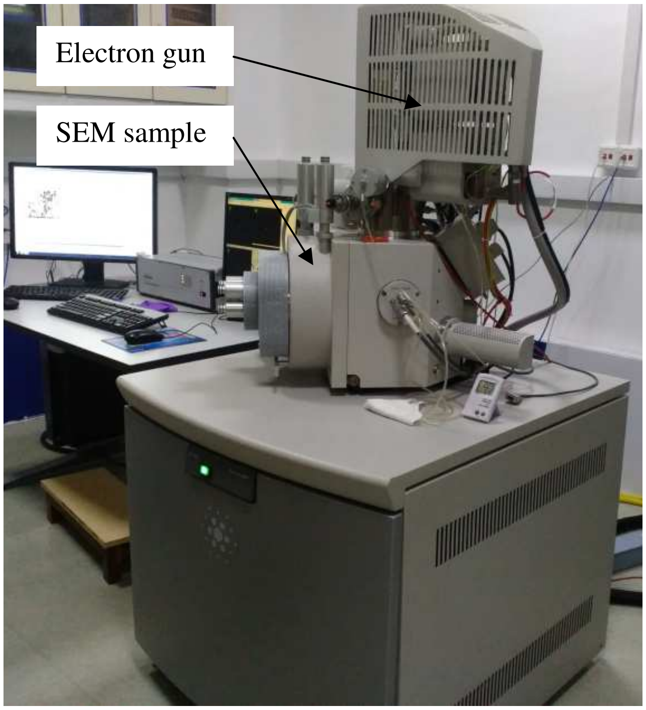

Figure 4.9: SEM

A gold coating has been given to the samples prior to the imaging process in order to avoid the charge accumulation on the non-conductive particles. These samples are placed in Quanta 400 (Figure 4.9) for imaging and energy dispersive X-ray analysis (EDXA).

The microstructure study of rubber and its mixtures are carried out with scanning electron micrograph (SEM) to substantiate the tests results of maximum dry unit weight and shear strength.

4.3.2 Image Analysis

Figure 4.10a to 4.10d shows the typical images of particulate rubber, particulate rubber-sand mixture, particulate rubber mixed with sand and fly ash, and particulate rubber-fly ash mixture respectively obtained using SEM. It is evident from Figure 4.10a that the particulate rubber used in this study has the highly irregular surface with significantly large specific surface area resulting in increase of inter-particle friction. Further, Figure 4.10a indicates that the surface of the particles possesses tiny voids which can be easily filled by fly ash particles rather than sand particles (refer Figure 4.10c and 4.10d). It is also evident from figure 4.10b that the contact of rubber with sand is relatively less while Figure 4.10c 4.10d depicts that the fly ash has contact over the full surface of rubber (In Figure 4.10c the elliptical mark is the particulate rubber covered by fly ash). Further, it can be stated that these increase in inter-particle contacts ensure the segregation resistance of fly ash mixtures containing higher rubber content. In general, the microstructure study reveals that the large amount of voids present in the higher rubber content (>30%) mixture matrix can be filled by smaller fly ash particles rather than sand particles. Hence, the unit weight of rubber-fly ash mixture is higher than rubber-sand mixture when the rubber content in the mixture is more than 30%. Furthermore, the increase in the shear strength of rubber-fly ash mixture over rubber-sand mixture is due to the higher inter-particles contact between rubber and fly ash.

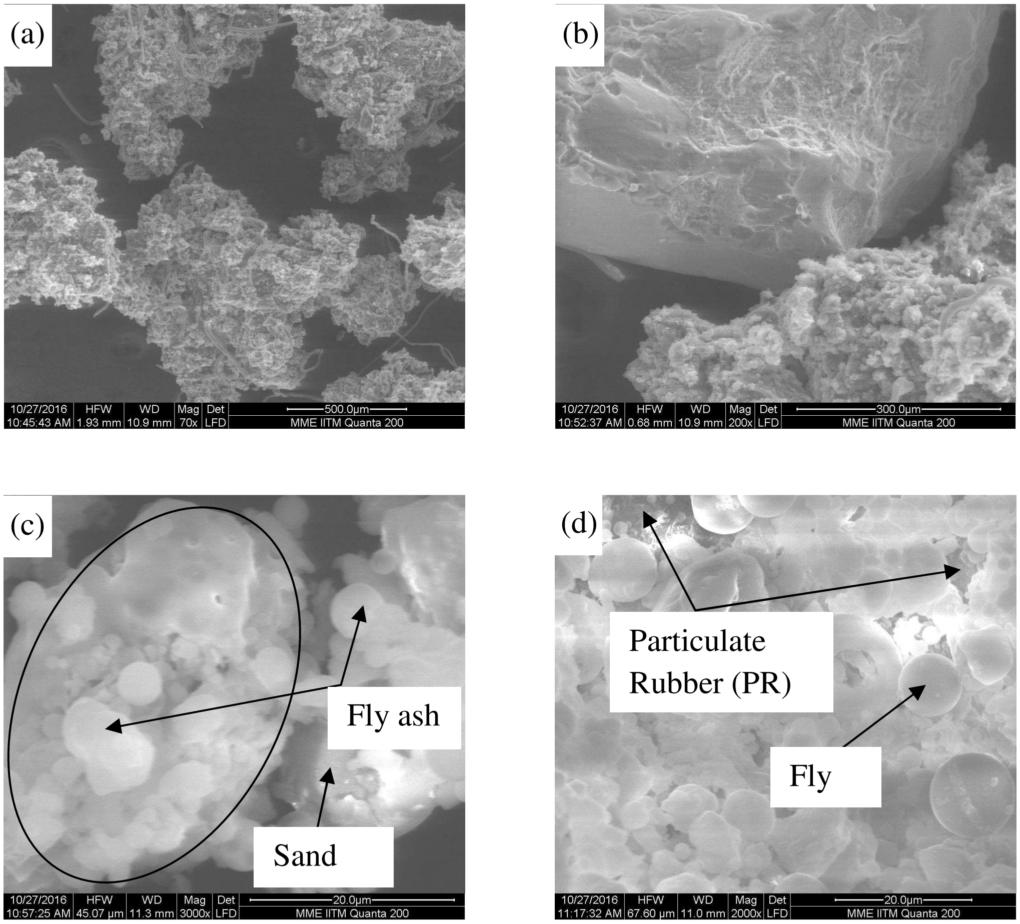

Figure 4.10: Typical SEM images of (a) particulate rubber, (b) particulate rubber-sand mixture, (c) particulate rubber mixed with sand and fly ash, and (d) particulate rubber-fly ash mixture

4.4 UNDRAINED BEHAVIOUR OF THE MIXTURES

The strain-controlled automated triaxial testing system (Make: VJ Tech, UK) used for the undrained triaxial testing of mixtures is shown in Figure 4.11. During the various stages of testing, the cell pressure and the backpressure are applied with help of the hydraulic system present inside the corresponding pressure volume controllers. The backpressure volume controller is also used to measure the volume changes of the sample during the consolidation stage. The axial load on the samples is measured with 10 kN load cell and the axial deformations are measured with 20 mm Linear Variable Differential Transducer (LVDT). The sample preparation and tests procedure are discussed in detail under the cyclic triaxial testing of the mixtures (Chapter 5). The triaxial samples prepared at 75% initial density is tested under the effective confining pressure of 100kPa. The strain rate 0.5mm/min is adopted for all the mixtures since it is highly permeable.

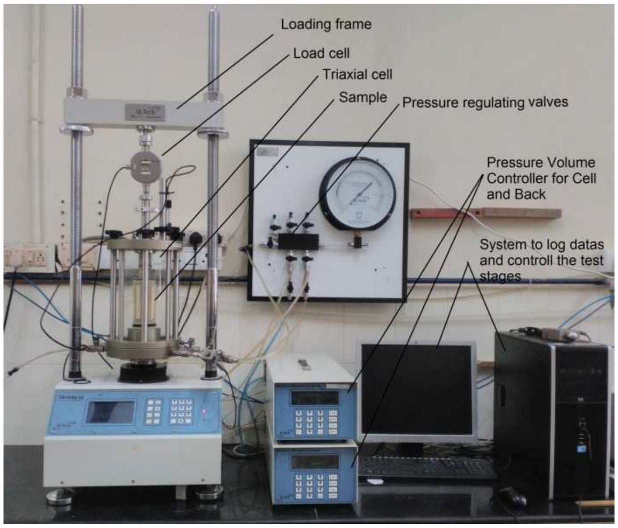

Figure 4.11: Triaxial tests setup

4.4.1 Stress-Strain Behaviour

The stress-strain plot of particulate rubber-sand mixtures and particulate rubber-fly ash mixtures is shown in Figure 4.12. The undrained shear strength of particulate rubber-sand mixtures is reduced with an increase in the rubber content. The particulate rubber-sand mixtures show a peak shear strength at very high axial strain (>15%) followed by a reduction. The undrained shear strength of particulate rubber-fly ash mixtures is increased with increase in the rubber content. The particulate rubber-fly ash mixture with 30% rubber content shows the shear strength equal to the particulate rubber-sand mixture with 10% rubber content. Further, the shear strength of particulate rubber-fly ash mixtures with 50% rubber content is observed to be more than that of any mixtures. The particulate rubber-sand mixtures show strain hardening up to a large strain (>15%) followed by a little reduction. However, the particulate rubber-fly ash mixtures, even at large strain, show only the strain hardening without any softening.

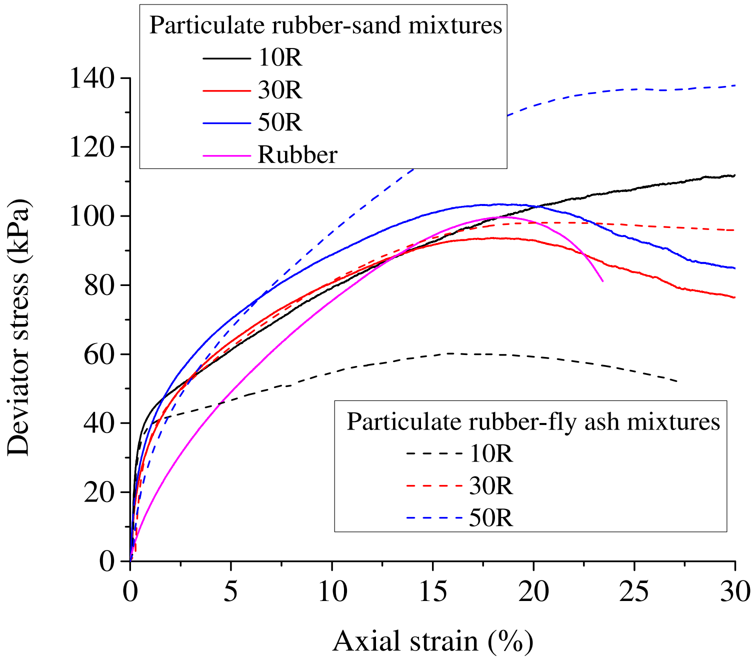

Figure 4.12: Stress-strain plot of mixtures (50% relative density and σ'_c=100kPa)

4.4.2 Pore Water Pressure Variation

The variation of pore water pressure with respect to axial strain is shown in Figure 4.13. The positive static pore water pressure of mixtures is observed to attain a peak followed by a reduction to a constant value. The pore pressure is decreased with increase in the rubber content. At-large strain, the pore pressure of particulate rubber-sand mixture with 10% rubber content is less than that of 30% and 50% mixtures. The 10% mixture shows sand like behaviour and hence the reduction is attributed to the dilative tendency of the mixture. As observed in the case of particulate rubber-sand mixtures, particulate rubber-fly ash mixtures also show the reduction in the pore pressure with an increase in the rubber content. Further, the pore pressure of particulate rubber-fly ash mixtures is more than that of the particulate rubber-sand mixtures.

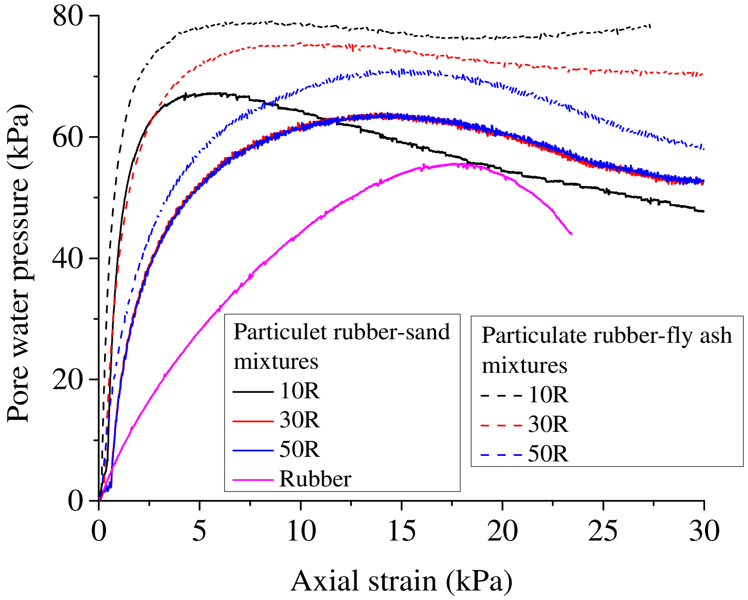

Figure 4.13: Pore water pressure variation of the mixtures (50% relative density and σ'$_c$=100kPa)

4.4.3 Stress Path

The stress path of particulate rubber-sand mixtures and particulate rubber-fly ash mixtures is shown in Figure 4.14. It is observed from the figure that the mean effective stress of all the mixtures decreases with increase in the deviator stress. It is due to the development of positive pore water pressure. The particulate rubber-sand mixture with 10% rubber is experienced the stress path reversal. It shows the dilative tendency of the mixtures. However, the particulate rubber-sand mixtures having rubber content greater than 10% is not shown any reversal rather a reduction in deviator stress due to post-peak softening at large strain (refer Figure 4.12). The particulate rubber-fly ash mixtures are shown the stress path reversal after experiencing the reduction in mean effective confining pressure. It is also observed that the amount of reduction in mean effective pressure is reduced with the increase in the rubber content.

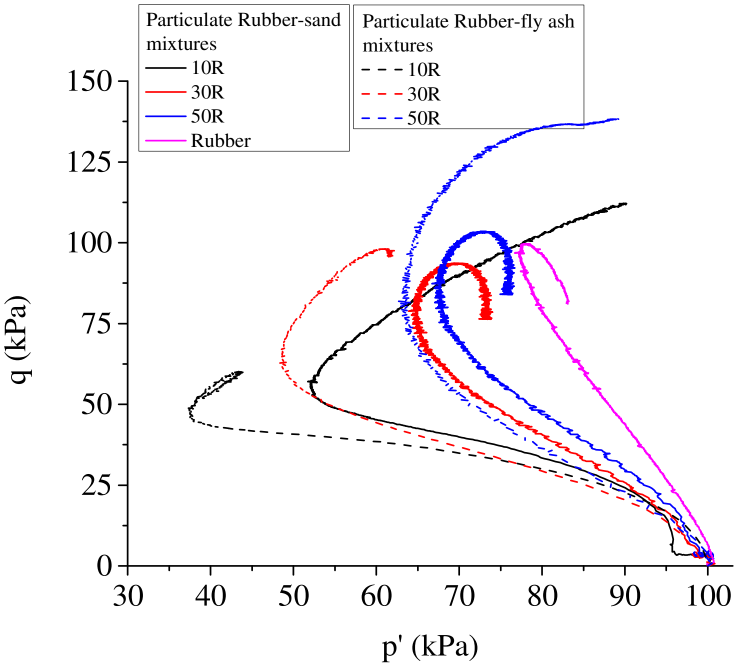

Figure 4.14: Stress path of the mixtures (50% relative density and σ'_c=100kPa)

4.4.4 Particulate Rubber-Sand-Fly Ash Mixtures

In this section, a particular mixture i.e., 50% rubber mixed with 50% sand is examined for the progressive replacement of sand with fly ash to identify an optimum mix proportion. The test results of two materials such as sand and rubber and four mixtures such as 50% rubber+50% sand, 50% rubber+40% sand+10% fly ash, 50% rubber+20% sand+30% fly ash, and 50% rubber+50% fly ash is discussed.

The plot of deviator stress versus axial strain for pure sand, particulate rubber, and particulate rubber-sand-fly ash mixtures is shown in Figure 4.15a and for clarity, only particulate rubber and particulate rubber-sand-fly ash mixtures are shown in Figure 4.15b. It is evident from Figure 4.15a that the sand gains strength with increase in the axial strain up to 8% followed by a reduction to a critical state. However, rubber and other mixtures show the increase in strength with increase in axial strain up to 20% without showing any post-peak softening. Until then, failure is not observed in the sample. It is interesting to note that the 1/3rd of the maximum strength of all the mixtures is attained at an axial strain less than 3%. It is evident from figure

4.15b that the deviator stress at particular axial strain increases with increase in the replacement of sand in the mixtures by fly ash.

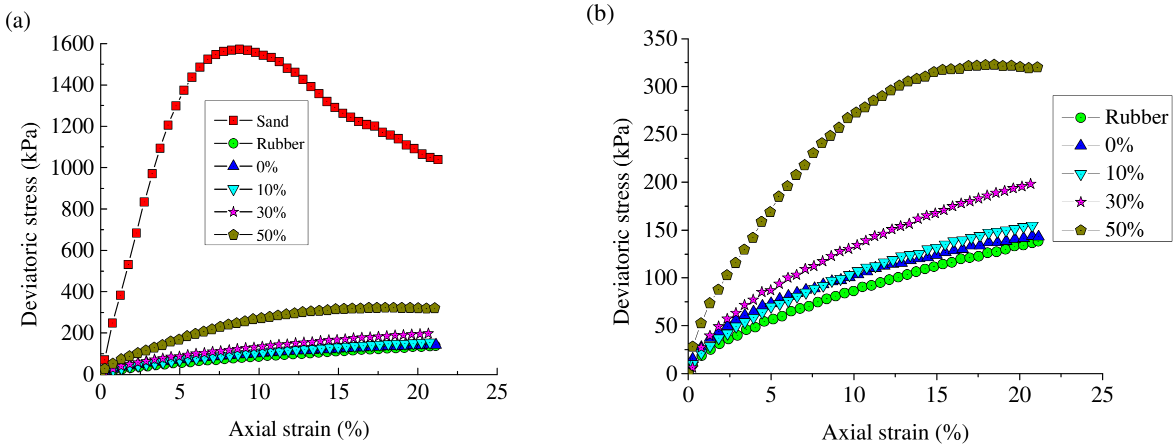

Figure 4.15: Variation of deviator stress with axial strain obtained from the triaxial tests (a) sand, rubber, and mixtures and (b) rubber and mixtures

The influence of fly ash on the shear strength of the particulate rubber-sand mixture is analyzed in terms of normalized maximum deviator stress, i.e., the maximum deviator stress of the mixtures divided by the maximum deviator stress of the sand and rubber. The variation of the normalized maximum deviator stress with respect to the fly ash percentage is shown in Figure 4.16. It is evident from Figure 4.16 that the normalized maximum deviator stress of particulate rubber-sand mixture with rubber is almost one, which shows that there is no significant increase in the shear strength of the rubber due to the addition of 50% sand by weight to it. However, the normalized maximum deviator stress of particulate rubber-sand mixture with sand is less than 0.1, which shows the drastic decrease in the shear strength of the sand as observed by Hong et al. 2015. It is also evident from Figure 4.16 that the normalized shear strength of the particulate rubber-sand mixture increases exponentially with the increase in the replacement amount of sand by fly ash. Among all the mixtures, the particulate rubber-fly ash mixture increases the shear strength twice as much as the particulate rubber-sand mixture.

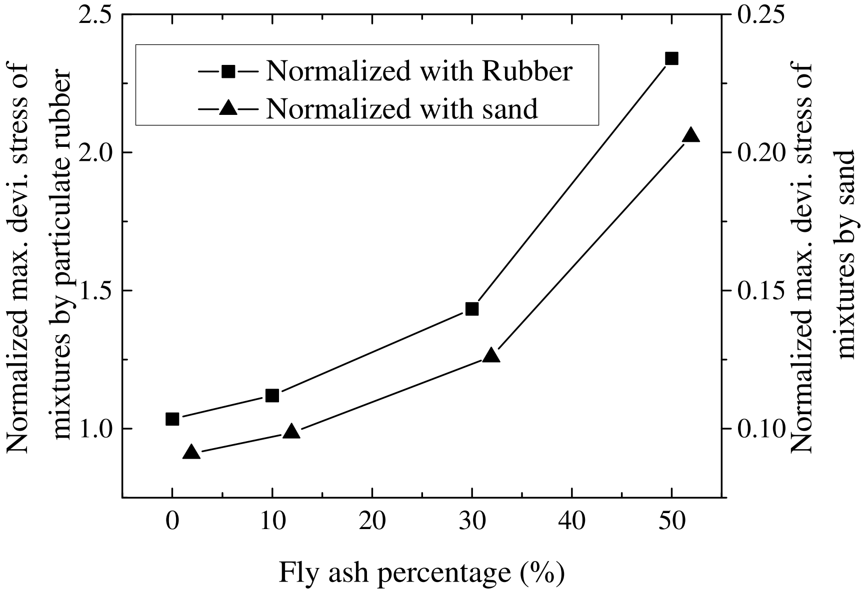

Figure 4.16: Variation of normalized maximum deviator stress with the fly ash percentage

It is observed during the triaxial test that the rubber and mixtures of rubber, sand, and fly ash regain their original shape once the load is removed. The samples are also intact, and there is no shear failure until the end of the test. However, the sand sample fails at the low axial strain. This observation clearly shows that the rubber mixtures are ductile in nature and can be subjected to reloading, but the sand samples are brittle in nature and not possible to reload once it fails. This observation also shows that the residual deformation is zero for mixtures due to its elastic behaviour and for sand it is significant. This residual deformation of the mixtures is expected to be less than the sand in case of dynamic loading. Though the sand has higher shear strength than the mixture, it will show instability due to the irrecoverable residual deformation, which is the main governing factor in earthquake analysis. Further, it is understood that the material, which possesses lesser residual deformation, always preferred for performance-based design (Priestley 2000). Hence, the rubber mixture especially particulate rubber-fly ash mixture, which possesses increased shear strength than rubber-sand mixture without compromising the elastic behaviour, can utilize for earthquake geotechnical engineering applications such as base isolation for low-rise buildings, lightly loaded foundations, etc.

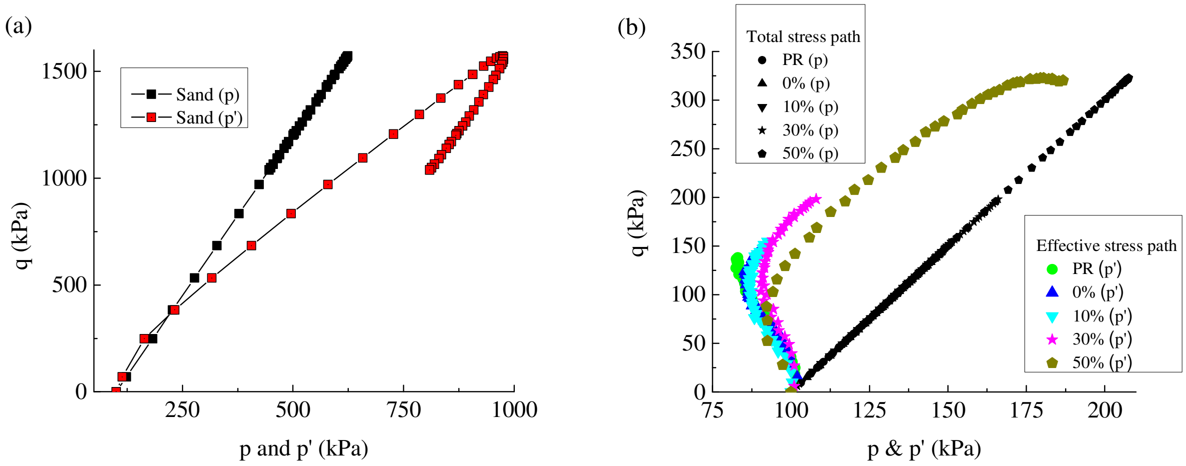

Figure 4.17: Variation of deviatoric stress (q’) with the total and effective mean stress (p and p’) (a) sand and (b) particulate rubber and mixtures

Variation of deviatoric stress (q’) with respect to total and effective mean stress (p and p’) for sand is shown in Figure 4.17a and only PR and mixtures are shown in Figure 4.17b. It is evident from Figure 4.17a and 4.17b that the total stress path for all the materials and mixtures coincides and has the typical slope of 1H : 3V. The effective stress path of sand initially moves left of its origin and then moves towards the right. It is the typical stress path for dilative sand. In Figure 4.17b, the stress path of rubber and its mixtures, except for the rubber sample, initially move left of their origin and then move right at the end of the test. The mixture containing 30% and 50% fly ash moves beyond its origin of stress path i.e., 100 kPa (refer figure 4.19b). It shows that the rubber completely compresses, and other mixtures show little dilation at the end of test except for 30% and 50% fly ash samples, which shows the bulging during the test itself.

The pore water pressure variation with respect to axial strain for sand, rubber, and mixtures is shown in Figure 4.18a and only rubber and mixtures are shown in Figure 4.18b to observe the clear variations. It is evident from Figure 4.18a that the sand develops initially positive and then negative pore water pressure due to its dilatancy behaviour. However, rubber develops entirely positive pore water pressure up to the end of the test, which shows the contractive behaviour of rubber. It shows increasing trend even at the end of the test as is evident from Figure 4.18b. The mixtures show increasing positive pore water pressure with the increase in the axial strain. At the large strain, all the mixtures except for the 50% fly ash mixture attain a constant value, which clearly shows the contractive behaviour of mixtures, but little less than the pure rubber at large strain. The 50% fly ash mixture shows initially increase followed by a decrease in pore water pressure at low strains and it could even become negative at higher axial strains as it is evident from Figure 4.18b. It clearly shows that the 50% fly ash mixture (particulate rubber-fly ash mixture) changes its behaviour from contractive to dilative at low strain.

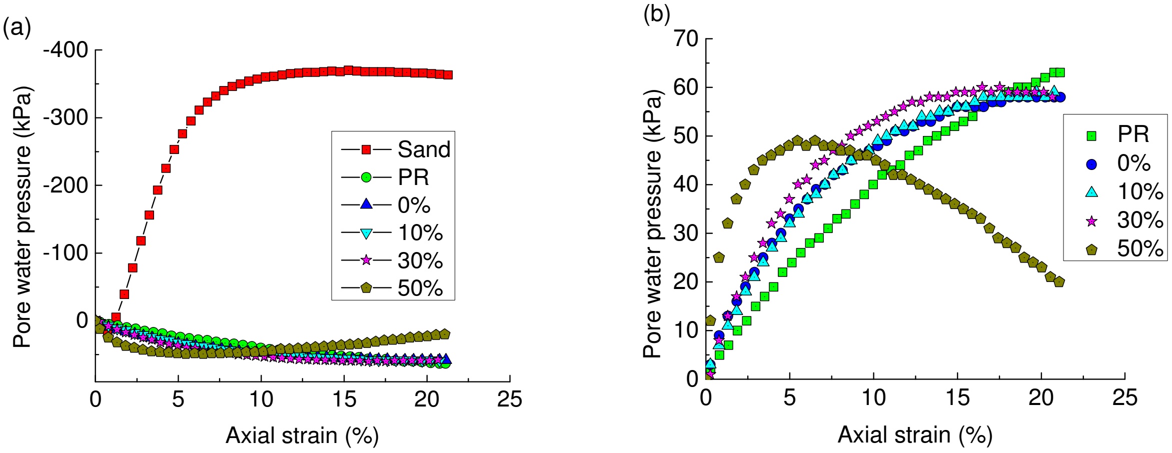

Figure 4.18: Variation of pore water pressure with axial strain (a) sand, PR, and mixtures and (b) particulate rubber and mixtures

4.5 INTERFACE SHEAR STRENGTH OF THE MIXTURES

4.5.1 Interface Direct Shear Tests

The shear box of size 60 mm x 60 mm is used for the interface direct shear testing. The size of the box used in this study is 30 times greater than that of the maximum size of the particle to be tested, which satisfies the minimum size limit of 10 as per ASTM D3080 (ASTM 2011). A concrete block of size 58 x 58 x 15 mm is used to determine the interface behaviour between concrete and particulate material.

In order to determine the interface friction between concrete and particulate material, the concrete block is always placed in the bottom half of the shear box and then the top box is assembled to prepare the sample in it. Next, to determine the interface behaviour between two different particulate materials, a separation plate of size 140mm x 65mm x 2mm is placed between the two boxes to prepare the samples. The direct shear setup used for the interface study is shown in Figure 4.19.

To prepare the sample for the concrete-particulate material interface, in the top box, the material is placed in three layers with the number of blows given to each layer is increased to achieve the uniform unit weight while the concrete block is placed in the bottom box. The top surface of each layer is scarified to have the better bonding between the layers. Preparing one sample over the other with different particulate material for sand-particulate material interface would affect the height of the sample present in the bottom box which in turn affects the density of the material.

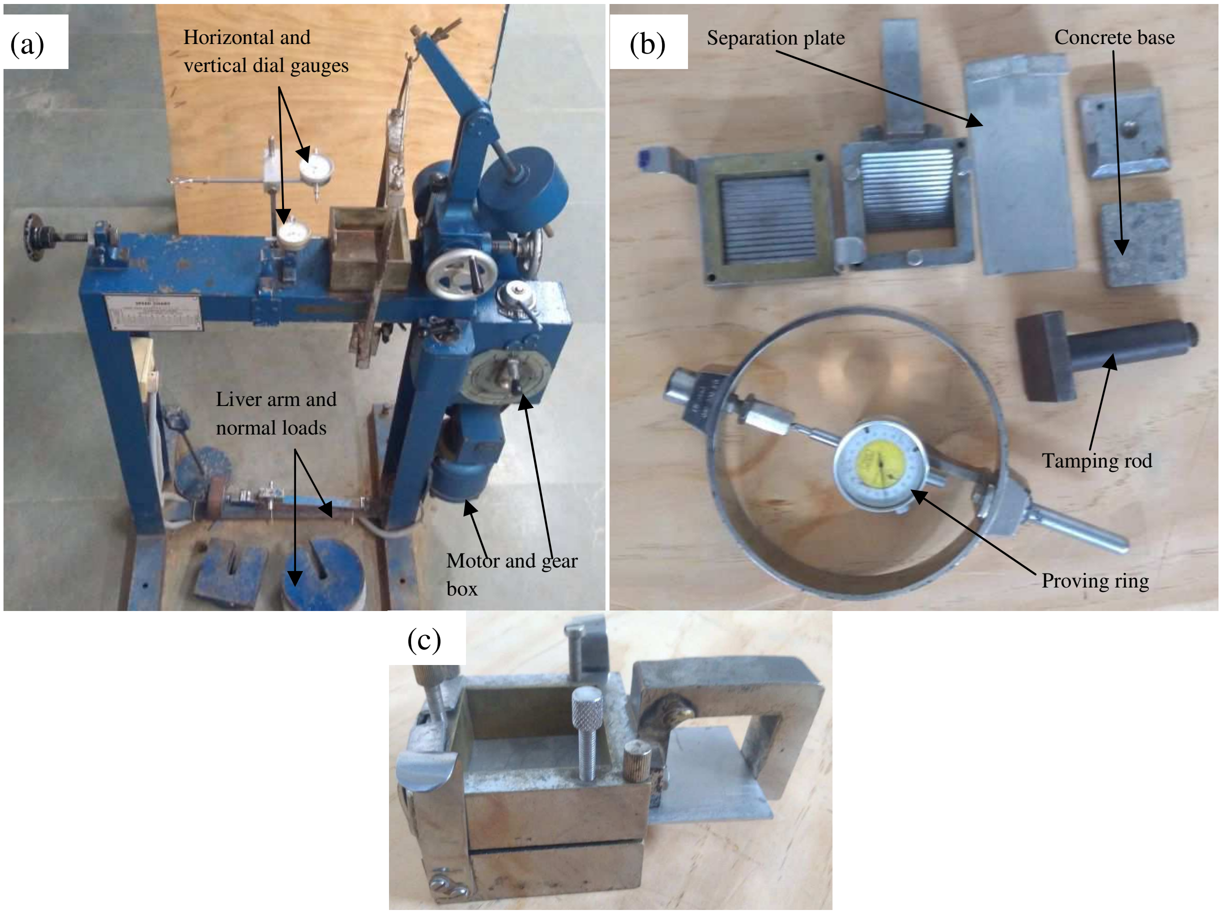

Figure 4.19: Experimental setup (a) direct shear apparatus (b) different parts used for the test (C) shear box with the separation plate

In addition, the shear plane would shift from the interface to the material within the top box. Hence a separation plate is used to prepare the sample in the top chamber without disturbing the sample in the bottom box. After preparing bottom box sample, the separation plate is placed in position (as shown in Figure 4.20) and then the top box is arranged over the separation plate. Then the particulate sample is prepared in the top box as in the bottom box, later the separation plate has been removed without disturbing the samples. It has been ensured that the samples are just in touch with the shear plane. The interface shear tests are carried out on sand, particulate rubber, particulate rubber-sand mixture and particulate rubber-fly ash mixture possessing 30% rubber. The tests are carried out with the samples prepared at three different initial relative densities such as 30, 60, and 85%. The effective normal pressure of 50, 100, and 150kPa is adopted for the interface shear tests.

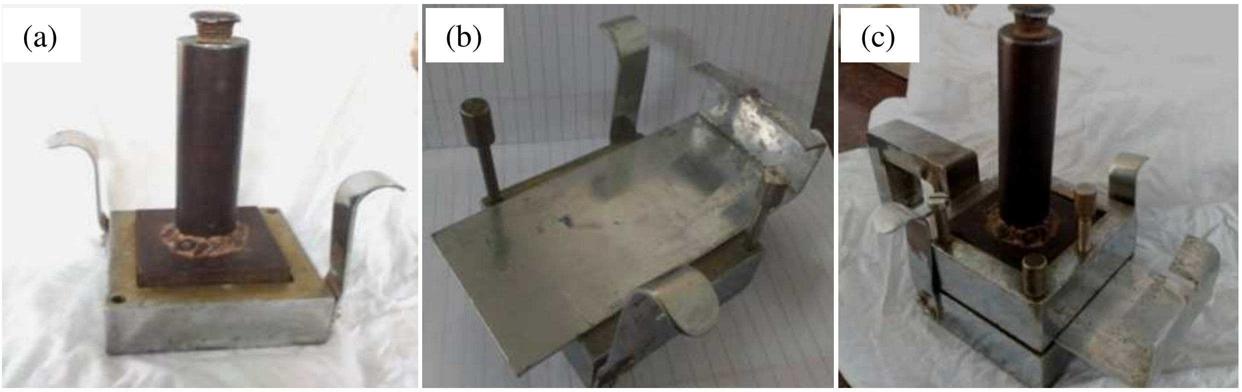

Figure 4.20: Preparation of sample with separation plate (a) preparation of sample in bottom box (b) arrangement of separation plate (c) preparation of sample in top box

The following section discusses the interface shear strength of pure particulate rubber, sand, particulate rubber-sand mixtures with 30% rubber, and particulate rubber-fly ash mixtures with 30% rubber. Two interface behavioue are examined such as concrete and sand.

Typical variation of interface shear stress with horizontal displacement for concrete-particulate materials is shown in Figure 4.21a. The figure shows that the interface shear strength of pure sand increases up to a peak followed by a reduction to the critical state. However, for pure particulate rubber, particulate rubber-sand mixture (with 30% rubber), and particulate rubber-fly ash mixture (with 30% rubber), the interface shear stress progressively increases to critical state with the increase in the horizontal displacement. A similar observation was reported by Xiao et al. (2015) for pure tire shreds. Figure 4.21a also shows that though the initial interface shear strength of rubber and mixtures are less than that of the sand, the ultimate interface shear strength of rubber and mixtures are observed to be same or more than that of sand. Moreover, it can also be seen that approximately 30% increase in interface shear strength due to the replacement of sand in the mixture (i.e., particulate rubber-sand mixture) with fly ash (i.e., particulate rubber-fly ash mixture). Furthermore, interface shear strength of rubber-sand mixture is observed to be higher than that of the interface shear strength of sand. The increase in the interface shear strength is attributed to the more number of particle interaction at the interface. Figure 4.22 shows the Scanning Electron Microscopic (SEM) image of the rubber-sand mixture and rubber-fly ash mixture. It is evident from SEM image that the replacement of sand with fly ash increases the number of particles around the rubber particles which in turn increased the interface shear strength of rubber-fly ash mixture.

Typical variation of interface shear stress with horizontal displacement for sand-particulate materials is shown in Figure 4.21b. As in Figure 4.21a, the interface shear stress of particulate rubber and particulate rubber-sand mixture monotonically increases with the increase in the horizontal displacement up to the critical state. However, for particulate rubber-fly ash mixture, the figure shows a distinct peak followed by a reduction of interface shear stress. Furthermore, particulate rubber-fly ash mixture shows higher interface shear strength than that observed for particulate rubber and rubber-sand mixture. It is also noted that particulate rubber-fly ash mixture shows approximately 18% increase in peak interface shear strength than that of particulate rubber-sand mixture.

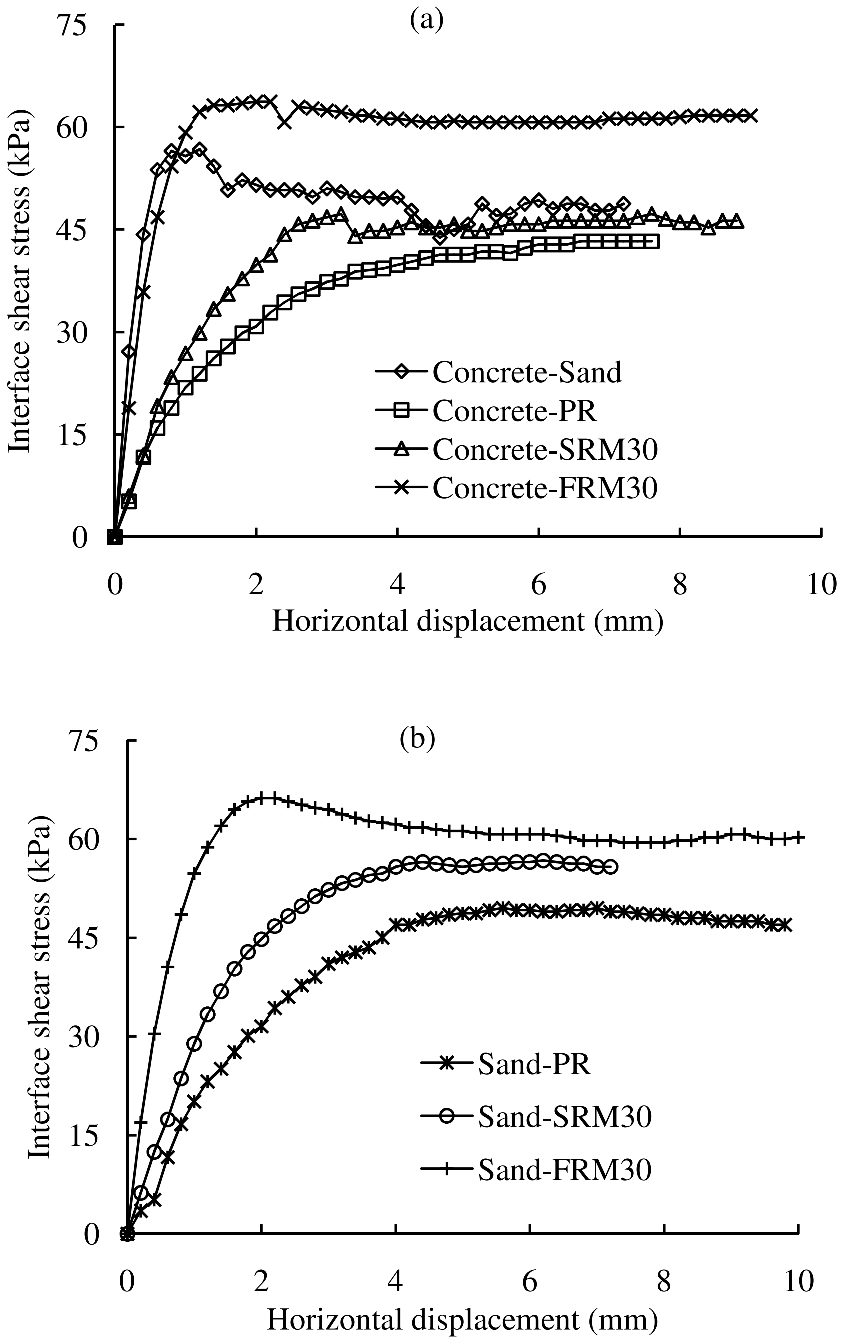

Figure 4.21: Interface shear stress versus horizontal displacement of concrete-particulate materials and sand-particulate materials (RD = 85% RD and σ' = 100 kPa, SRM30- particulate rubber-sand mixture with 30% rubber, FRM30- particulate rubber-fly ash mixture with 30% rubber)

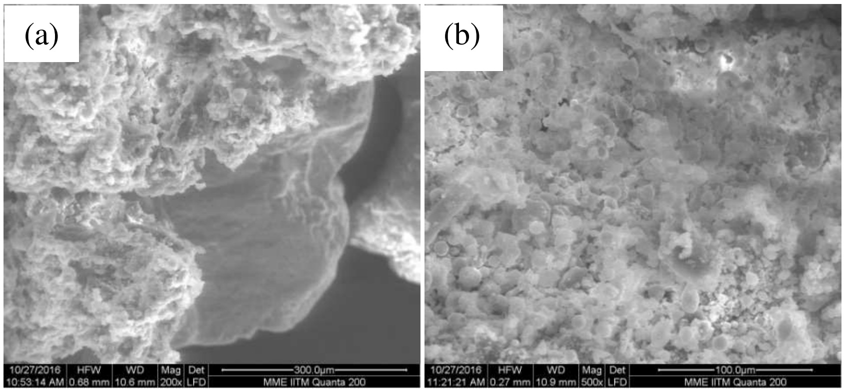

Figure 4.22: Interaction of particles in (a) particulate rubber-sand mixture (b) particulate rubber-fly ash mixture

Variation of the peak interface friction angle with the initial relative density is shown in Figure 4.23. The figure shows that there is no significant influence of initial relative density on the interface shear strength of the materials and mixtures examined in the present study except for the concrete-rubber sand mixture and concrete-rubber fly ash mixture interfaces. The concrete interface shear strength of particulate rubber-sand mixture and particulate rubber-fly ash mixture is increased with an increase in the initial relative density. Further, there is a significant increase in the interface shear strength when the concrete (i.e., rigid) interface is replaced with soil (i.e., particulate). It is also observed that the interface friction angle of sand-particulate materials is 1.5° to 3° higher than that of concrete-particulate material. In addition, concrete and sand interface friction angle (i.e., concrete and sand) of particulate rubber-fly ash mixture is observed to be higher than that of particulate rubber-sand mixture. It is due to the fact that the higher number of particle interaction at the interface.

Interface shear strength properties of large size rubber tire with different interface material as reported in the available literature are given in Table 4.1 along with the results from the present study. It is evident from the table that the particulate rubber (small size rubber) possesses lower interface shear strength than that of shredded rubber (large size rubber). In addition, the interface friction angle observed by Ghaaowd et al. (2017) for concrete-tire shreds is the lowest among the other studies. It is attributed to the lower initial unit weight of the tested samples.

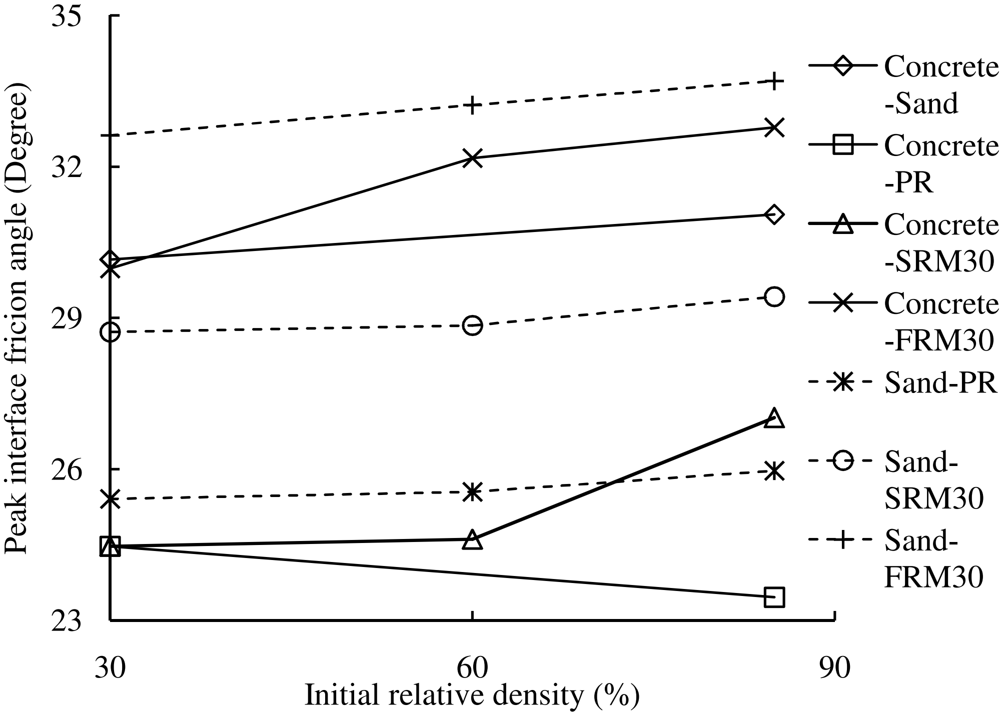

Figure 4.23: Peak interface friction angle versus initial relative density of materials and mixtures with different interfaces (SRM – PR-sand mixture and FRM – PR-fly ash mixture)

Table 4.1: Interface shear strength of pure rubber observed from different studies

Literature	Rubber tire size (mm)	Sand-rubber		Concrete-rubber	
		C (kPa)	Φ (°)	C (kPa)	Φ (°)
Gebhardt 1997*	20 to 450	2.1	33	-	-
Reddy et al. 2010	130 to 229	0.8	35.8	-	-
Xiao et at. 2015	25 to 75	6.6	39.3	6.3	35.5
Ghaaowd et al. 2017	30 to 320	-	-	-	22.9
Present study	0.425 to 2	-	25.6$^{\$}$	-	23.9$^{\$}$

*interface shear between tire shreds and glacial till

$^{\$}$friction angle determined by passing the failure envelope through the origin

4.5.2 Interface Shear Stiffness

Typical variation of the initial interface shear stiffness with the initial relative density is shown in Figure 4.24. The initial interface shear stiffness is the slope of the straight line portion of the plot between the interface shear strength and the horizontal displacement. It is evident from the figure that though the peak interface shear strength and friction angle of the sand-particulate materials is higher than that of concrete-particulate materials, the initial interface shear stiffness of sand-particulate materials is observed to be lower. It is due to the fact that the different particulate materials (i.e., interface between sand-particulate materials) have to make an initial adjustment to gain the interface shear strength. Further, it is also evident from the figure that particulate rubber-fly ash possesses higher interface shear stiffness than particulate rubber-sand mixture for concrete and sand interface.

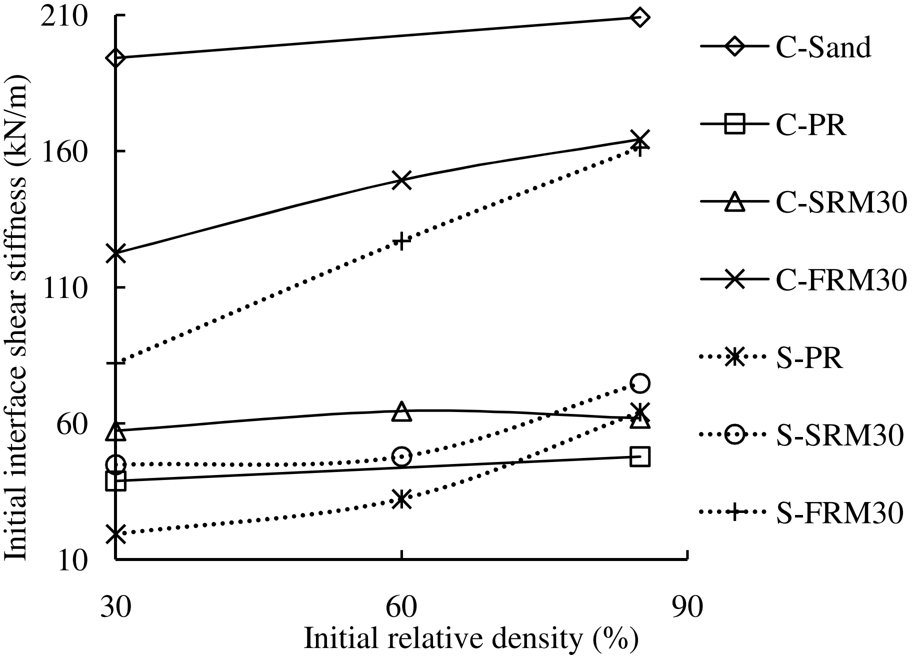

Figure 4.24: Variation of initial interface shear stiffness with initial relative density at σ’ = 50 kPa (C - Concrete and S - Sand)

4.5.3 Interface Coefficient

The interface coefficient used in this study is the ratio of peak interface friction angle to the peak friction angle of materials or mixtures. The interface coefficients of material and mixtures at different RD with different interfaces are given in Table 4.2. It is evident from the table that the interface coefficient is increased for both the interfaces due to the replacement of sand in the mixture with fly ash. In addition, as in the case of peak interface friction angle, the interface coefficient of the sand-particulate material is observed to be higher than that of concrete-particulate material.

Table 4.2: Interface coefficients of materials and mixtures

Sample in bottom box	RD (%)	Sample in top box			
		Sand	PR	Rubber-sand mixture	Rubber-fly ash mixture
Concrete	30	0.76	0.99	0.90	0.99
	60	-	-	0.82	0.96
	85	0.67	0.89	0.88	0.96
Sand	30	-	1.03	1.05	1.07
	60	-	1.0	0.96	0.99
	85	-	0.98	0.96	0.99

Interestingly, the interface coefficient is observed to decrease with an increase in the relative density. It shows that the increase in the interface friction angle with an increase in the initial relative density is lesser than that of the material friction angle. It is due to the fact that the increase in the density of the mixture increases the apparent cohesion (e.g., Ghazavi and Sakhi 2005) which in turn increases the integrity of the sample due to which the sample acts as a unit rather than the particulate material. Hence, the reduction in the interface coefficient is attributed to the reduction in the interaction of particulate material at the interface. On the other hand, the higher interface coefficient of sand-particulate material at lower initial relative density, at which the sample experience the lower integrity, is due to the more interaction between sand and mixture particle at the interface. In general, the concrete-particulate materials possess the interface coefficient of 0.85 and 0.95 for particulate rubber-sand mixture and particulate rubber-fly ash mixture respectively. However, this interface coefficient is increased to 0.95 and 1 in the case of the sand-particulate material interface due to the more interaction between sand and the particulate samples.

4.6 SUMMARY

The shear strength of particulate rubber-sand mixtures and particulate rubber-fly ash mixtures is reduced with increase in the rubber content. When the rubber content is more than 10%, particulate rubber-fly ash mixtures shows higher shear strength than that of the particulate rubber-sand mixtures. The undrained behaviour of the mixtures shows that the increase in the rubber content, in general, reduces the development of positive pore water pressure. Further, it is observed that the progressive replacement of sand with fly ash in a particular particulate rubber-sand mixture results in the increase in shear strength. The maximum shear strength increment of 100% is observed when the sand is fully replaced with fly ash (i.e., for the particulate rubber-fly ash mixture). In addition, the interface shear strength of particulate rubber-fly ash mixture is observed to be higher than that of the particulate rubber-sand mixture. Further, the mixture with concrete interface shows higher interface shear strength than that of mixtures with sand interface.

CHAPTER 5

LIQUEFACTION AND POST-LIQUEFACTION BEHAVIOUR OF THE MIXTURES

5.1 INTRODUCTION

Liquefaction occurs in saturated cohesionless materials subjected to dynamic loading. The mixture of rubber and sand is susceptible to liquefaction since the rubber does not possess cohesion. The liquefaction studies of these mixtures have been carried out only since 2008 even though the applications of the mixtures have been examined since early 1990's. The liquefaction resistance of particulate rubber-sand mixtures should be studied for its effective use in the earthquake-prone areas. The previous studies have examined the liquefaction resistance of the mixtures using cyclic triaxial apparatus which is widely available. However, none of the previous studies have examined the post-liquefaction behaviour of the mixtures. The post-liquefaction behaviour of the materials needs to be examined for the analysis of settlement, lateral spreading, and development of p-y curves. In the present study, the liquefaction and post-liquefaction behaviour of the mixtures are examined using multi-stage cyclic triaxial testing. The different responses such as pore pressure variation and axial strain development are discussed in the present chapter along with the liquefaction resistance of the mixtures.

5.2 CYCLIC TRIAXIAL TESTS

5.2.1 Experimental Setup

Servo controlled automated cyclic triaxial apparatus (Make: VJ Tech) as shown in Figure 5.1 available at Geotechnical Engineering division of Indian Institute of Technology Madras is used to carry out the liquefaction and post-liquefaction behaviour of the particulate rubber mixtures.

Figure 5.1: Cyclic triaxial setup

In the cyclic triaxial apparatus, the load cell of 5 kN capacity and the vertical encoder of 100mm capacity is used to measure the sample load and deformation. The automated hydraulic pressure controller of capacity 1000kPa is used to apply back pressure while the pneumatic pressure controller along with air-water interface of 1000kPa capacity are used to apply the cell pressure. The developed pore water pressure is measured with the pore pressure transducer of capacity 1000kPa.

The load cell of the cyclic triaxial is calibrated before using it for the present study. The calibration is carried out using the reference load cell with the capacity of 5kN. The calibration frame and the reference load cell used to calibrate the load cell of the cyclic triaxial is shown in Figure 5.2. The reference load cell is placed in the calibration frame having pneumatic jack which in turn connected to load cell of the cyclic triaxial. The reference load cell is connected to the digital indicator to measure its load value. The reference load cell is loaded with help of pneumatic pressure and the load measured in the load cell of the cyclic triaxial is noted down. The plot between applied and measured load for the cyclic triaxial load cell is shown in Figure 5.3a. These values are the calibration input for Clisp Studio which is the operating software for cyclic triaxial apparatus.

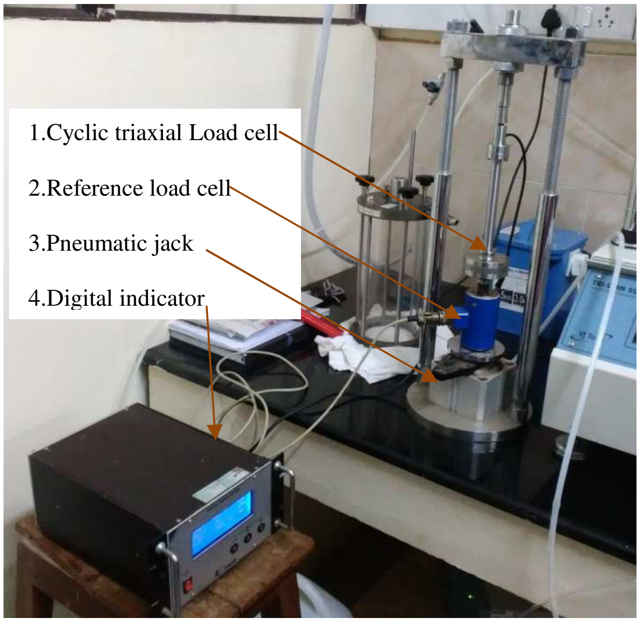

Figure 5.2: Calibration of cyclic triaxia load cell

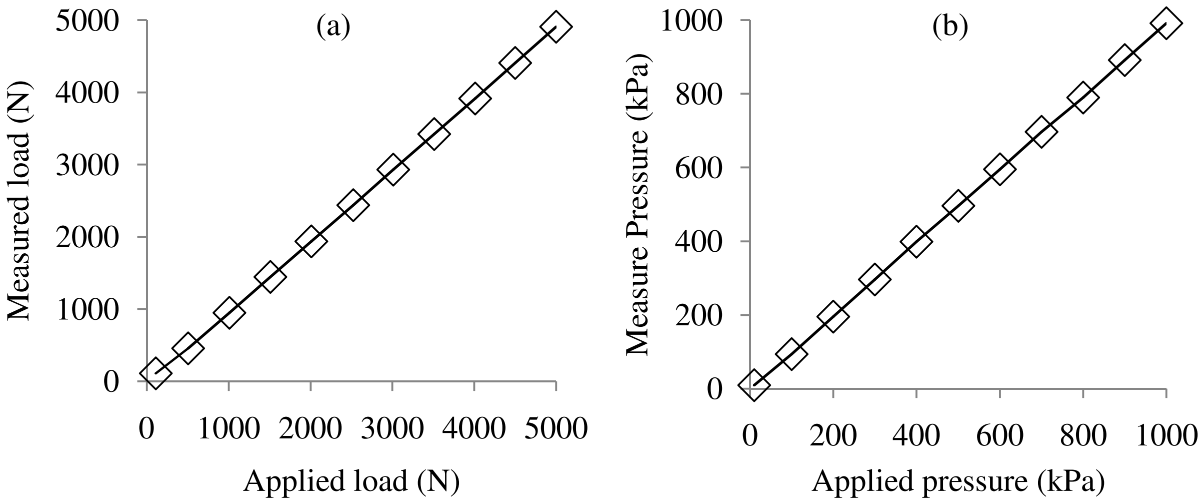

Figure 5.3: Calibration chart for (a) cyclic triaxial load cell (b) pore water pressure transducer

As in the case of the load cell, the pore water pressure transducer and the back pressure controller are also calibrated using reference pressure gauge. The typical applied and measured plot of the pore water pressure transducer is shown in Figure 5.3b.

5.2.2 Sample Preparation and Test Program

All the mixtures are prepared with certain quantity and stored in an airtight bag. A required mixture is then taken out from the bag and mixed it thoroughly before taking it for the test. Ladd's (1978) under compaction method is used to prepare the sample. The samples are prepared with 5 layers as shown in Figure 5.4 and the relative density of each layer is calculated based on the Equation 4.1. The calculation of relative density for the particulate rubber-sand mixtures is discussed in chapter 3.

$$u_n = u_{ni} - [\frac{u_{ni} - u_{nt}}{n_t - 1}(n - 1)] \tag{5.1}$$

where u_{ni} is percent under-compaction selected for the first layer, u_{nt} is percent under-compaction selected for the first layer (usually zero), n is the number of layer being considered, n_i is first (initial) layer and n_t is the total number of layers (final layer).

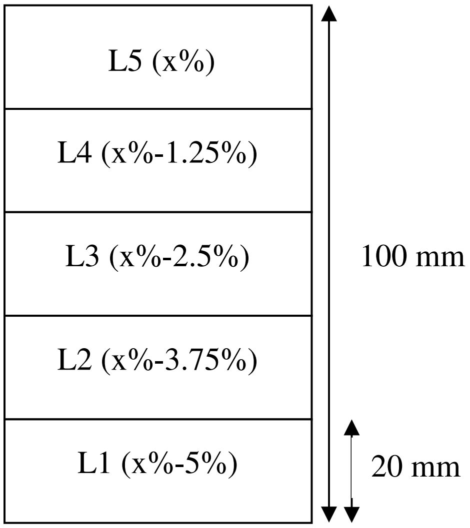

Figure 5.4: Density of the sample at each layer with 5% undercompaction

The rubber membrane for 50mm diameter and 100mm height sample is stretched and placed in the sample formation split mould. Then the mould is placed on the pedestal which has the porous stones and filter paper. The vacuum pressure of about 10kPa is applied to the split mould to hold the membrane firmly with the mould. The material required for under compaction is taken out separately as shown in Figure 5.5a. The dry samples are prepared inside the mould with 5 layers and the layer density is increased from the bottom to top as shown in Figure 5.4. This procedure is followed to prepare the sample with uniform density. Each layer is poured into the sample formation mould with zero drop height and compacted to the height of 20mm. The compaction rod of 2.88 N (0.294 kg) weight and the base diameter of 25 mm is used to prepare the sample. The sample of particulate rubber-sand mixture prepared using the above is shown in Figure 5.5b. A filter paper followed by a porous stone and top cap is placed after preparing the sample. Then 4 ‘O’ rings, 2 each on the pedestal and top cap are placed before stop applying the vacuum pressure. The mixture sample prepared for the cyclic triaxial testing is shown in Figure 5.5c. After which, the cell is placed in position and the submersible load cell is connected to the sample with help of a mechanical hard lock.

The prepared samples are subjected to three stages such as saturation, consolidation and cyclic loading. In saturation stage, the samples are saturated from the bottom to top. Initially, 20kPa of cell pressure and 10kPa of back pressure is applied while the top cap valve is open to take out the air bubbles along with the water. It is followed by the saturation is carried out by increasing the back pressure step by step till it achieves the required B value which is defined as the change in the pore pressure to the cell pressure ($\Delta u/\Delta\sigma$). The saturation of the sample is assumed to be achieved when the B value is greater than or equal to 0.95. Then the consolidation of the sample is carried out with the effective confining pressure of 100 kPa. The consolidation is ensured when the volume change is less than 5 mm^3 in 5 minutes. After which, the undrained cyclic load is applied with the frequency of 1 Hz and effective confining pressure of 100 kPa. It is followed by the post-liquefaction undrained monotonic strain controlled test is carried out without dissipating the excess pore water pressure once the liquefaction condition is achieved. It is also to be noted that the post-liquefaction undrained monotonic strain controlled test is carried out after the attainment of constant excess pore water pressure for the samples those are not liquefied.

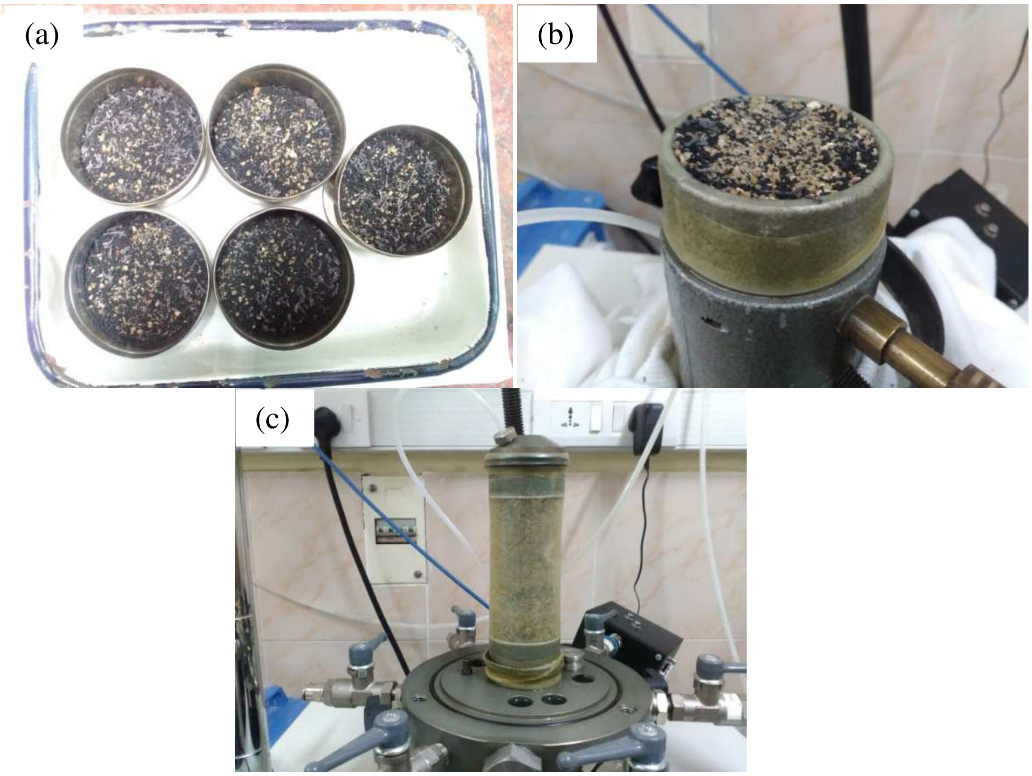

Figure 5.5: Sample preparation (a) material for five layers (b) prepared sample (c) sample with O ring and top cap

The cyclic triaxial testing is carried out with the samples of pure sand, particulate rubber, fly ash and three mixtures each in particulate rubber-sand mixtures and particulate rubber-fly ash mixtures with varying rubber content. Two relative densities such as 50% and 75% are studied since 50% is corresponding to the density of the mixtures subjected to the nominal compaction. On the other hand, approximately, the relative density of 75% is the maximum density of the mixtures which has been achieved in the site (Bosscher et al. 1992; Yoon et al. 2006). These samples are studied with 100 kPa effective confining pressure (σ'_c) since the material is being studied for shallow depth applications, 1 Hz frequency, and the cyclic stress ratio ($\sigma_d/2\sigma'_c$) in the range of 0.1 to 0.25. Test program for the present study is shown in Table 5.1. The relative density of the material and mixtures are calculated with the maximum unit weight determined from the compaction method and the minimum unit weight determined from the index density method.

Table 5.1: Test program for cyclic triaxial

Materials	CSR ($\sigma_d/2\sigma'_c$)	RD (%)	Confining pressure (kPa)	Frequency (Hz)
Rubber-sand mixtures				
Sand	0.1, 0.14, 0.18, 0.23	50	100	1
10%R	0.1, 0.11, 0.14, 0.18, 0.23	50, 75		
30%R	0.1, 0.15, 0.2, 0.23	50, 75		
50%R	0.1, 0.15, 0.2, 0.23	50, 75		
Rubber-fly ash mixtures				
Fly ash	0.1	50	100	1
10%R	0.1	50		
30%R	0.1	50		
50%R	0.1	50		
Rubber	0.1, 0.15, 0.2	50, 76		

5.3 CYCLIC BEHAVIOUR OF THE RUBBER-SAND MIXTURES

Isotropically consolidated samples are subjected to sinusoidal stress controlled cyclic loading. The loading is termed as cyclic stress ratio (CSR) which is defined as the ratio of deviator stress to the effective confining pressure ($\sigma_d/2\sigma'_c$). The typical cyclic loading applied during the tests is shown in Figure 5.6.

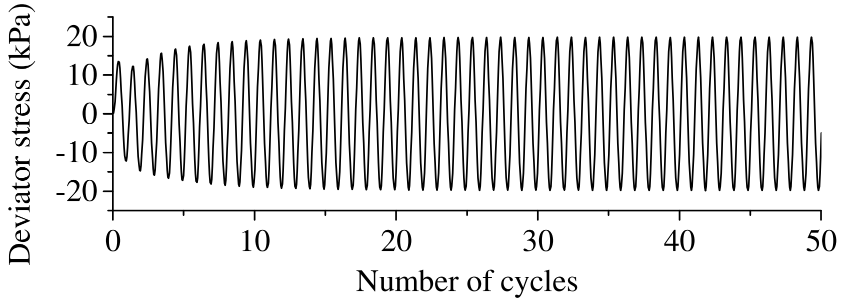

Figure 5.6: Typical loading cycles (CSR = 0.1)

The tests results are examined in terms of the variation of excess pore water pressure ratio ($r_u = u/\sigma'_c$) and axial strain with the number of loading cycles, stress-strain behaviour, and stress path for the sand, particulate rubber, and particulate rubber-sand mixtures and particulate rubber-fly ash mixtures having rubber content between 10% to 50%.

5.3.1 Pore Water Pressure Response of the Particulate Rubber-Sand Mixtures

The pore water pressure response of the mixtures is shown in Figure 5.7. The pore water pressure is depicted in terms of pore water pressure ratio which is defined as the ratio of excess pore water pressure to the effective confining pressure ($r_u = u/\sigma'_c$). In general, it is evident from the figure that the pore water pressure ratio is increased with increase in the number of cycles. The pore water pressure of the mixture having rubber content of 10% is rapidly increased and with this progression it would reach the maximum pore water pressure ratio of about unity. It shows that the mixture with 10% of rubber content would show initial liquefaction. Initial liquefaction is defined as the state of excess pore water pressure equals the effective confining pressure (Seed and Lee 1968). It is also to be noted that the mixture having rubber content of 10% shows higher pore water pressure ratio than that of sand. Further, it is observed that these mixtures show initial liquefaction. The excess pore pressure of mixtures reaches a constant value in about 20 numbers of loading cycles. The developed pore water pressure in the mixture with the rubber content of 50% is same as that of pure particulate rubber. Further, it is also evident from Figure 5.7b that the development of pore water pressure is reduced with the increase in the initial relative density of the mixtures.

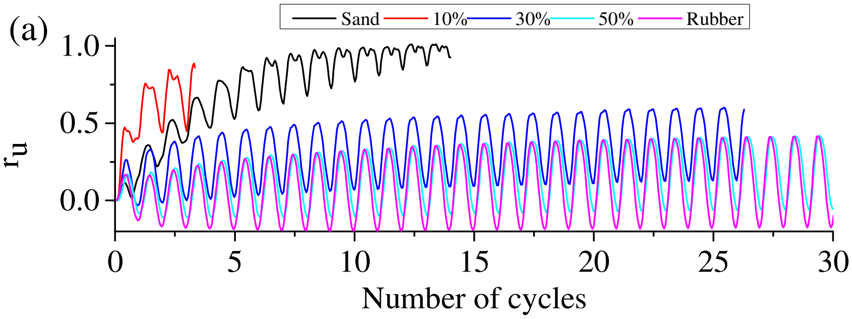

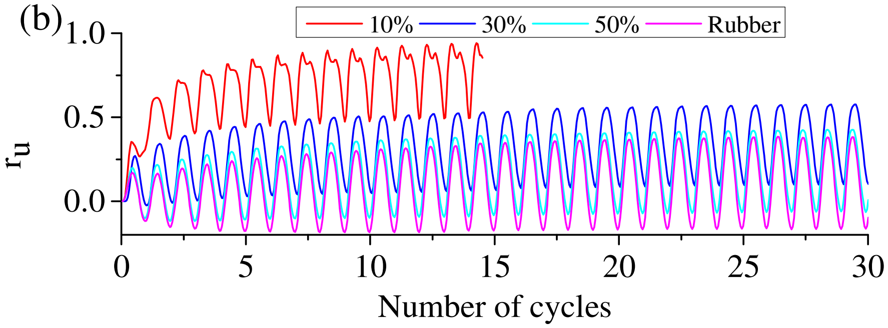

Figure 5.7: Excess pore water pressure variation of different mixtures at the initial relative density of (a) 50% (b) 75% (CSR 0.2)

5.3.2 Axial Strain Response of the Particulate Rubber-Sand Mixtures

Figure 5.8 plots the axial strain variation of the mixtures with the number of loading cycles. The axial strain shows an insignificant increase for sand during initial loading cycles. However, a rapid increase is observed for sand when the pore water pressure ratio is about 0.9. The double amplitude axial strain of sand was observed to be within 5% when the excess pore water pressure reaches the effective confining pressure (i.e., the condition of initial liquefaction). The similar behaviour of the sand is also observed for all the CSR which are examined in the present study. This shows that the sand samples are failed by reaching the initial liquefaction. For mixtures with the particulate rubber content of 10%, the axial strain is rapidly increased from the beginning of the loading cycles. The rapid increase in the axial strain of these mixtures is attributed to the rapid increase in the pore water pressure and the reduced stiffness of the mixture matrix. The axial strain of the mixtures with the particulate rubber content between 10% and 50% is gradually increased to a constant value within 15 numbers of loading cycles. The developed axial strain for these mixtures is also within 5% when the CSR is less than 0.2. Further, it is observed that the axial strain for the mixtures is reduced with the increase in the initial relative density of the mixtures. It is attributed to the increase in the stiffness of the samples with the increase in the initial relative density.

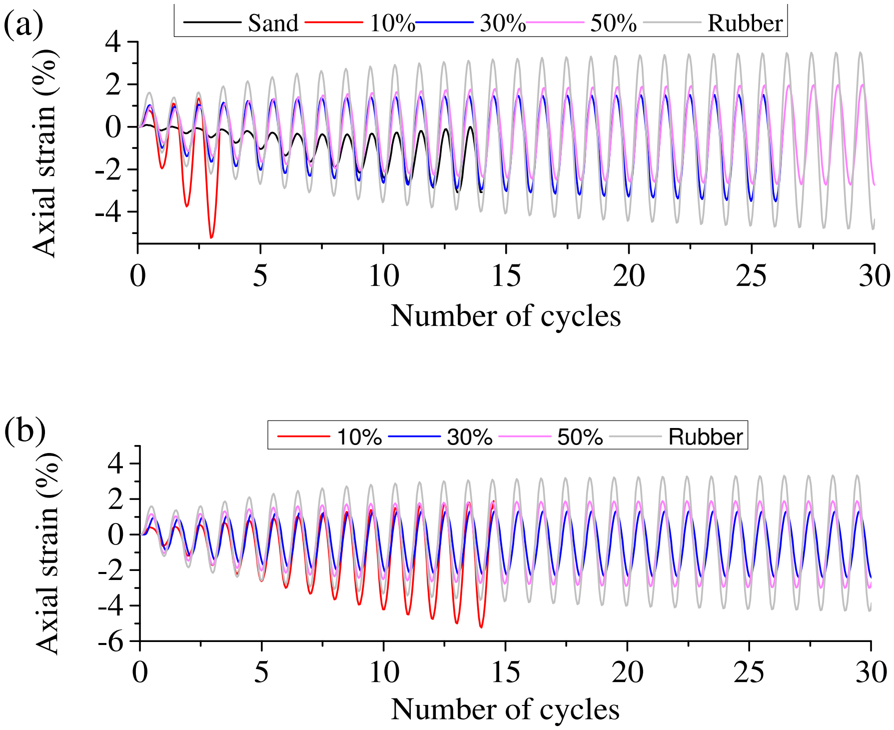

Figure 5.8: Axial strain variation of different mixtures at the relative density of (a) 50% (b) 75% (CSR 0.2)

5.3.3 Stress Path of the Particulate Rubber-Sand Mixtures

The stress path which is the variation of deviator stress (q) with the effective mean stress (p') for the different rubber content mixture is shown in Figure 5.9. The mean effective stress (p') of the mixtures is reduced with the increase in the loading cycles. The reduction in the mean effective stress is due to the increase in the pore water pressure. The mean effective stress of sand is reduced to zero. It is due to the increase in the excess pore water pressure. Further, the rapid decrease in the mean effective stress is observed for mixture with a rubber content of 10%. However, the mixture with 10% rubber content has shown the liquefaction failure before it reaches the zero mean effective stress. Further, the mean effective stress is not reduced significantly for the mixtures with rubber content greater than 10%. It confirms that the mixture with rubber content more than 10% does not show initial liquefaction. The reduction in the mean effective stress is reduced with an increase in the initial relative density. It is attributed to the reduction in the development of the pore pressure with the increase in the initial relative density.

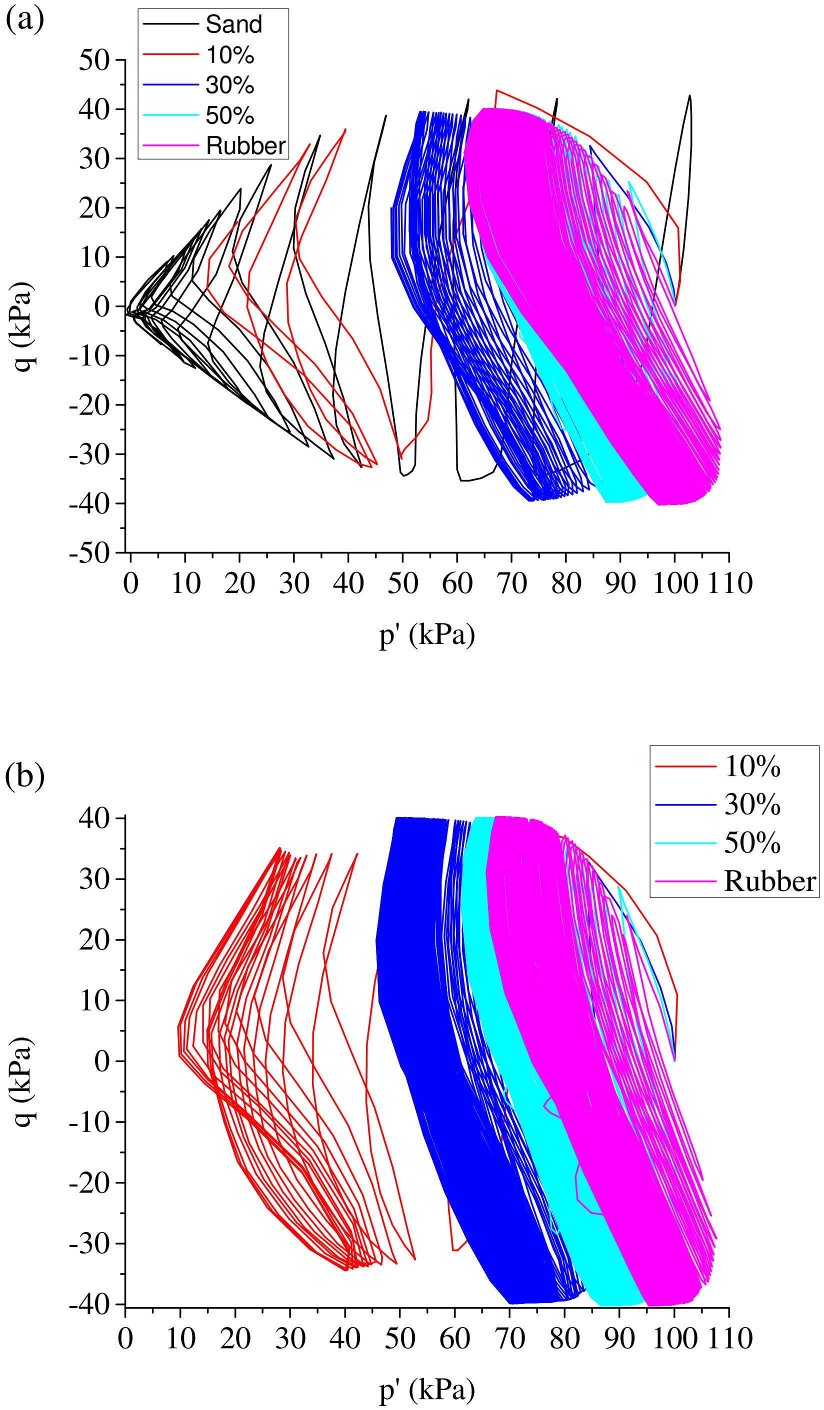

Figure 5.9: P'-q plot of different mixtures at the relative density of (a) 50% (b) 75% (CSR 0.2)

5.3.4 Stress-Strain Behaviour of the Particulate Rubber-Sand Mixtures

Figure 5.10 shows the stress-strain behaviour of the mixtures with different rubber content. It is evident from the figure that the hysteretic behaviour of sand is asymmetric. The deformation of sand is observed to be more in tension than that of in compression. It shows that the sand deforms more in tension to take the given axial load than that of in compression. However, the hysteretic behaviour of the sand becomes symmetric with the addition of the rubber. It shows that the addition of rubber to sand induces the elasticity. Further, the addition of rubber to sand reduces the modulus of the mixtures. The mixtures with the increase in the rubber content persuade the elasticity and reduce the modulus. It is also observed that there is no significant reduction in the modulus of the mixtures with higher rubber content (> 30%) due to the increase in the number of cycles. The mixture with the rubber content more than 50% behaves like rubber material with improved stiffness owing to the presence of sand particles. Further, it is evident from the figure that the unsymmetrical behaviour of the mixtures is changed to symmetric when the mixture with the rubber of 50%.

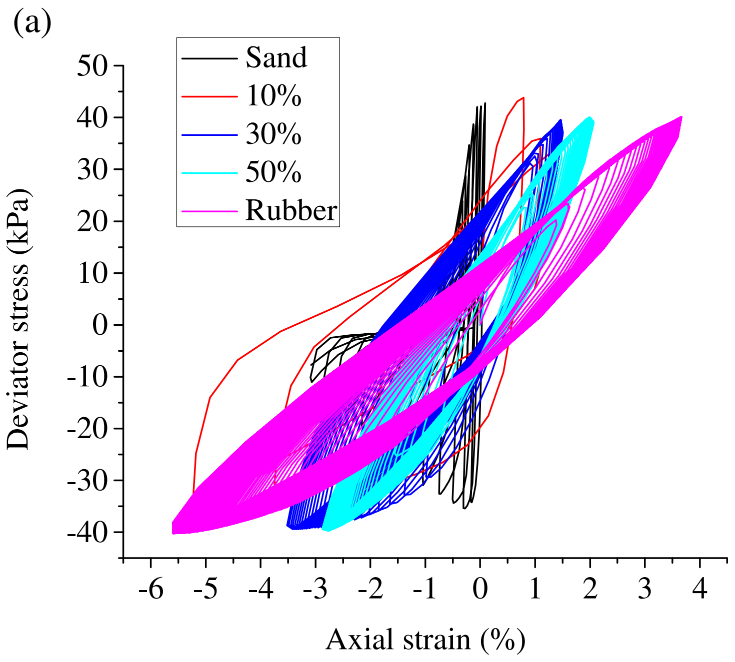

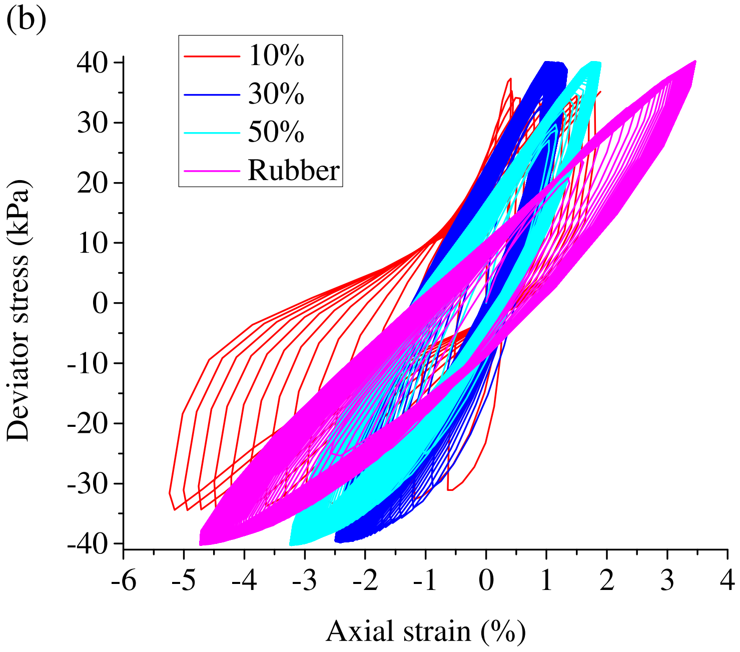

Figure 5.10: Cyclic stress-strain behaviour of different mixtures at the initial relative density of (a) 50% (b) 75% (CSR 0.2)

5.3.5 Factors Affecting the Pore Pressure and Axial Strain Response

Effect of rubber content

The variation of the maximum pore water pressure ratio with an increase in the rubber content is shown in Figure 5.11a. The curves are plotted for different cyclic stress ratio (CSR) which is defined as the ratio of deviator stress to the effective confining pressure ($\sigma_d/2\sigma'_c$). In general, the pore pressure ratio decreases with increase in the rubber content. The decrease in the pore pressure ratio is insignificant for the mixtures with the rubber content less than 10%. Further, the mixture with rubber content of 10% shows sand like behaviour, hence the pore water pressure is increased nearer to one. When the rubber content more than 10%, the reduction in pore pressure is rapid. However, the reduction is insignificant for the mixture with the rubber content more than 50%. It is attributed to the fact that the mixture having rubber content more than 50% behaves more like pure particulate rubber.

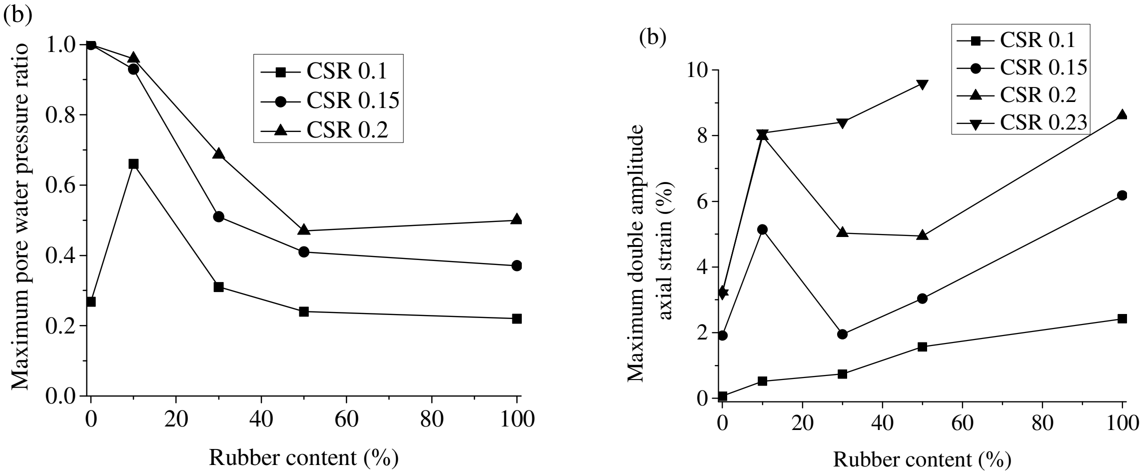

Figure 5.11: Effect of rubber content on (a) maximum pore water pressure ratio (b) maximum double amplitude axial strain (RD = 50%)

Figure 5.11b plots the variation of maximum double amplitude axial strain with the increase in rubber content. It is evident from the figure that the axial strain is gradually increased with increase in the rubber content at lower CSR. Meanwhile the axial strain rapidly increased for the sample with 10% rubber when the CSR is more than 0.1. It is due to the reduction in the stiffness because of the addition of rubber and increase in the pore water pressure. The axial strain of the sample with the rubber content between 10% and 50% is observed to be less than that of 10% sample when the CSR is greater than 0.1. Further increase in the rubber content more than 50%, the axial strain is increased more than that of the sample with the rubber content of 10%. The increase in the axial strain is due to only the reduction in the stiffness of the sample. The mixture having rubber content more than 50% shows rubber-like behaviour and the presence of sand particles does not increase the stiffness.

Effect of loading magnitude

The cyclic loading on the sample is termed as the cyclic stress ratio (CSR). It is the ratio of the deviator stress ($\sigma_d/2$) to the effective confining pressure (σ'_c). The variation of maximum pore water pressure ratio and axial strain for different rubber content mixtures with the variation of CSR is shown in Figure 5.12a. The pore water pressure ratio is observed to increase with an increase in the loading magnitude. The mixture having the rubber content of 10% shows higher pore water pressure at lower loading magnitude (CSR<0.1). The maximum pore water pressure ratio of sand and the mixture with 10% rubber content is reached about unity with the increase in the loading magnitude. The mixtures with the rubber content greater than 10% are also shown the increase in the pore pressure with an increase in the loading magnitude. However, the maximum increase is only about 0.6. It shows that the mixture with the rubber content greater than 10% does not show initial liquefaction.

Figure 5.12b shows the variation of maximum double amplitude axial strain of the mixtures with an increase in the loading magnitude. In general, the axial strain increases with an increase in the loading magnitude for all the mixtures. Of all the mixtures, rubber shows higher axial strain for all the loading magnitude. It is followed by the mixture with the rubber content of 10%. The mixture with the rubber content between 10% and 50% shows lower axial strain and the maximum axial strain is less than 5% when the CSR is less than 0.2.

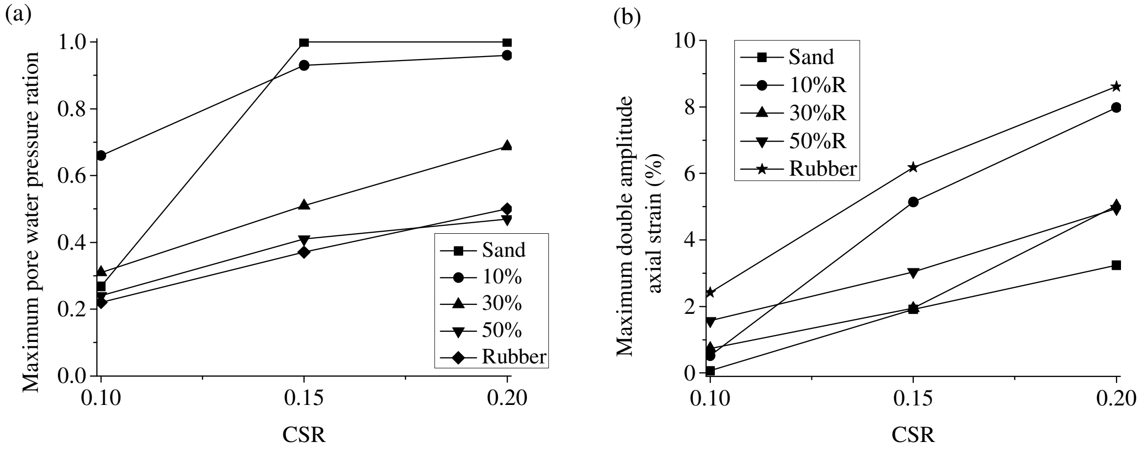

Figure 5.12: Effect of loading magnitude on (a) maximum pore water pressure ratio (b) maximum double amplitude axial strain (RD = 50%)

Effect of relative density

The influence of density on the maximum pore water pressure ratio is shown in Figure 5.13a. It is evident from the figure that the increase in the density decreases the development of the pore pressure. Further, Figure 5.13b shows the effect of density on the maximum double amplitude axial strain. The axial strain is also reduced with an increase in the relative density. The reduction in the axial strain is due to the increase in the stiffness of the sample. The effect of the increase in the relative density is more pronounced in decreasing the axial strain than decreasing the pore water pressure.

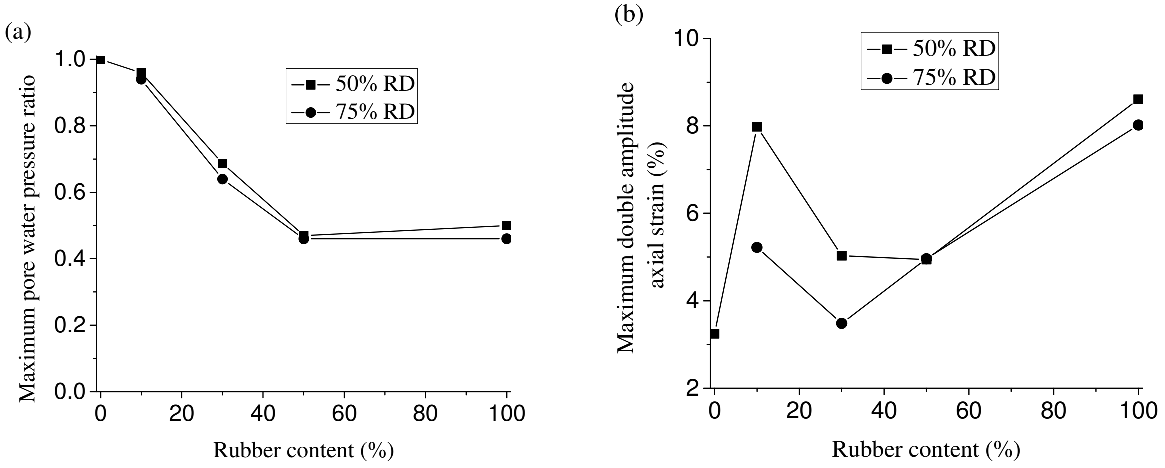

Figure 5.13: Effect of relative density on (a) maximum pore water pressure ratio (b) maximum double amplitude axial strain (CSR 0.2)

5.3.6 Liquefaction Resistance of the Particulate Rubber-Sand Mixtures

The liquefaction resistance of the mixtures is defined in terms of Cyclic Resistance Ratio (CRR). In the present study, the CRR at specific numbers of cyclic loading is obtained based on the two criteria: one is reaching of value r_u equals to unity and the other is reaching of 5% double amplitude axial strain, whichever occurs earlier. The liquefaction resistance of mixtures with different rubber content is shown in Figure 5.14. It is observed form the figure that the particulate rubber-sand mixtures with 10% rubber is not liquefied when the CRR is less than or equal to 0.1. In addition, the liquefaction resistance of mixture reduces due to the addition of 10% rubber to sand when the CRR is more than 0.1. Further, the liquefaction resistance of the other mixtures is more than that of sand for the CRR less than 0.23. It is also observed that the rubber-sand mixtures with 30% and 50% rubber content were not liquefied when the CRR is less than 0.15 and 0.2 for the initial relative density of the mixture is 50%. However, the pure rubber sample shows liquefaction strength more than that of sand for the CRR of up to 0.15. Further increase in the CRR is resulted into reduction of the liquefaction resistance of the pure rubber.

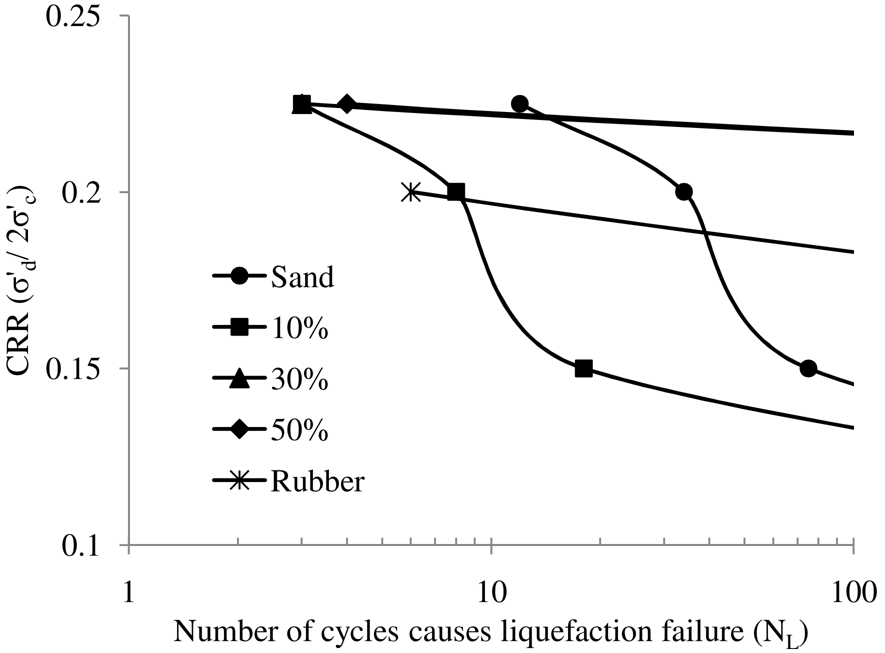

Figure 5.14: Liquefaction resistance of the mixtures (50% RD)

The increase in the density of the mixture (i.e., at 75%) increases the CRR below which the mixture does not liquefy. The particulate rubber-sand mixture with 30% rubber is not liquefied at 50% RD with the CRR of less than 0.15. However, increase in the relative density to 75% is increased the CRR of the mixture with 30% rubber content from 0.15 to 0.2. Further, the liquefaction strength of the mixtures is increased with an increase in the RD of the mixtures.

Figure 5.15 plots the Cyclic Resistance Ratio (CRR) versus the rubber content for 10 and 30 numbers of cyclic loading. The number of cycles 10 is corresponding to the earthquake magnitude (Mw) of 6.5 and 30 numbers of cycles corresponding to the earthquake magnitude of 9 (Seed et al. 1975). The figure shows that the liquefaction strength initially reduces till the addition of 10% rubber followed by an increase till 50% rubber content in the mixture. Further, the liquefaction strength of the mixture is reduced for the mixture with rubber content more than

50%. The initial reduction in the liquefaction strength is attributed to the rapid increase in the pore pressure and axial strain of the mixtures. The reduction in higher rubber content mixture is attributed to the reduction in the stiffness of the mixtures which increases the accumulation of axial strain.

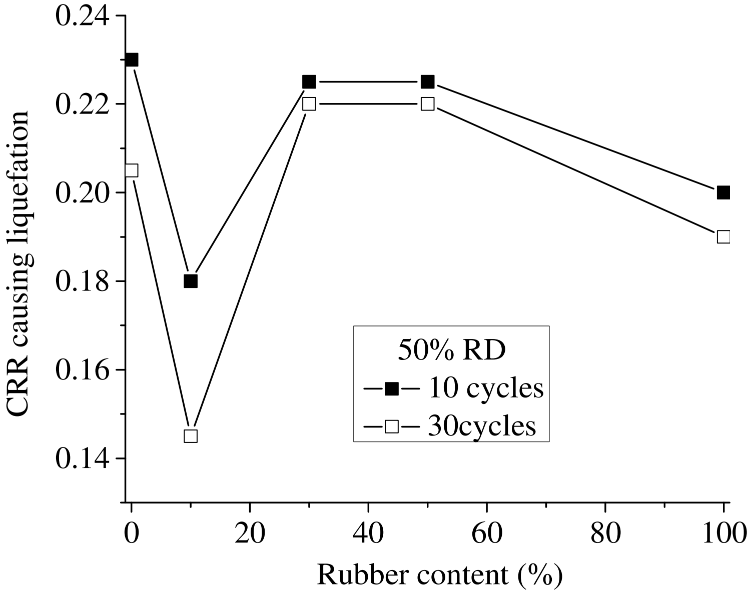

Figure 5.15: Liquefaction resistance of the rubber-sand mixtures

5.3.7 Post-Liquefaction Strength of the Particulate Rubber-Sand Mixtures

The variation of post-liquefaction monotonic deviator stress and excess pore water pressure with the axial strain for all the mixtures are shown in Figure 5.16a and 5.16b at 50 and 75% RD respectively. Figure 51.6a shows that the sand initially posses the shear strength close to zero owing to the fact that the material is in the liquefied state. However, with the increase in the axial strain, the samples gain strength. The strain at which the significant load is taken by the sample is termed as take of strain (Rouholamin et al. 2017). The take of strain in the post-liquefaction monotonic behaviour of sand is equal to the strain at which excess pore pressure start diminishing or the load taken by the sample is significant. The take of strain of 4% to 5%, which is termed as post-dilation shear strain, is observed by Rouholamin et al. (2017) for the sand at

50% relative density. In addition, the excess pore water pressure starts dissipating when the specimen started taking the load. In general, the sand attains denser configuration after liquefaction even though it is prepared in the loose state. Hence, further loading of sand after liquefaction would dilate which result into the decrease in the excess pore water pressure.

The post-liquefaction monotonic behaviour of the mixtures in Figure 5.16a and 5.16b shows that, unlike sand, the mixtures immediately takes loading during the post-liquefaction monotonic behaviour. Hence, the mixtures show higher post-liquefaction shear strength than that of sand till the axial strain of about 5%. It is evident from the figure that the mixtures initially posses sharp increase in the shear strength followed by a gradual increase. The strain at which such phase change occurs increases with the rubber content. Nevertheless, the post-liquefaction strength of the mixture is decreased with the increase in the rubber content. It is also observed that the post-liquefaction strength of the mixture is increased with an increase in the relative density. Figure 5.17 shows the variation of post-liquefaction excess pore water pressure with axial strain. The excess pore water pressure developed during the cyclic loading is marginally increased at first for mixture with 10% rubber content due to the post-liquefaction undrained monotonic loading followed by a reduction. It indicates that the mixture initially shows little compression followed by a steady dilation. However, all other mixtures and pure rubber show the increase in the excess pore water pressure with the increase in the post-liquefaction loading. It shows that the mixtures are compressive in nature during the post-liquefaction monotonic loading.

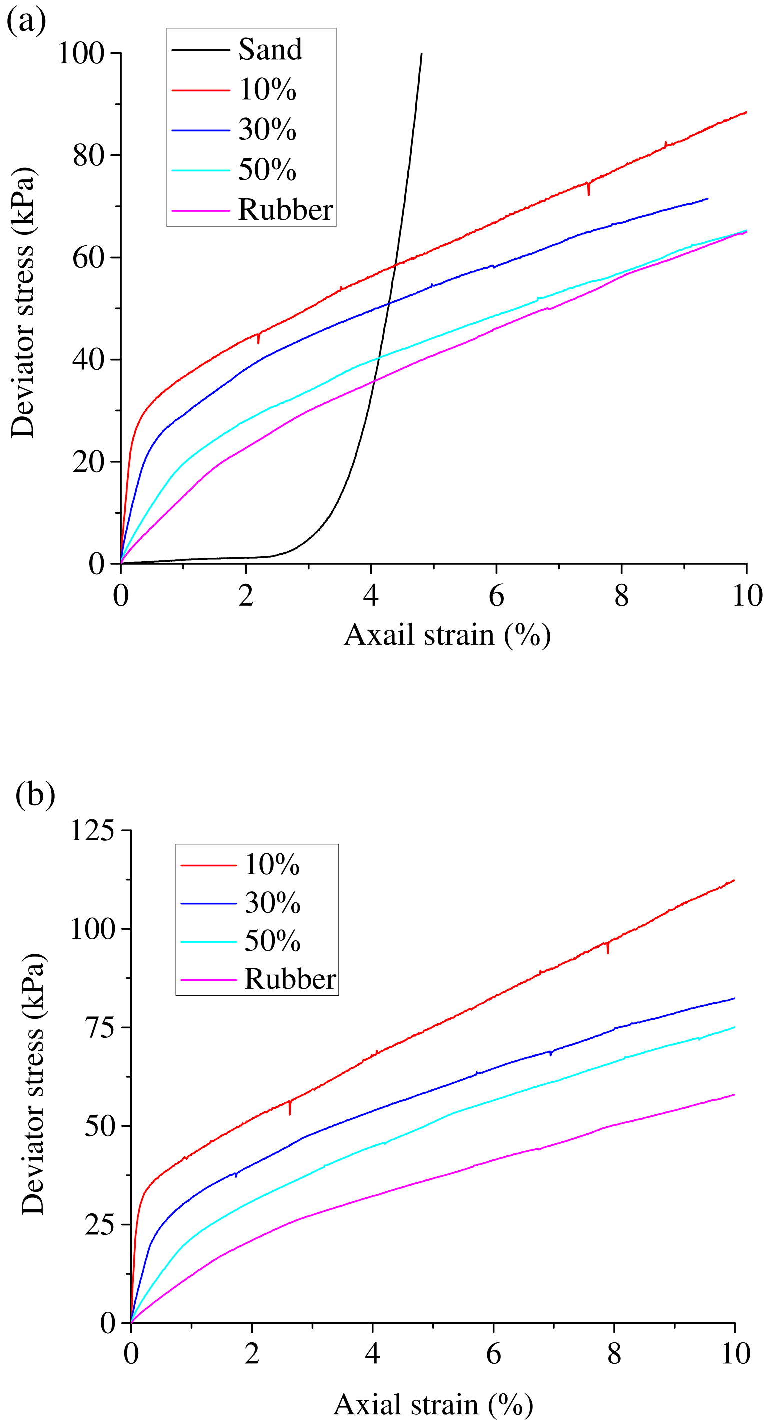

Figure 5.16: Typical post-liquefaction monotonic deviator stress-strain behaviour of mixtures at (a) 50% RD (b) 75% RD

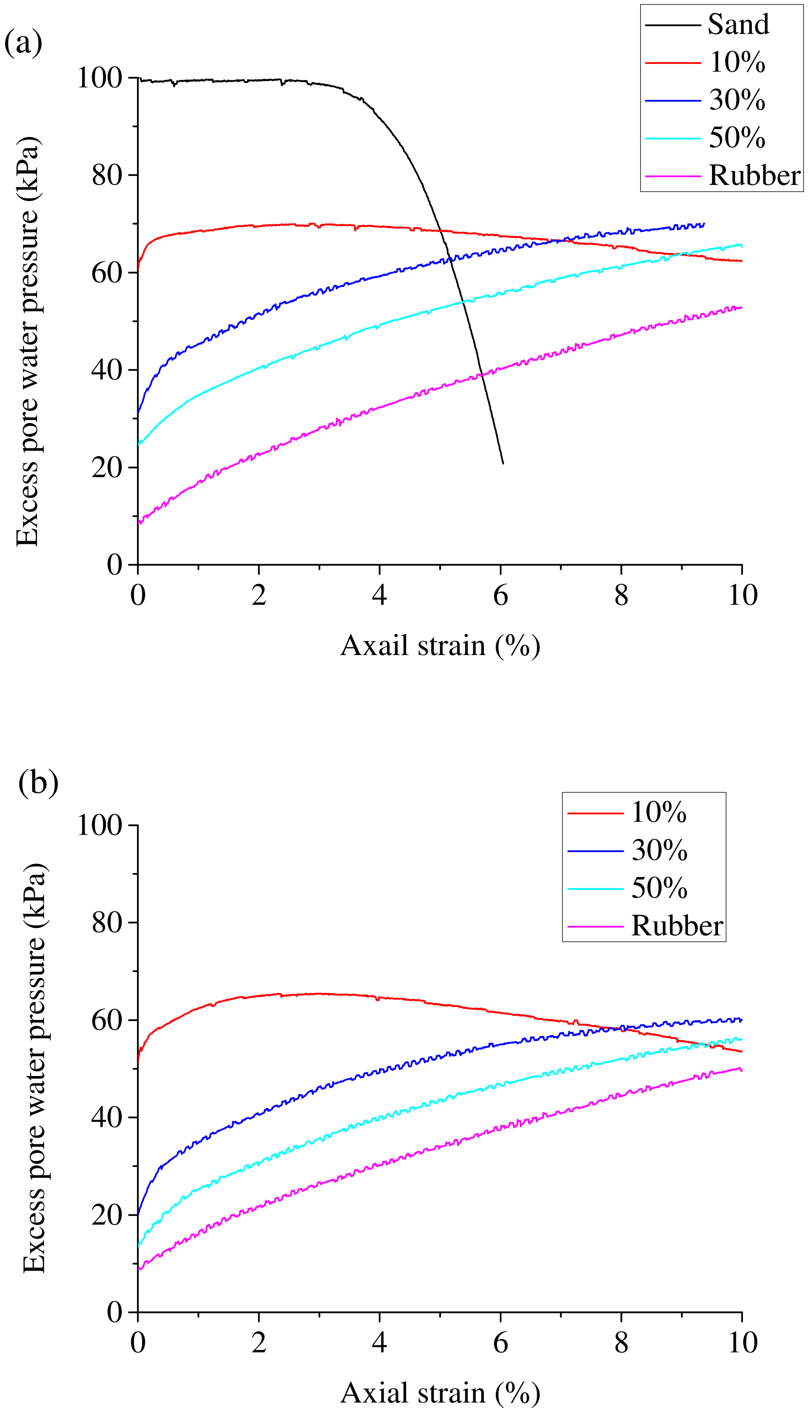

Figure 5.17: Typical post-liquefaction monotonic excess pore water pressure-axial strain plot of mixtures at (a) 50% RD (b) 75% RD

Typical stress-strain plot of the post-liquefaction behaviour of the mixture with 30% rubber content is shown in Figure 5.18 for different CSR and density. It is evident from the figure that the CSR does not have the influence on the post-liquefaction stress-strain behaviour of the mixtures. However, the post-liquefaction strength of the mixtures is observed to be increased with increase in the initial relative density of the mixture.

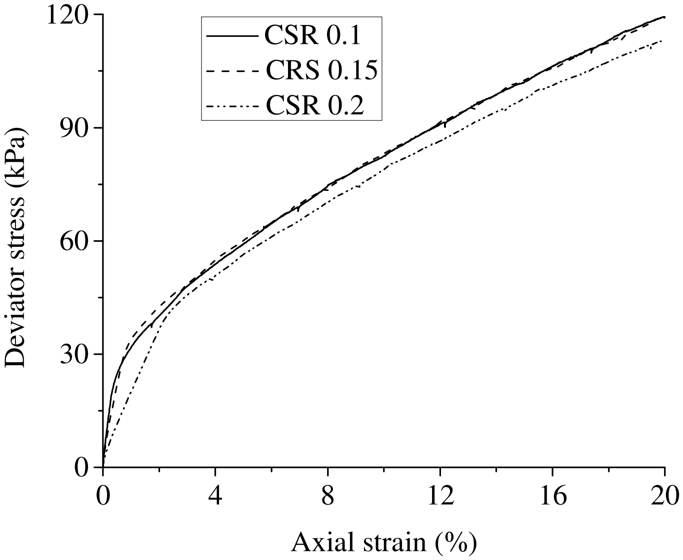

Figure 5.18: post-liquefaction monotonic deviator stress-strain behaviour of mixtures subjected to different CSR (75% RD)

It can be easily noticed from Figures 5.16 (a) and 5.16 (b) that the general behaviour of the mixtures during the post-liquefaction monotonic loading is observed to be elastic-hardening. Therefore, the mixture behaviour is idealized to have two moduli such as modulus for initial elastic and modulus for hardening behaviour. Both the modulus of the mixtures normalized to RD for the mixtures with the rubber content between 10 to 100% are given in Figure 5.19. It is evident from the figure that both the modulus of the mixtures reduces significantly till the rubber content of 50% followed by a slight reduction up to the rubber content of 100%. It is also noted that the change in initial elastic modulus with the increase in density is pronounced for the rubber content less than 50% in the mixture. However, the hardening modulus is not significantly varied with the increase in the density for all the rubber content mixtures.

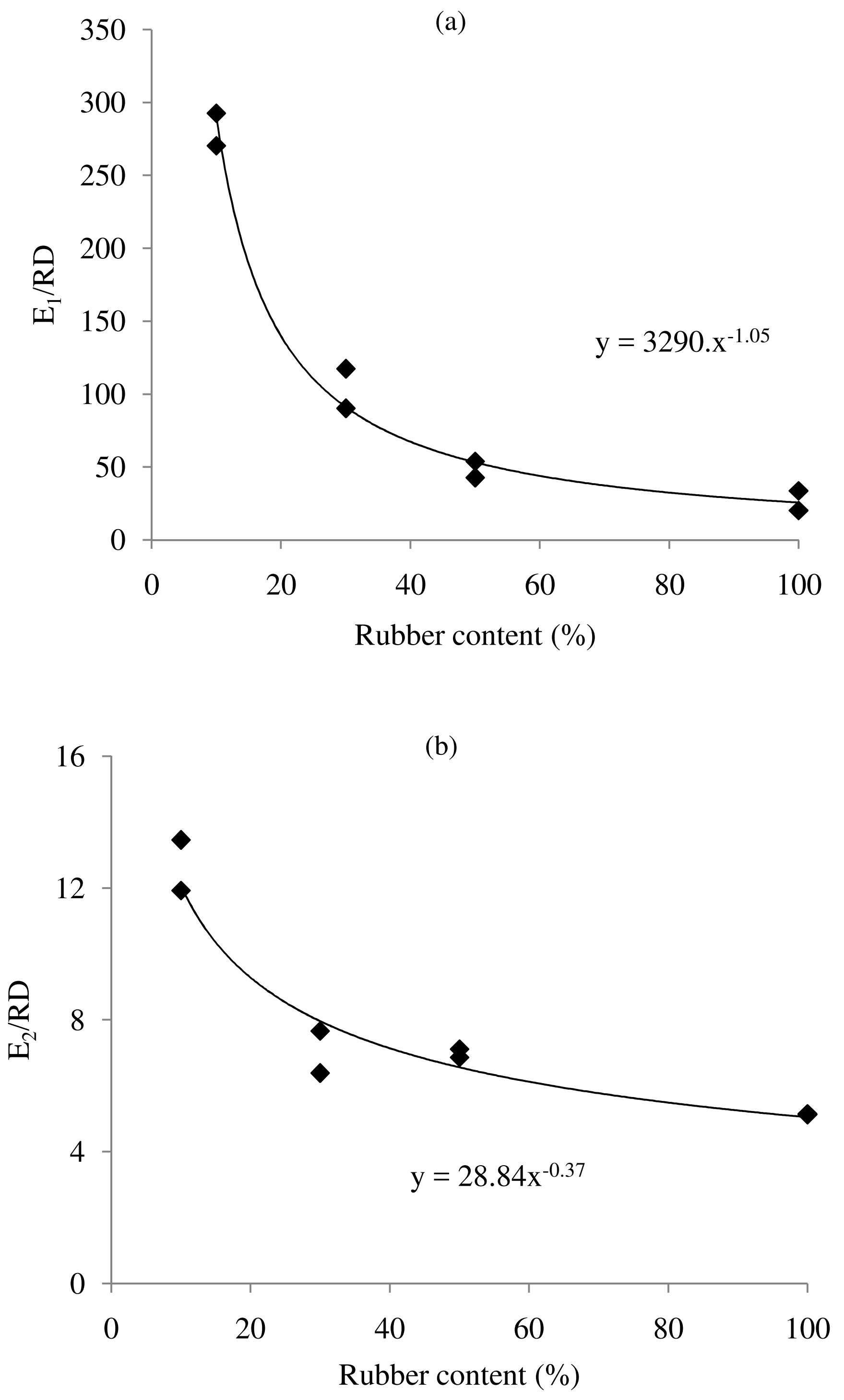

Figure 5.19: post-liquefaction monotonic (a) elastic modulus (b) hardening modulus of the mixtures

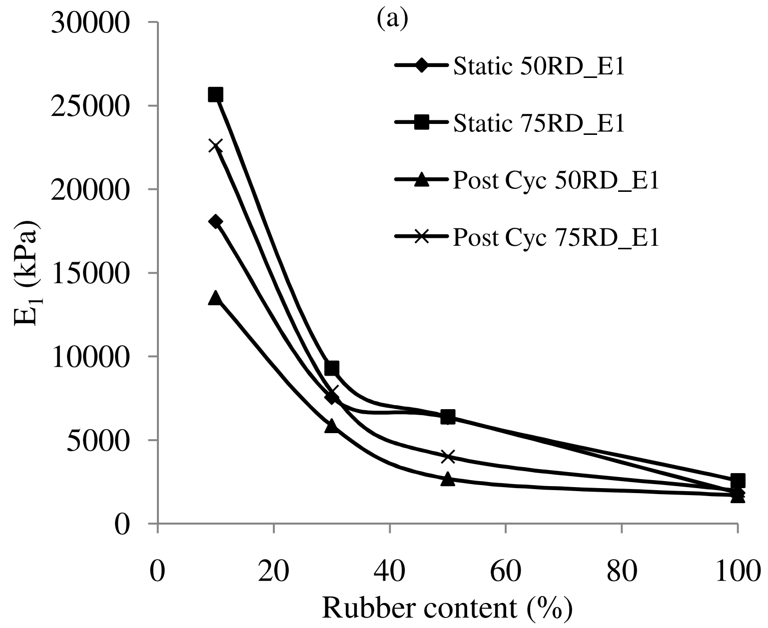

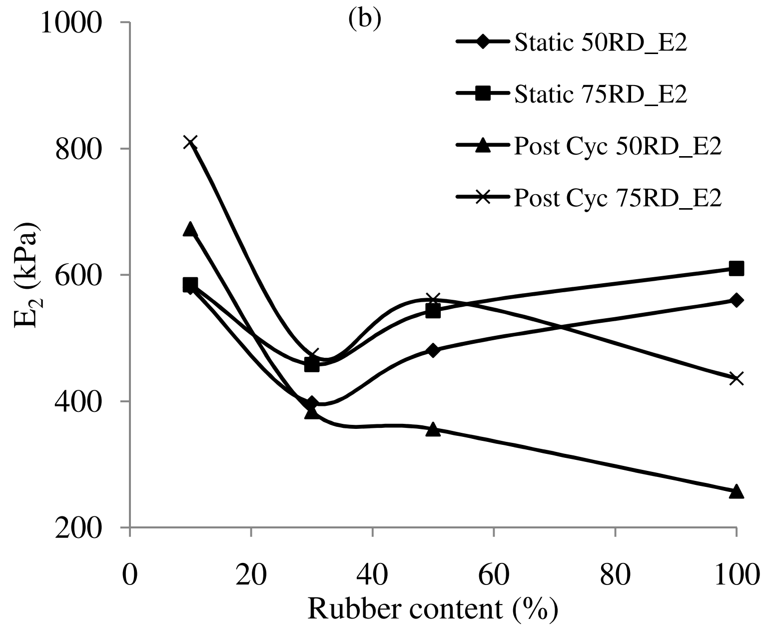

Figure 5.20: Static and post-liquefaction monotonic (a) elastic modulus (b) hardening modulus of the mixtures

The generalized relation between the modulus, relative density, and rubber content is given in Equation 5.2 (Initial elastic modulus) and Equation 5.3 (Hardening modulus).

$$E_1 = RD * 3290\chi^{-1.05} \tag{5.2}$$

$$E_2 = RD * 28.84\chi^{-0.37} \tag{5.3}$$

where, E1 is initial elastic modulus, E2 is hardening modulus, RD is the relative density of the mixture, χ is rubber content in the mixture which should be greater than 10%.

The post-liquefaction modulus of the mixtures is compared with the static modulus in Figure 5.20. The post-liquefaction initial elastic modulus of the mixture is less than that of the static modulus. The reduction for 10% mixture is more than that of other mixtures. The reduction is less significant for the mixtures with rubber content more than 10%. The development of pore water pressure during the cyclic stage is attributed to the reduction in the initial elastic modulus of the mixtures with 10% rubber content. The hardening modulus of the mixtures shows marginal variation between static and post-liquefaction behaviour. The mixture having 10% rubber content shows higher post-liquefaction hardening modulus than static hardening modulus. It is perhaps due to the dilation of the mixtures at large strain (as seen in post-liquefaction pore pressure).

5.4 CYCLIC BEHAVIOUR OF THE PARTICULATE RUBBER-FLY ASH MIXTURES

The following sections discuss the undrained cyclic behaviour such as pore water pressure, axial strain, and the number of cycles cause liquefaction of the particulate rubber mixed with fly ash.

5.4.1 Pore Water Pressure and Axial Strain Response

The variation of excess pore water pressure ratio with the increase in the number of cycles for the different mixture is shown in Figure 5.21. The pore water pressure ratio is rapidly increased for fly ash and the mixture with rubber content less than 30% rubber content. In addition, the pore water pressure ratio of mixtures with rubber content less than 30% is more than that of fly ash. The pore water pressure ratio is retarded when the rubber content is more than 30%. The maximum pore water pressure ratio of one is observed for fly ash and mixtures with the rubber content less than 30%. The maximum pore water pressure ratio of about 0.85 is observed for the mixture with the rubber content of 50%. It shows that the mixture with rubber content of 50% does not show initial liquefaction.

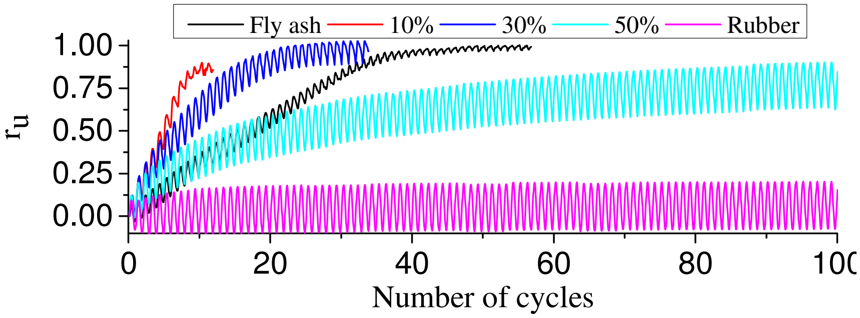

Figure 5.21: Excess pore water pressure variation particulate rubber-fly ash mixtures at (50% RD and CSR 0.1)

The axial strain of different mixtures with the increase in the number of loading cycles is shown in Figure 2.22. The axial strain of fly ash initially shows the insignificant increase. However, the rapid increase in axial strain is observed for fly ash when the pore pressure is more than 0.8. The mixture having rubber content less than 30% is shown higher axial strain than that of fly ash at the initial number of loading cycles. It is due to the development of higher excess pore water pressure than that of fly ash at that point. As in the case of fly ash, the mixture with rubber content less than 30% is also shown the rapid increase in the axial strain when the excess pore water pressure ratio is about 0.8.

The stress path for particulate rubber-fly ash mixtures is shown in Figure 5.23. It is observed from the figure that the mean effective stress of fly ash is reduced to zero. It shows that the fly ash experiences the initial liquefaction. Unlike the particulate rubber-sand mixture, the particulate rubber-fly ash mixture would experiences the initial liquefaction when the rubber content is less than 30%. However, the liquefaction failure of the particulate rubber-fly ash mixtures is governed by the axial strain criterion as in the case of particulate rubber-sand mixtures. In the present study, the particulate rubber-fly ash mixtures have shown the liquefaction failure by reaching 5% axial strain before it reaches the initial liquefaction. Further, the figure shows that the mean effective stress is reduced with the increase in the rubber content of the mixtures.

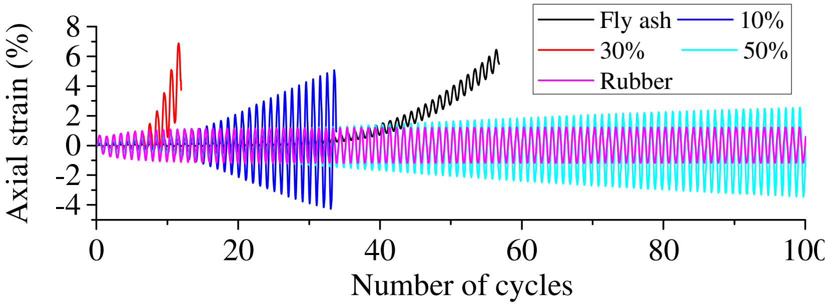

Figure 5.22: Axial strain variation of particulate rubber-fly ash mixtures at (50% RD and CSR 0.1)

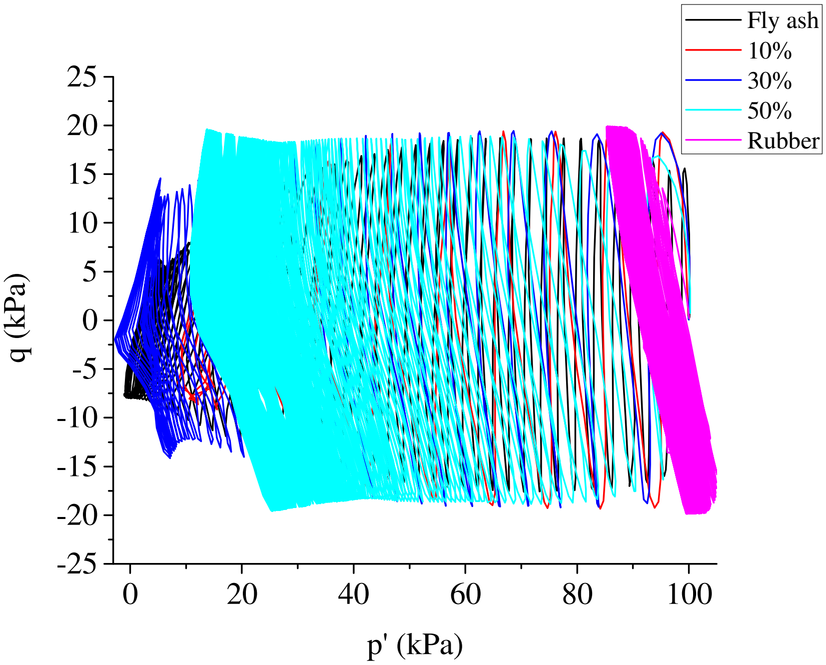

Figure 5.23: Stress path of particulate rubber-fly ash mixtures at (50% RD and CSR 0.1)

The stress-strain plot of the particulate rubber-fly ash mixtures is shown in Figure 5.24. It is evident from the figure that the hysteretic behaviour of the fly ash is asymmetric. The fly ash deforms more in compression than in tension. It shows that there is a permanent set during the compression cycles of loading. The mixture with 10% rubber content is also shown the same behaviour. The hysteretic loop of the mixture has become symmetric when the rubber content is increased in the mixture. Also, it is observed that the mixtures behave like elastic material when the rubber content is increased in the mixture.

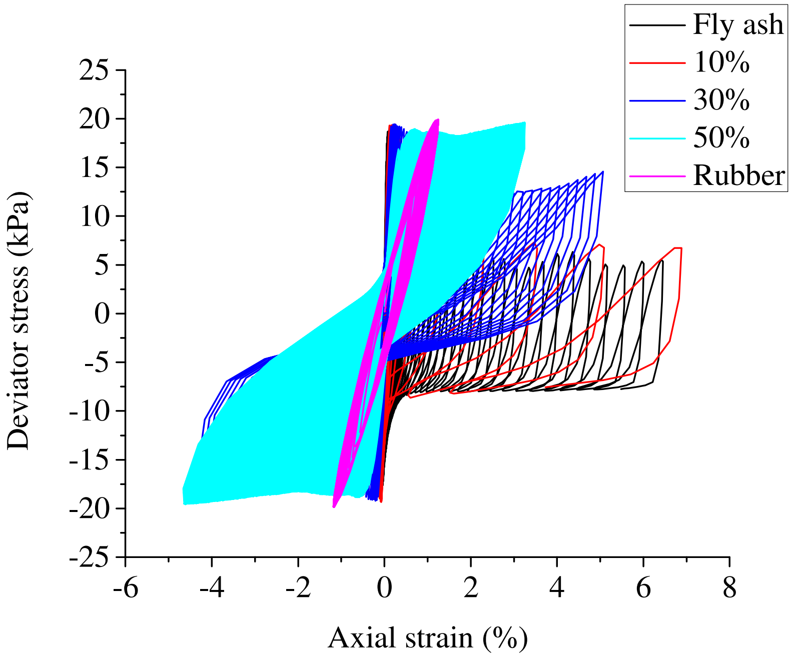

Figure 5.24: Stress-strain behaviour of particulate rubber-fly ash mixtures at (50% RD and CSR 0.1)

5.4.2 Liquefaction Strength of the Particulate Rubber-Fly Ash Mixtures

Figure 5.25 shows the number of cycles causes liquefaction, N_L (the number of cycles required to cause initial liquefaction or the double amplitude axial strain reaching 5%, whichever occurs first) with the increase in the rubber content for particulate rubber-fly ash mixtures. The liquefaction strength of the mixtures initially observed to be decreased with an increase in the rubber content. The liquefaction resistance is increased when the rubber content is more than 30% in the mixture. The mixture having rubber content of 50% is shown the liquefaction resistance more than that of fly ash and sand. Therefore it can be stated that the particulate rubber-fly ash mixture possesses higher liquefaction resistance when the rubber content is more than 30%.

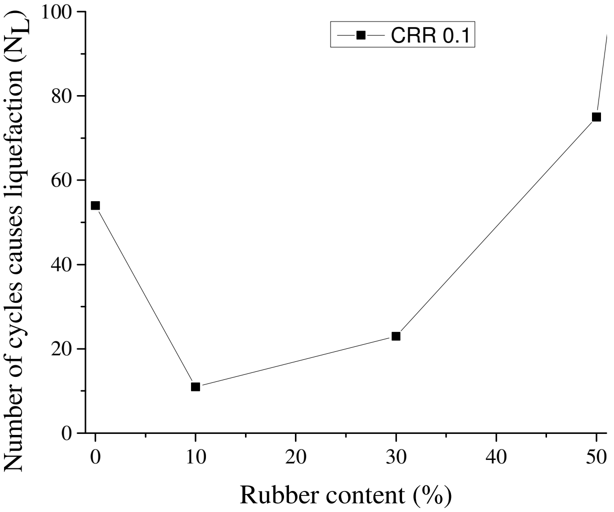

Figure 5.25: Liquefaction strength of particulate rubber-fly ash mixtures at (50% RD and CSR 0.1)

5.4.3 Post-Liquefaction Behaviour of the Particulate Rubber-Fly Ash Mixtures

The immediate undrained behaviour of particulate rubber-fly ash mixtures after the stress controlled cyclic loading is presented in Figure 5.26. It is observed from the figure that the post-liquefaction shear strength of the mixtures is increased with an increase in the axial strain without showing any post-peak softening. Further, the mixtures possess lower shear strength than that of fly ash at the low axial strain. However, the mixtures possess higher shear strength than pure fly ash at the higher axial strain. The particulate rubber-fly ash mixture with the rubber content of 50% is shown higher post-liquefaction shear strength than that of other mixtures. It is also evident from Figure 4.14 that the static strength of the particulate rubber-fly ash mixture with 50% rubber content is more than that of any mixtures. Figure 5.27 shows the peak deviator stress of the particulate rubber-sand mixtures and particulate rubber-fly ash mixtures. The post-liquefaction peak deviator stress of particulate rubber-sand mixtures is reduced with the increase in the rubber content. However, the shear strength of the particulate rubber-fly ash mixture is increased with the increase in the rubber content when the rubber content is more than 10%.

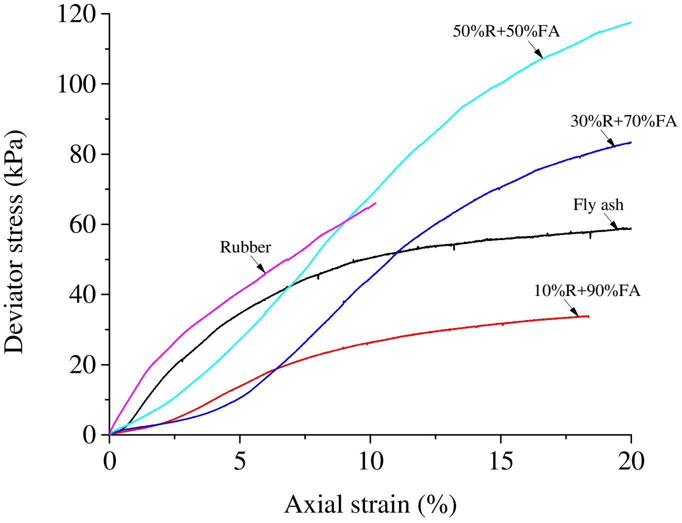

Figure 5.26: Post-liquefaction stress-strain behaviour of particulate rubber-fly ash mixtures at (50% RD and CSR 0.1)

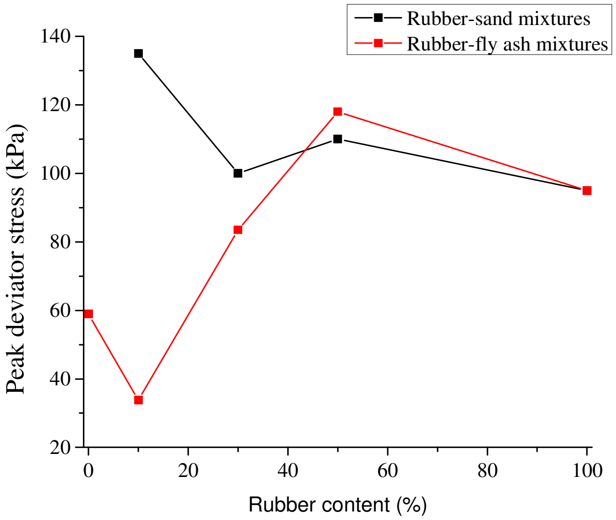

Figure 5.27: Peak post-liquefaction strength of particulate rubber-fly ash mixtures and particulate rubber-sand mixtures at (50% RD and CSR 0.1)

5.5 CYCLIC BEHAVIOUR OF PARTICULATE RUBBER-SAND-FLY ASH MIXTURES

The following section examines the optimum content of particulate rubber, sand and fly ash in the mixtures for the higher liquefaction resistance. The sand in the mixture is progressively replaced with fly ash to obtain the mixtures with particulate rubber, sand and fly ash. In each rubber content, two mixtures of particulate rubber-sand-fly ash mixtures along with the particulate rubber-sand mixtures and particulate rubber-fly ash mixtures are examined in the following section. The mixture with 10% rubber content is examined with the CSR of 0.1 since the particulate rubber-sand mixture shows the liquefaction failure when the CSR is more than 0.1. The particulate rubber-sand mixtures with rubber content more than 10% are liquefied only when the CSR is greater than 0.2. Therefore, the mixtures in this section with rubber content more than 10% are examined with the CSR of 0.2.

5.5.1 Pore Water Pressure and Axial Strain Response of the Particulate Rubber-Sand-Fly Ash Mixtures

Figure 5.28a shows the pore water pressure ratio variation of different mixtures with the rubber content of 10%. It is evident from the figure that the mixture with the addition of 10% fly ash initially retards the pore water pressure ratio. However, the pore water pressure ratio of the mixture with the addition of 10% fly ash is more than that of particulate rubber-sand mixtures at a large number of loading cycles. Further, it is observed from the figure that the addition of fly ash to particulate rubber-sand mixtures rapidly increases the pore water pressure ratio. The axial strain response of the mixtures is shown in Figure 5.28b. It is evident from the figure that the particulate rubber-sand mixture (10PR+90S) with 10% fly ash has shown the insignificant change in the axial strain up to 80 numbers of loading cycles. Further increase in the loading cycles causes the rapid increase in the axial strain which is attributed to the rapid increase in the pore water pressure ratio at that point. The axial strain of mixtures with fly ash content more than 30% is rapidly increased at the lower number of loading cycles. Further, it is observed that the axial strain development is shifted from compressive to tensile side with the increase in the fly ash content.

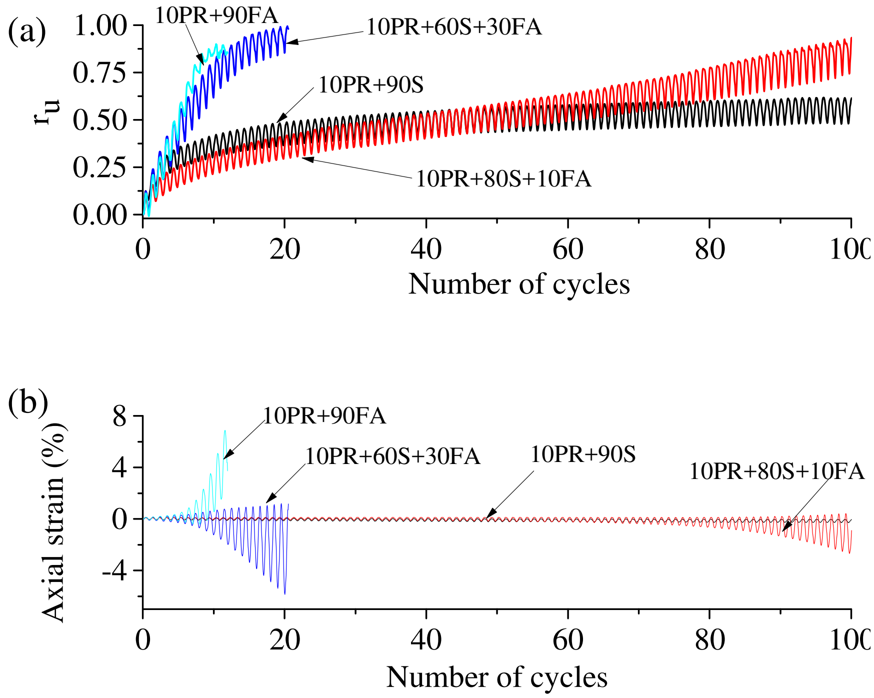

Figure 5.28: Particulate rubber-sand-fly ash mixtures with 10% rubber (a) pore pressure response (b) axial strain response (50% RD and CSR 0.1)

The pore water pressure response of 30% rubber content mixture with varying proportion of sand and fly ash is shown in Figure 5.29a. It is evident from the figure that the excess pore water pressure ratio of the particulate rubber-sand mixture is increased gradually with increase in the loading cycles. The mixture attains a constant pore water pressure ratio at about 20 numbers of cycles. Addition of fly ash to the particulate rubber-sand mixture is increased the pore water pressure ratio. However, the maximum increase is much lower than the pore water pressure ratio of one. The maximum pore pressure of 0.6 and 0.7 is observed for the mixtures having fly ash of 10% and 30% respectively. The axial strain response of 30% rubber mixtures is shown in Figure 5.29b. It is evident from the figure that the particulate rubber-sand mixture shows the gradual increase in the axial strain to a maximum value of about 5%. However, the addition of fly ash to the mixture rapidly increases the axial strain. The axial strain development is observed to be increased in tensile side, unlike the 10% rubber mixtures. The increase in the axial strain attributed to the increase in the pore water pressure and the reduction in the stiffness of the mixture matrix.

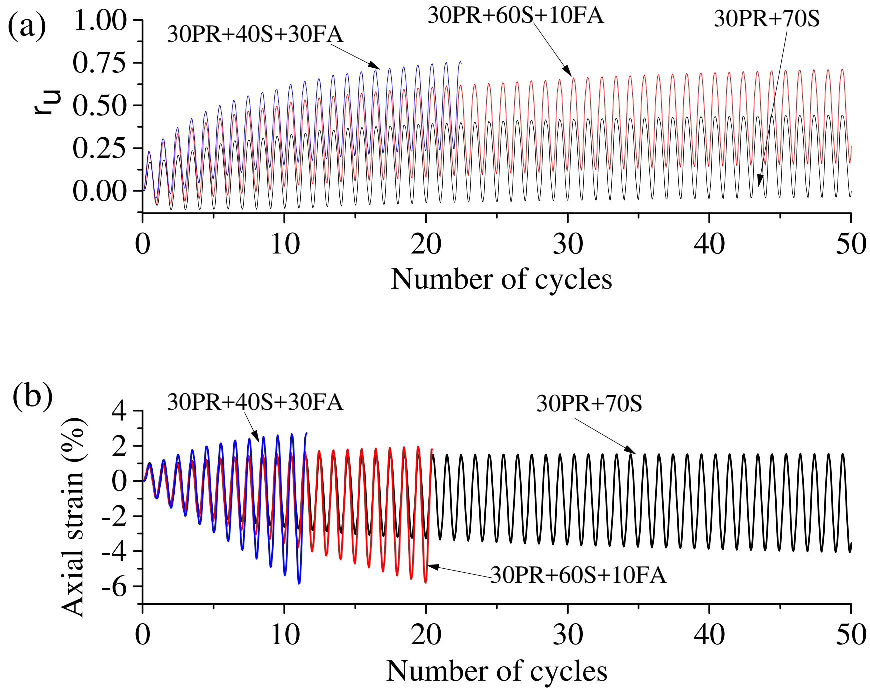

Figure 5.29: Particulate rubber-sand-fly ash mixtures with 30% rubber (a) pore pressure response (b) axial strain response (50% RD and CSR 0.2)

Figure 5.30a shows the pore water pressure response of mixtures having rubber content of 50%. It is evident from the figure that the pore water pressure ratio of the particulate rubber-sand mixture is increased to the maximum value of 0.5. Further, the addition of the fly ash to the mixture is increased the pore water pressure ratio. However, the maximum pore water pressure ratio of the mixtures is observed to be 0.7 and 0.8 for the mixtures with the fly ash content of 10% and 30% respectively. The axial strain variation of the mixtures with different fly ash content is shown in Figure 5.30b. The axial strain of particulate rubber-sand mixture is gradually increased to reach a maximum value of 3%. Further, the addition of fly ash to the mixture is increased the axial strain. The increase in the axial strain with the increase in the fly ash content is attributed to the development pore water pressure and the reduction in the stiffness of the mixtures.

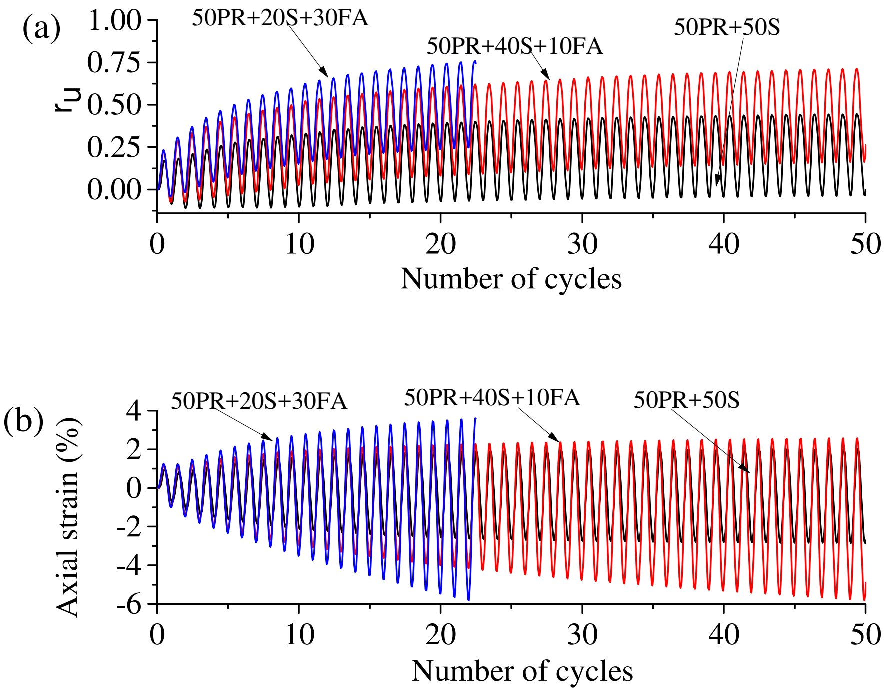

Figure 5.30: Particulate rubber-sand-fly ash mixtures with 50% rubber (a) pore pressure response (b) axial strain response (50% RD and CSR 0.2)

5.5.2 Liquefaction strength of rubber-sand-fly ash mixtures

The effect of sand replacement with fly ash on the liquefaction resistance of the mixtures is shown in Figure 5.31. The particulate rubber-sand mixture with 10% rubber content shows the significant decrease in the liquefaction resistance with an increase in the replacement of sand with fly ash. The mixtures with rubber content more than 10% is initially shown a decrease with increase in the fly ash content followed by an increase. Eventually, for the mixtures with rubber content of 30% and 50%, the full replacement of sand with fly ash is shown the increase in the liquefaction resistance than that of particulate rubber-sand-fly ash mixtures. The particulate rubber-fly ash mixture with rubber content 50% shows higher liquefaction resistance than that of other particulate rubber-fly ash mixtures and particulate rubber-sand-fly ash mixtures. The progressive replacement of sand with fly ash is carried out to examine the optimum content of rubber, sand and fly ash for the liquefaction resistance. These series of cyclic triaxial tests show that, in general, the liquefaction resistance decreases with increase in the fly ash content. It is also evident from the literature that the liquefaction resistance of sand increases with the addition of fly ash up to 6% (Keramatikerman et al. 2017). However, the liquefaction resistance of sand with the addition of the higher amount of fly ash is not reported in the literature. It is believed that the addition of higher amount of fly ash to sand would reduce the liquefaction resistance.

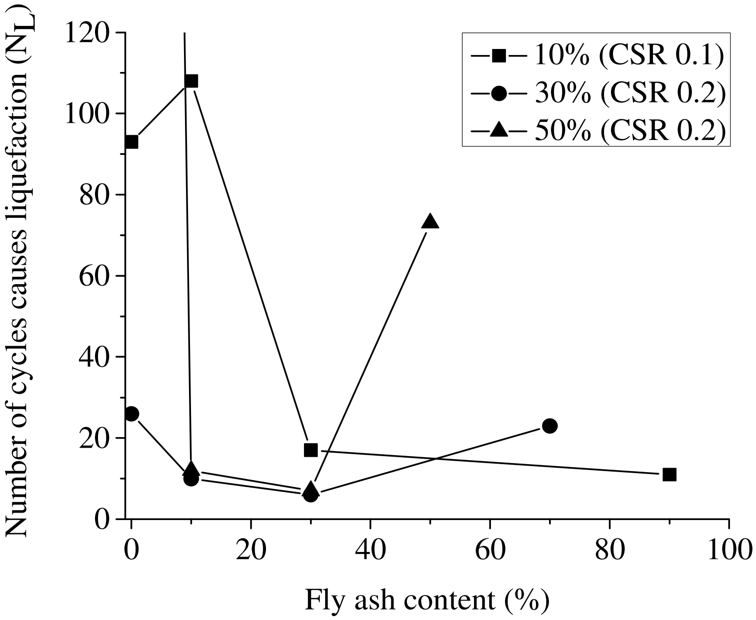

Figure 5.31: Liquefaction strength curve of particulate rubber-sand-fly ash mixtures (50% RD)

5.6 MODELING THE CYCLIC BEHAVIOUR OF PARTICULATE RUBBER-SAND MIXTURES

Numerous models are available to study the liquefaction behaviour of the saturated cohesionless materials. However, the available models require monotonous calibration parameters. Further, it is very difficult to calibrate the existing model for the particulate rubber-sand mixtures. Therefore, it is required to formulate a simple model for the cyclic undrained behaviour of the mixtures.

The preceding laboratory results for the particulate rubber sand mixture provide the basis for the proposed semi-empirical constitutive framework. The constitutive framework is based on hyperbolic backbone curve relating deviator stress and generalized shear strain. The unloading and reloading behaviour of the mixtures is modeled using Masing's rules (Pyke 1979) while cyclic degradation is modeled using the degradation index (Idriss et al. 1978).

5.6.1 Initial Loading Portion

The hyperbolic relation developed to model the backbone curve is given in Equation 5.4 (Subramaniam and Banerjee 2013). The original form of the equation is for the strain controlled testing which is rearranged for the stress controlled test and given in Equation 5.5. It is also to be noted that the G_{max} is changed to E_1 (Secant modulus of 1st cycle) to suit the mixture behaviour.

$$q_r = q_f - \frac{1}{3R}\left[\frac{3G_{max}}{1 + 3R\varepsilon_r}\right] \tag{5.4}$$

$$\varepsilon_r = \frac{1}{3R}\left[\frac{3E_1}{3R(q_f - q_r)} - 1\right] \tag{5.5}$$

where, ε_r is the axial strain, E_1 is the secant modulus of 1st cycle, q_f is the deviatoric stress at failure, q_r is the deviator stress and R is the modulus ratio,

$$R = \frac{E_N}{q_f} \tag{5.6}$$

The deviator stress at failure is defined as,

$$q_f = \frac{Mp'}{2^r} \tag{5.7}$$

where, p' is the mean effective confining pressure, r is the calibration parameter of the model which depends on the rubber content and relative density, M is the function of friction angle which is expressed as,

$$M = \frac{6\, sin\phi}{3 - sin\phi} \tag{5.8}$$

The calibration parameter (r) for rubber sand mixture is given in Figure 5.32.

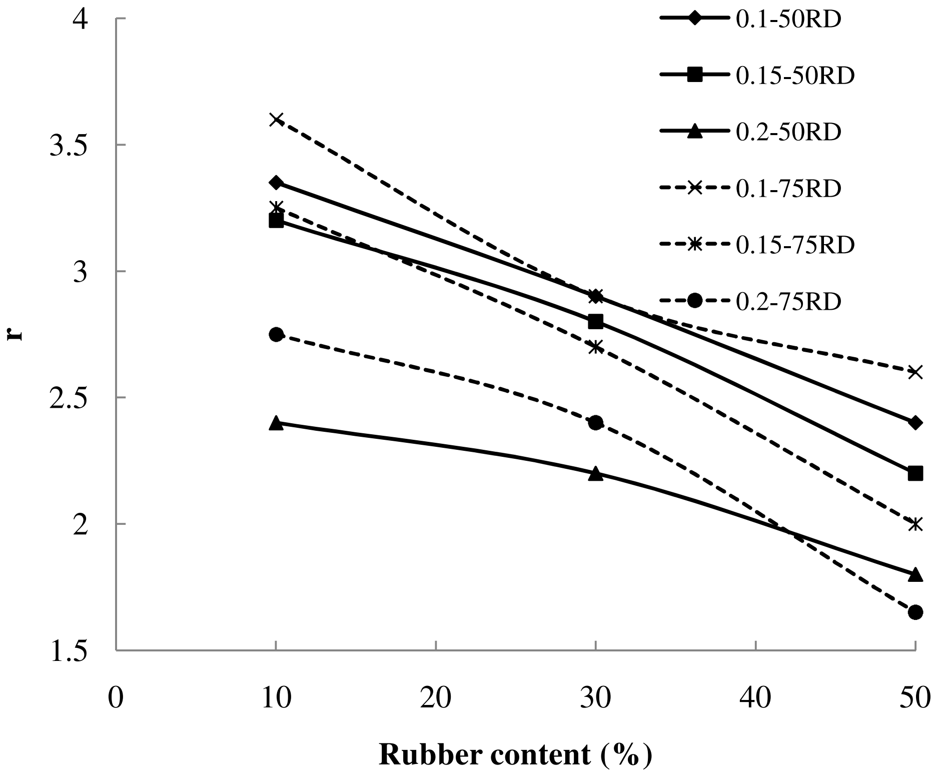

Figure 5.32: Calibration parameter (r) for rubber-sand mixtures

Figure 5.33 shows the typical initial loading portion of the test result and initial loading portion obtained using Equation 5.5. It is evident from the figure that the modification to the hyperbolic relation reasonably predicts the behaviour of the mixture with different rubber content in the range of 10% to 50% by weight. It is also to be noted from Figure 5.33a that the present study experimental results along with the model behaviour are matched reasonably with the experimental results given in Hazarika et al. (2007).

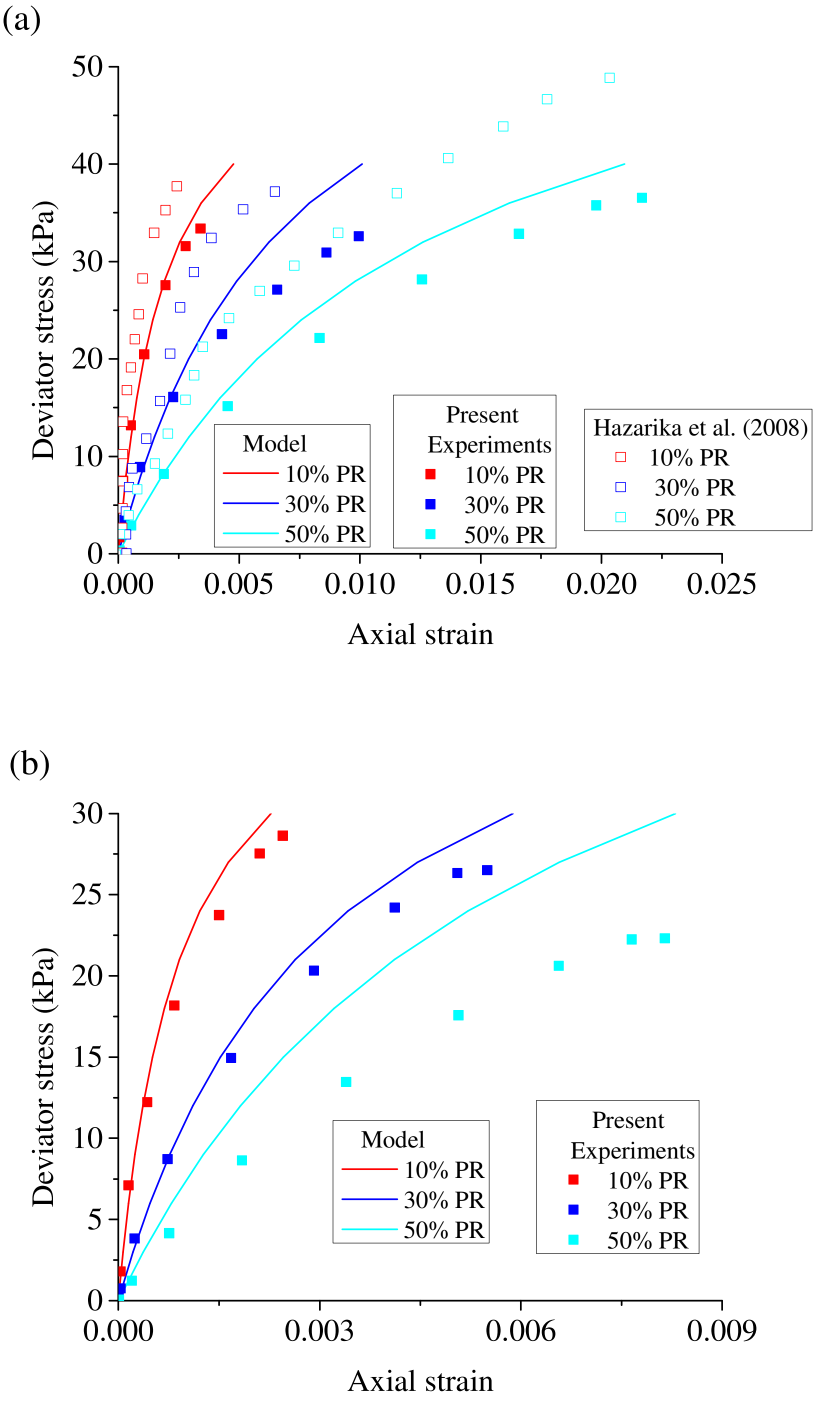

Figure 5.33: Initial loading of rubber-sand mixtures with relative density of (a) 50% (b) 75%

5.6.2 Modeling the Loading-Unloading Behaviour of the Mixture

The unloading and reloading path of the mixture is modeled using Masing's rule (1926). Loading and unloading equation for strain controlled tests is given as,

$$q = -2q_f - \frac{2}{3R}\left[\frac{3G_{max}}{1 + \frac{3R}{2}(\varepsilon_{r1} - \varepsilon_s)}\right] + q_{r1} \tag{5.9}$$

$$q = 2q_f - \frac{2}{3R}\left[\frac{3G_{max}}{1 + \frac{3R}{2}(\varepsilon_s - \varepsilon_{r2})}\right] - q_{r2} \tag{5.10}$$

Equation 5.9 and 5.10 are modified to model the loading and unloading path of the mixtures obtained from stress controlled tests and presented in Equation 5.11 and 5.12.

$$\varepsilon_s = \varepsilon_{r1} - \frac{1}{3R/2}\left[\frac{3E_N}{\frac{3R}{2}\left(q + 2q_f - q_{r1}\right)} - 1\right] \tag{5.11}$$

$$\varepsilon_s = \varepsilon_{r2} - \frac{1}{3R/2}\left[\frac{3E_N}{\frac{3R}{2}\left(q - 2q_f + q_{r2}\right)} + 1\right] \tag{5.12}$$

The notation used in the equation has the same expression and meaning as mentioned in the modeling of initial loading portion. In Equation 5.11 and 5.12, ε_{r1} and ε_{r2} are the axial strain at the point of stress reversal while q_{r1} and q_{r2} are the deviator stress at the point of stress reversal.

Figure 5.34 shows the first cycle of the test results and the model behaviour of the mixtures using Equation 5.11 and 5.12. It is evident from the figure that the loading and unloading path obtained using the equations matches well with the test results. Further, the first hysteresis loop observed from Hazarika et al. (2007) is also presented in Figure 5.31a which shows that the model behaviour and present experimental results match reasonably with the reported literature.

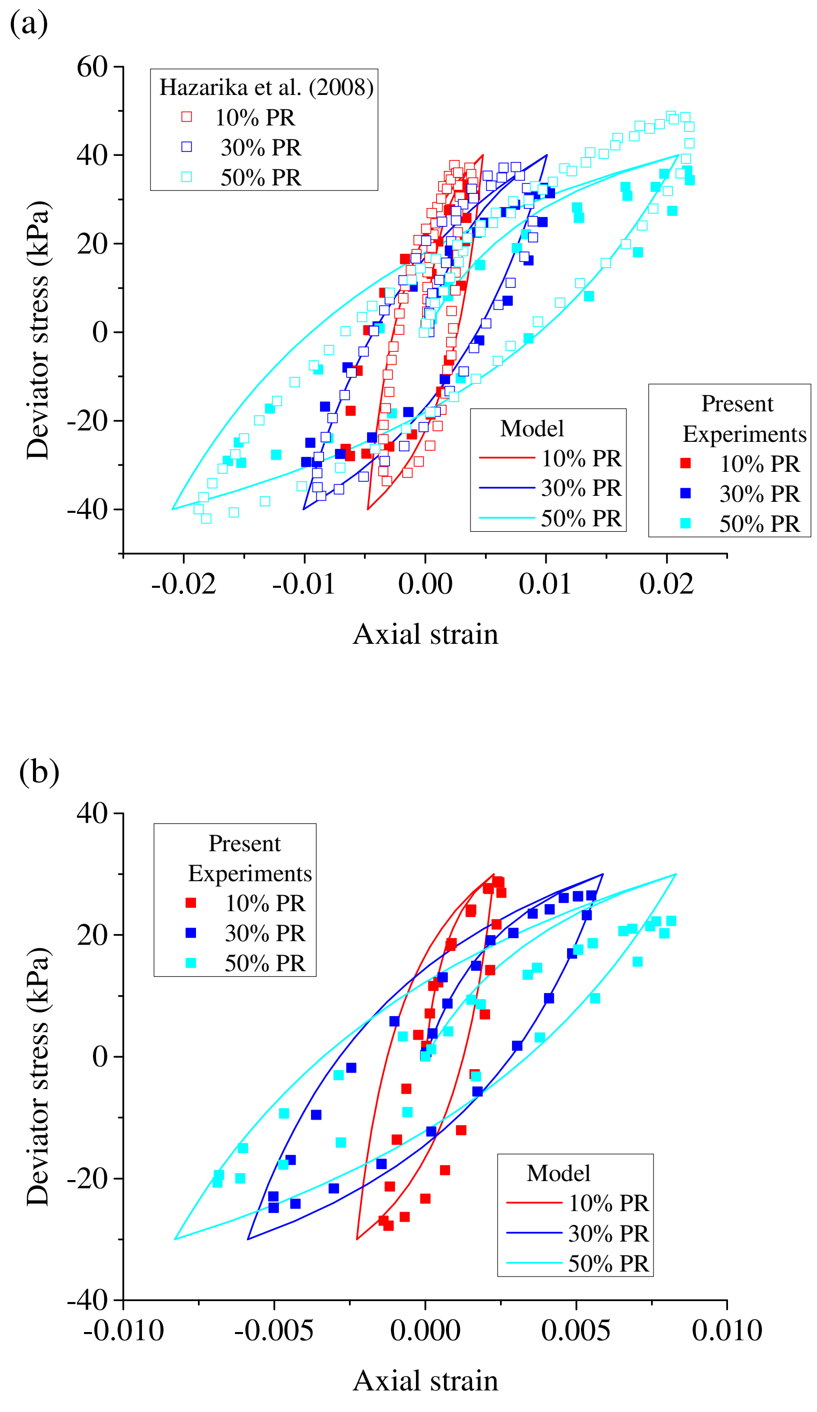

Figure 5.34: First cycle of rubber-sand mixtures with relative density of (a) 50% (b) 75%

Typical modulus degradation parameter (Idriss et al. 1978), which is given in Equation 5.13, is defined as the ratio of the secant modulus of the current number cycle to the first cycle. The degradation parameter for different rubber content at 50% RD is given in Figure 5.35. The figure shows that the degradation of modulus is reduced as the rubber content increases in the mixture. It is also to be noted that the modulus is not degraded significantly when the rubber content is more than 30% by weight subjected to low CSR (CSR = 0.1). Further, it is observed that the modulus degradation of the mixtures depends on the CSR, i.e., when the CSR increases the modulus degradation is pronounced.

$$\delta = \frac{E_N}{E_1} \tag{5.13}$$

The modulus is not fully degraded for the mixtures. The maximum degradation value is decreased with the increase in the rubber content. The decrease in the modulus of the mixture is insignificant for the loading cycles more than 20.

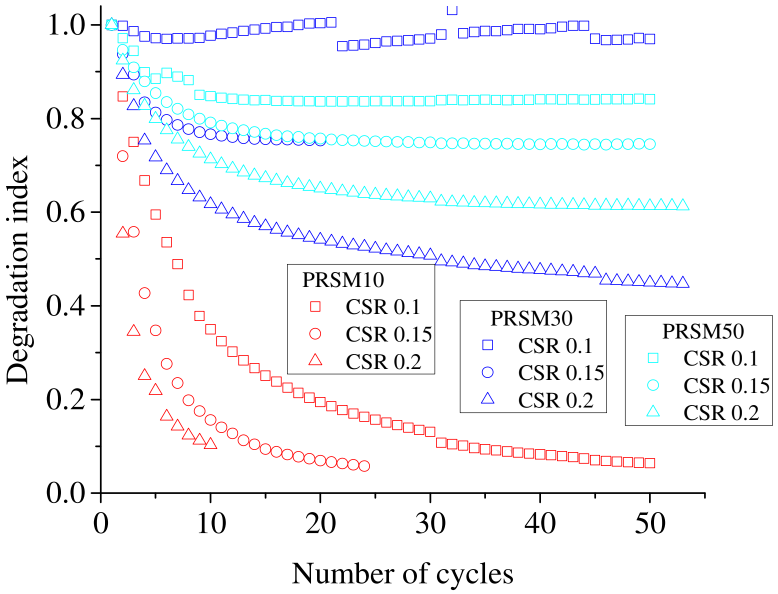

Figure 5.35: Typical modulus degradation curve of rubber-sand mixtures at different CRS

5.6.3 Modeling the Pore Water Pressure Development

It is well-known that, in clayey soils, the development of the pore pressure due to the cyclic loading is a function of the cyclic modulus degradation (Matasovic and Vocitic 1995). Similarly, the present study noted that there exists a correlation between developed pore water pressure ratio due to the cyclic loading and the degradation index of the mixture. In general, the relationship between excess pore water pressure ratio and the degradation index can be expressed as (Matasovic and Vocitic 1995),

$$u_N = A\delta^3 + B\delta^2 + C\delta + \mathrm{D} \tag{5.14}$$

Where, u_n (σ_u/σ_3) is the excess pore water pressure ratio at the n^{th} cycle, A, B, C, and D are the curve fitting parameters and δ is the degradation index.

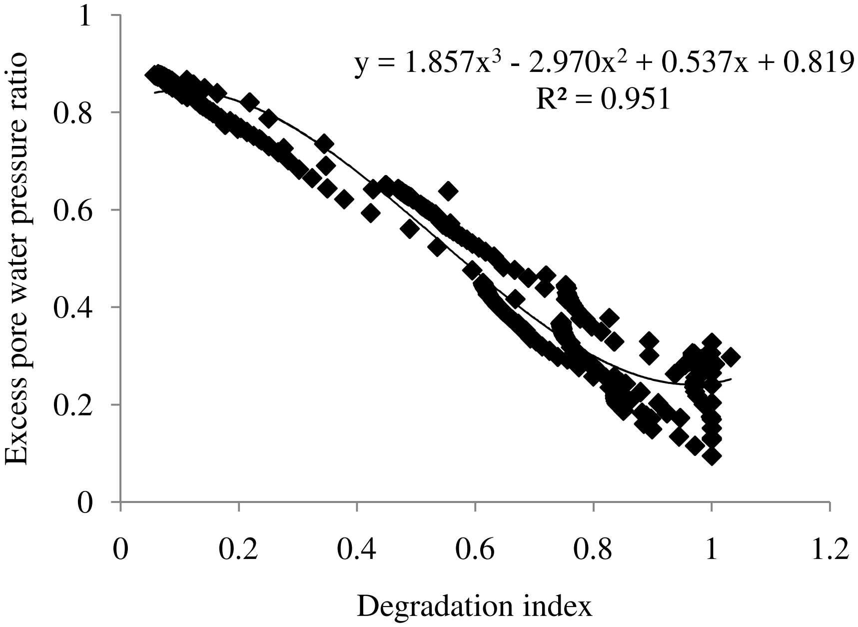

Figure 5.36: Variation of excess pore pressure with degradation index of rubber-sand mixtures

Figure 5.36 shows the variation of excess pore water pressure ratio with the degradation index of the mixtures. It is to be noted that the developed pore water pressure has attained a saturation point when the rubber content increases in the mixture. The saturation point depends on the CSR and rubber content present in the mixture. It is also to be noted that the excess pore water pressure ratio and the modulus degradation varies insignificantly with an increase in the CSR. The general relation between excess pore water pressure ratio and degradation index for different rubber content mixture is given as,

$$u_N = 1.857\delta^3 - 2.970\delta^2 + 0.537\delta + 0.819 \quad (5.15)$$

Equation 5.15 is valid for the mixtures with rubber content between 10 and 50%. However, degradation index should be restricted to 0.9, 0.65, and 0.4 for the mixtures with rubber content 10%, 30%, and 50% respectively.

5.7 SUMMARY

A series of cyclic triaxial tests were carried out with particulate rubber mixed with sand and fly ash to examine the liquefaction and post-liquefaction behaviour of the mixtures. Before the testing, the different parts of the cyclic triaxial equipment such as load cell, controllers and transducers are calibrated. The samples for different mixtures sample are prepared using Ladd's under-compaction method to ensure a uniform density of the samples. The pore pressure and axial strain response of the samples are examined with the stress controlled sinusoidal loading. It is observed that the rubber mixed with sand can attain initial liquefaction when the rubber content in the mixture is less than or equal to 10%. However when the rubber content more than 10%, the mixture does not show initial liquefaction instead fails by attaining a double amplitude axial strain of 5%. However, in the literature it is evident that the rubber content more than 10% in the mixture of rubber tire chips (i.e., large size rubber, size > 50mm) and sand would show initial liquefaction. It is to be noted that the mixture contains tire chips which has the size of approximately 25 times more than that of sand cannot make the mechanical bonding in the matrix. It is the reason why the tire chips mixtures have shown the initial liquefaction although the rubber content in the mixture is more than 10%. However, the present study shows that the mechanical bonding in particulate rubber sand mixture is much more pronounced which helps the sample to act as unit rather than individual particles. Further, the post-liquefaction behaviour of the mixture is idealized as elastic-hardening. The modulus of the elastic and hardening portion of the mixtures is reduced with the increase in the rubber content. Further, the post liquefaction-modulus is varied marginally with the static modulus of the particulate rubber-sand mixtures.

The particulate rubber-fly ash mixtures are initially observed to reduce the liquefaction resistance with the increase in the rubber content. However, the mixture shows increased liquefaction resistance when the rubber content is more than 30%. The post-liquefaction strength of the mixture is initially reduced followed by an increase when the rubber content is more than 30%. The post-liquefaction strength of the particulate rubber-fly ash mixture is observed to be more than particulate rubber-sand mixture when the rubber content is 50%.

The particulate rubber-sand-fly ash mixtures are also examined to find the optimum ratio for higher liquefaction resistance. It is observed that the liquefaction resistance of the mixture is reduced with increase in the replacement of sand with fly ash. However, the higher rubber content mixtures (i.e., 50% rubber content) with complete replacement of sand with fly ash shows higher liquefaction resistance than that of pure sand and pure fly ash.

The undrained cyclic behaviour of the mixtures is modeled using the hyperbolic relation. The loading and unloading portion of the cycles is modeled using Masin’s rule. A calibration parameter is introduced in the model to predict the cyclic behaviour of the different rubber content mixtures. It is observed that both the modified hyperbolic equation and Masing’s rule are able to predict reasonably the cyclic behaviour of the mixtures with rubber content 10% to 50% by weight. Further, in the present study the pore pressure response of the mixtures is modeled indirectly with the modulus degradation.

CHAPTER 6

SUMMARY AND CONCLUSIONS

6.1 INTRODUCTION

The rubber-sand mixture is widely examined for various engineering applications such as embankment, lightweight retaining wall backfill, buried pipeline backfill, and base isolation. The present study is intended to propose an alternative material for sand in the rubber-sand mixtures considering the scarcity of sand and the depletion of natural resources. Fly ash is examined as an alternative material for sand in particulate rubber-sand mixtures. The mixtures with the particulate rubber content of 10%, 30% and 50% by weight are examined in the present study. The shear strength, liquefaction and post-liquefaction behaviour of particulate rubber-sand mixtures and particulate rubber-fly ash mixtures are mainly examined in the present study. The conclusions derived from the present study are applicable to the mixtures with the particulate rubber content between 10% and 50%.

6.2 SUMMARY

The literature pertaining to the density, shear strength, interface shear behaviour, liquefaction resistance and the modeling of the mixture behaviour are examined. It is found that the appropriate technique to find the maximum density of the mixture is lacking in the literature. Further, the interface behaviour of the mixtures is not examined. The liquefaction resistance of the mixtures is limited to the initial liquefaction analysis. In addition, the post-liquefaction behaviour of the mixtures has not been examined.

The material of shredded rubber from scrap tire with size less than 2mm, river sand, and fly ash of Class F are used in the present study. Three mixtures such as particulate rubber-sand mixtures, particulate rubber-fly ash mixtures, and particulate rubber-sand-fly ash mixtures are examined using various tests in the laboratory. Three different techniques such as vibratory table method, Proctor compaction, and mini compaction are used to find the suitable method for particulate rubber-sand mixtures and particulate rubber-fly ash mixtures. Further, the segregation is a major problem which has been observed in the mixture of tires chips and sand. Hence, the particulate rubber-sand mixture and particulate rubber-fly ash mixture is analyzed for the segregation resistance.

The shear strength of the mixtures is examined using direct shear tests while the interface shear strength is examined using interface direct shear tests. A new sample preparation technique is proposed for the particulate-particulate samples for the interface direct shear tests. In addition, the undrained behaviour of the mixtures is studied using undrained triaxial tests.

Servo controlled automated cyclic triaxial (Make: VJ Tech, UK) is used to carry out multistage cyclic testing on the mixtures. The samples are prepared in five layers using Ladd's (1978) under compaction method. A sample is first subjected to stress controlled cyclic loading for liquefaction analysis which is immediately followed by undrained monotonic strain controlled loading without dissipating the excess pore water pressure for post-liquefaction analysis. The liquefaction behaviour of the mixtures is modeled using hyperbolic relation and Masing's rule. The excess pore pressure is modeled indirectly using the modulus degradation.

6.3 CONCLUSIONS

The following major conclusions are arrived from the present study:

6.3.1 Characteristics of the Mixtures

- ✓ The maximum dry unit weight of the particulate rubber-sand mixtures obtained using Proctor compaction technique is higher than that of vibratory table method with increased surcharge. Further, the vibratory table method is not suitable to obtain the maximum dry unit weight of the rubber-sand mixtures due to the factors such as vibration absorbent nature of rubber, rebounding of mixtures, and inadequate surcharge. Hence, the Proctor compaction method is recommended for finding the maximum dry unit weight of the particulate rubber-sand mixtures.

- ✓ The vibratory table method and the Proctor compaction method are not suitable for the particulate rubber-fly ash mixtures due to the spillage of fly ash. However, the spillage of fly ash is reasonably controlled in mini compaction method. Hence, the mini compaction method is recommended for finding the maximum dry unit weight of the particulate rubber-fly ash mixtures.
- ✓ The particulate rubber-sand mixtures and the particulate rubber-fly ash mixtures do not segregate unlike tire chips-sand mixtures and tire shreds-sand mixtures due to the maximum particle size ratio which is one for the particulate rubber-sand mixtures and the stronger inter-particle contacts.

6.3.2 Static Behaviour of the Mixtures

- ✓ Both particulate rubber-sand mixtures and particulate rubber-fly ash mixtures exhibit ductility when the rubber content is more than 30%. Hence, the larger quantity of scrap tire can be used in the form of particulate rubber for earthquake engineering applications.
- ✓ The compressibility of the particulate rubber-sand mixtures is significantly reduced due to the full replacement of sand in the mixtures with fly ash.
- ✓ For all the mixtures, the ultimate shear strength and friction angle of the particulate rubber-fly ash mixtures is observed to be higher than that of particulate rubber-sand mixtures. The microstructure study shows that the increase in shear strength is attributed to the stronger inter-particle contacts between the rubber and fly ash.
- ✓ The undrained shear strength of the particulate rubber-sand mixtures is increase with an increase in the replacement content of sand in particulate rubber-sand mixtures by fly ash. The shear strength of the particulate rubber-fly ash mixture increases by more than 100% compared to the particulate rubber-sand mixtures. In addition, the particulate rubber-fly ash mixtures show similar ductile behaviour as that of particulate rubber-sand mixtures, which is essential for earthquake geotechnical engineering applications.
- ✓ The contractive behaviour of rubber changes to the dilative at large strain due to the increase of sand replacement with fly ash in the mixture. However, higher content fly ash mixture, i.e., particulate rubber-fly ash mixtures, dilates at low strain.

- ✓ The pore water pressure of the mixtures decreases with the increase in the replacement content of sand by fly ash.
- ✓ The particulate rubber-fly ash mixture shows 30% and 18% higher interface shear strength than that of the particulate rubber-sand mixture for the interfaces of concrete and sand respectively.
- ✓ The peak interface friction angle of sand-particulate material is1.5° to 3° higher than that of concrete-particulate material. However, the initial interface shear stiffness of the sand-particulate material is observed to be lower than that of the concrete-particulate material. It is due to the initial adjustments between the particles present at the interface of sand-particulate material.
- ✓ The interface coefficient of both the sand-particulate material and concrete-particulate material decreases with an increase in the relative density. It is due to the increase in the integrity of sample with an increase in the relative density which reduces the particles interaction at the interface.
- ✓ The interface coefficient for the concrete-particulate material can be considered as 0.85 and 0.95 for particulate rubber-sand mixtures and particulate rubber-fly ash mixtures, respectively. Further, the interface coefficient of 0.95 and 1 can be considered for particulate rubber-sand mixtures and particulate rubber-fly ash mixtures, respectively, in the case of the sand-particulate material interface.

6.3.2 Liquefaction and Post-liquefaction Behaviour of the Mixtures

- ✓ The sand and mixture with the rubber content of 10% have experienced the rapid build-up of the pore water pressure and subsequently shows initial liquefaction at relatively less number of cycles of loading. However, the mixtures with rubber content more than 10% shows a gradual increase of pore water pressure to the maximum pore water pressure ratio of 0.5. It shows that the mixtures with the rubber content more than 10% do not show initial liquefaction.
- ✓ The liquefaction resistance of the particulate rubber-sand mixtures with the rubber content between 10% and 50% is approximately equal to that of sand. In addition, the mixtures with the rubber content greater than 10% show higher liquefaction resistance than that of sand

when the CSR is greater than 0.23 owing to the reason that the reduction in the development of pore water pressure. The particulate rubber-sand mixture with the rubber content of 10% always show lesser liquefaction resistance than that of sand due to the reduction in the stiffness of the sample and increase of the pore water pressure. Further, the pure rubber shows lesser liquefaction resistance than that of 30% and 50% particulate rubber-sand mixtures when CSR is greater 0.15 due to the lesser stiffness.

- ✓ The post-liquefaction strength of the mixtures is more than that of sand at the lower axial strain. Further, the post-liquefaction strength of the mixtures is observed to be less than its static strength. The post-liquefaction behaviour is idealized as elastic hardening. The elastic modulus is significantly reduced than hardening modulus with the increase in the rubber content.
- ✓ The liquefaction resistance of the particulate rubber-fly ash mixture is initially reduced till 30% rubber content followed by an increase. The liquefaction resistance of the mixture is observed to be more than fly ash and sand when the rubber content is 50%.
- ✓ In addition, the post-liquefaction strength of particulate rubber-fly ash mixtures is more than that of particulate rubber-sand mixtures when the rubber content is more than 30%.
- ✓ The partial replacement of sand with fly ash in the particulate rubber-sand mixtures reduces the liquefaction resistance of the mixtures. It is also found that there is no optimum mixture content with particulate rubber, sand, and fly ash.
- ✓ A semi-empirical constitutive model is proposed based on the experimental results. Hysteretic behaviour is modeled using Masing's rule while the pore pressure is modeled indirectly with help of degradation index. The proposed model is able to predict the liquefaction behaviour of the particulate rubber-sand mixtures with the rubber content between 10 and 30%. Further, the model is validated using the data given in an experimental study.

As discussed in the present study, the full replacement of sand in particulate rubber-sand mixture with fly ash significantly enhances the static properties and possesses satisfactory liquefaction resistance. Therefore, particulate rubber-fly ash mixtures, in general, can be preferred for various geotechnical applications such as embankment, lightweight backfill, buries pipeline backfill and base isolation.

6.4 LIMITATIONS OF THE PRESENT STUDY

The conclusions from the vibratory table method are derived by increasing only the surcharge. Further, the conclusions from the compaction methods are for the standard energies given in ASTM D698 (ASTM 2012a), ASTM D1557 (ASTM 2012b), and Sridharan and Sivapullaiah (2005).

The static and liquefaction behaviours are observed from the element tests in the lab. However, the behaviour would be changed if the mixture will be examined in the model tests or the field study. Therefore, the behaviours reported in this study are the representative from the element tests.

The present study examines the mixtures behaviour under confined condones. Hence, the results of the present study are valid only for the confined condition applications such as retaining wall backfill, base isolation, and buried pipeline backfill. However, the literature shows that the rubber-sand mixtures can also be used for the embankments of pavements which are of open bounded condition. Therefore the rubber-fly ash mixtures can also be used in the applications of open bounded conditions. However, the rubber-fly ash mixtures possess environmental issues (e.g., disseminating of ashes in the air). Further, the flow of water through these mixtures would cause the loss of fines. Therefore, to mitigate these problems, minimum soil cover is necessitated to maintain the environmental standards and to avoid the loss of fines during the rainy seasons. Further, the use of the mixtures for open bounded conditions like embankments would require a model study or full-scale field study.

6.5 MAJOR CONTRIBUTIONS

- ✓ An appropriate technique to determine the maximum unit weight of the mixtures is recommended.
- ✓ A new sample preparation technique is proposed for the interface behaviour of the particulate-particulate material. Further, the two different interface shear strength of the mixtures are reported.

- ✓ The fly ash is identified as an alternate material for sand in particulate rubber-sand mixtures. The particulate rubber-fly ash mixture with higher rubber content is found to significantly improves the static behaviour and possess the satisfactory liquefaction resistance.
- ✓ It is the first kind of study to examine the post-liquefaction behaviour of the mixture. In addition, a semi-empirical analytical model is proposed for the liquefaction behaviour of the mixtures.

6.6 FUTURE SCOPE OF WORK

- ✓ The present study is limited to the laboratory examination of static, liquefaction and post-liquefaction behaviour of the particulate rubber-sand mixtures and particulate rubber-fly ash mixtures. However, the dynamic properties such as modulus degradation and damping ratio are needed to examine the suitability of the mixtures in earthquake-prone area.
- ✓ The proposed analytical model in the present study can be implemented as User Defined Model (UDM) in the commercial software packages. Then the model can be used to analyze the mixtures for many field applications.
- ✓ A model study is necessary to examine the behaviour in large scale. Further, before implementing these mixtures, it is also required to conduct a full-scale field study.
- ✓ The lower liquefaction resistance of the particulate rubber-fly ash mixtures is observed for the rubber content less than 30%. It is beloved that any reinforcement such as geosynthetics or fibers would increase the liquefaction resistance. Further, the reinforcement would also increase the static strength. It can be recommended to study static and liquefaction behaviour of the reinforced mixtures.

REFERENCES

1. Ahmed, I., and Lovell, C. W. (1993). "Rubber soils as lightweight geomaterials." *Transportation Research Record,* 1422, 61-70.
2. Anastasiadis, A., Senetakis, K., and Pilitakis, K. (2011). "Small-strain shear modulus and damping ratio of sand-rubber and gravel-rubber mixtures." *Geotech. Geol. Eng.,* 30(2), 363–382.
3. Anbazhagan, P., Manohar, D. R., and Rohit, D. (2016) "Influence of size of granulated rubber and tyre chips on the shear strength characteristics of sand-rubber mix." *Geomech. Geoeng.,* 10.1080/17486025.2016.1222454.
4. Anubhav and Basudhar, P. K. (2013). "Interface behavior of woven geotextile with rounded and angular particle sand." *J. Mater. Civil Eng.,* 10.1061/(ASCE)MT.1943-5533.0000774.
5. ASTM. (2011). "Standard test methods for Direct shear test of soils under consolidated drained conditions." ASTM D3080, West Conshohocken, PA.
6. ASTM. (2012a). "Standard test methods for laboratory compaction characteristics of soil using standard effort (12,400 ft-lbf/ft3 (600 kN-m/m3))." ASTM D698-12ε2, West Conshohocken, PA.
7. ASTM. (2012b). "Standard test methods for laboratory compaction characteristics of soil using modified effort (56,000 ft-lbf/ft3 (2,700 kN-m/m3))." ASTM D1557-12e1, West Conshohocken, PA.
8. ASTM. (2012c). "Standard practice for use of scrap tires in civil engineering applications." ASTM D6270-12, West Conshohocken, PA.
9. ASTM. (2016a). "Standard test methods for maximum index density and unit weight of soils using a vibratory table." ASTM D4253-16, West Conshohocken, PA.
10. ASTM. (2016b). "Minimum index density and unit weight of soils and calculation of relative density." ASTM D4254-16, West Conshohocken, PA.
11. Balunaini, U., Prezzi, M., Mohan, V. K. D., and Salgado, R. (2014). "Shear strength of tyre chip–sand and tyre shred–sand mixtures." *Geotech. Engg.,* 10.1680/geng.13.00097.
12. Bernal, A., Swan, R. H., and Lovell, C. W. (1997). "Interaction between tire shreds, rubber-sand, and geosynthetics." *Geosynthetics International,* 4(6), 623-643.
13. Bolton, M. D. (1986). "The strength and dilatancy of sands." *Geotechnique,* 36(1), 65-78.

14. Bosscher, P. J., Edil, T. B., and Eldin, N. N. (1992). “Construction and performance of a shredded waste tire test embankment.” *Transportation Research Record,* 1345, 44-52.
15. Cabalar, A. F. (2011). “Direct shear tests on waste tires-sand mixtures.” *Geotech. Geol. Eng.,* 29(4), 411–418.
16. Chauhan, M. S., Mittal, S., and Mohanty, B. (2008). “Performance evaluation of silty sand subgrade reinforced with fly ash and fibers.” *Geotextiles and Geomembranes,* 26(5), 429-435.
17. Chu, L. M., and Yin, J. H. (2005). “Comparison of interface shear strength of soil nails measured by both direct shear box tests and pullout tests.” *J. Geotech. Geoenviron. Eng.,* 10.1061/(ASCE)1090-0241(2005)131:9(1097).
18. Dixit, P. M., and Dixit, U. S. (2015). *Plasticity fundamentals and applications (Chapter 11.6: Ductile fracture),* CRC Press, Taylor and Francis Group, UK.
19. Edil, T. B., and Bosscher, P. J. (1992). “Development of engineering criteria for shredded waste tires in highway applications.” Final Report to Wisconsin Departments of Transportation and Natural Resources, Madison, WI, Research Report GT-92-9.
20. Edil, T. B., and Bosscher, P. J. (1994). “Engineering properties of tire chips and soil mixtures.” *Geotech. Test. J.,* 17(4), 453–464.
21. Edincliler, A., Baykal, G., and Saygili, A. (2010). “Influence of different processing techniques on the mechanical properties of used tires in embankment construction.” *Waste Management,* 30(6), 1073–1080.
22. Edincliler, A., and Ayhan, V. (2010). “Influence of tire fiber inclusions on shear strength of sand sand.” *Geosynth. Int.,* 10.1680/gein.2010.17.4.183.
23. Feng, Z. Y., and Sutter, K. G. (2000). “Dynamic properties of granulated rubber/sand mixtures.” *Geotech. Test. J.,* 23(3), 338–344.
24. Feng, S. J., and Cheng, D. (2014). “Shear strength between Soil/Geomembrane and Geotextile /Geomembrane Interfaces.” *Tunneling and Underground Construction GSP 242,* doi.org/10.1061/9780784413449.054.
25. Foose, G. J., Benson, C. H., and Bosscher, P. J. (1996). “Sand reinforced with shredded waste tires.” *J. Geotech. Eng.,* 122(9), 760–767.

26. Fuchiyama, M., Hyodo, M., Nakata, Y., Yoshimoto, N., Imada, K., and Konja, A. (2015). "Monotonic and cyclic shear behaviour of tire chips." Proc., Int. Symposium on Geomech. from Micro to Macro (IS-Cambridge 2014), Taylor and Francis, London, 1383–1387.
27. Garga, V. K., and O'Shaughnessy, V. 2000 "Tire-reinforced earthfill. Part 1: Construction of a test fill, performance, and retaining wall design." Canadian Geotechnical Journal 37 (1): 75-96.
28. Gebhardt, M. A. (1997). "Shear strength of shredded tires as applied to the design and construction of a shredded tire stream crossing." M.S. thesis, Iowa State Univ., Ames, IA.
29. Ghaaowd, I., McCartney, J. S., Thielmann, S. S., Sanders, M. J., and Fox, P. J. (2017). "Shearing behavior of tire-derived aggregate with large particle size. I: internal and concrete interface direct shear." J. Geotech. Geoenviron. Eng.,10.1061/(ASCE)GT.1943-5606.0001775.
30. Ghazavi, M. (2004). "Shear strength characteristics of sand-mixed with granular rubber." Geotech. Geol. Eng., 22(3), 401–416.
31. Ghazavi, M., and Amel Sakhi, M. (2005). "Influence of optimized tire shreds on shear strength parameters of sand." Int. J. Geomech., 5(1), 58–65.
32. Hazarika, H., Kohama, E., and Sugano, T. (208). "Underwater shake table tests on waterfront structures protected with tire chips cushion." J. of Geotech. Geoenv. Engg. 134(12), 1706-1719.
33. Holtz, R. D., Kovacs W. D., and Sheahan, T. C. (2011). An introduction to geotechnical Engineering, Pearrson, India.
34. Hong, Y., Yang, Z., Orense, R. P., and Lu, Y. (2015). "Investigation of sand-tire mixtures as liquefaction remedial measure." Proc., 10th Pacific Conf. on Earthq. Eng., Sydney, Australia.
35. Hyodo, M., Yamada, S., Orense, R. P., Okamoto, M., and Hazarika, H. (2007). "Undrained cyclic shear properties of tire chip-sand mixtures." Proc., Int. Workshop IW-TDGM 2007, Taylor and Francis, London, 187–196.
36. Hu, L., and Pu, J. (2004). "Testing and modeling of soil-structure interface." J. Geotech. Geoenviron. Eng.,10.1061/(ASCE)1090-0241(2004)130:8(851)
37. Humphrey, D. N. (2007). "Tire derived aggregate as lightweight fill for embankments and retaining walls." Proc., Int. Workshop IW-TDGM 2007, Taylor and Francis, London, 59–81.

38. Idriss, I.M., Dobry, R., and Singh, R.M. (1978). “Nonlinear behaviour of soft clays during cyclic loading.” J. of Geotech. Engg. 104, GT12, 1427-47.
39. Kaneko, T., Orense, R. P., Hyodo, M., and Yoshimoto, N. (2013). “Seismic response characteristics of saturated sand deposits mixed with tire chips.” J. Geotech. Geoenviron. Eng., 139(4), 633–643.
40. Kawata, S., Hyodo, M., Orense, R. P., Yamada, S., and Hazarika, H. (2007). “Undrained and drained shear behaviour of sand and tire chips composite material.” Proc., Int. Workshop IW-TDGM 2007, Taylor and Francis, London, 277–283.
41. Kim, K. H., and Santamarina, J. C. (2008). “Sand-rubber mixtures (large rubber chips).” Can. Geotech. J., 45(10), 1457–1466.
42. Ladd, R. S.(1978).“Preparing test specimens using under compaction.” Geotech. Test. J., 1(1), 16–23. https://doi.org/10.1520/GTJ10364J.
43. Lee, J. H., Salgado, R., Bernal, A., and Lovell, C. W. (1999). “Shredded tires and rubber-sand as lightweight backfill.” J. Geotech. Geoenviron. Eng., 125(2), 132-141.
44. Li, B., Huang, M., and Zeng, X. (2016). “Dynamic behavior and liquefaction analysis of recycled-rubber sand mixtures.” J. Mater. Civ. Eng., 10.1061/(ASCE)MT.1943-5533.0001629.
45. Masad, E., Taha, R., Ho, C., and Papagiannakis, T. (1996). “Engineering properties of tire/soil mixtures as a lightweight fill material.” Geotech. Test. J., 19(3), 297–304.
46. Mashiri, M. S. (2014). “Monotonic and cyclic behaviour of sand-tyre chip (STCh) mixtures.” Ph.D thesis, University of Wollongong, Australia.
47. Mashiri, M. S., Vinod, J. S., and Sheikh, M. N. (2015). “Shear strength and dilatancy behaviour of sand–tyre chip mixtures.” Soils and Foundations, 55(3), 517–528.
48. Mashiri, M. S., Vinod, J. S., and Sheikh, M. N. (2015). “Constitutive model for sand-tire chip mixture.” International Journal of Geomechanics, 16(1), 04015022-1-10.
49. Mashiri, M. S., Vinod, J. S., and Sheikh, M. N. (2016). “Liquefaction potential and dynamic properties of sand-tyre chip (STCh) mixtures.” Geotechnical Testing Journal, 39(1), 69–79.
50. Ngo, A. T., and Valdes, J. R.(2007). “Creep of sand-rubber mixtures.” J. Mater. Civ. Eng., https://doi.org/10.1061/(ASCE)0899-1561(2007)19:12(1101)
51. Noorzad, R., and Ravesshi, M. (2017). “Mechanical behavior of waste tire crumbs-sand mixtures determined by triaxial tests.” Geotech. Geol. Eng., 10.1007/s10706-017-0209-9.

52. Priyadarshee, A., Gupta, D., Kumar, V., and Sharma, V. (2015). “Comparative study on performance of tire crumbles with fly ash and kaolin clay.” Int. J. of Geosynth. and Ground Eng., 10.1007/s40891-015-0033-3.
53. Promputthangkoon, P., and Hyde, A. L. F. (2007). “Compressibility and liquefaction potential of rubber composite soils.” Proc., Int. Workshop IW-TDGM 2007, Taylor and Francis, London, 59–81.
54. Pyke, R. (1979) “Nonlinear soil models for irregular cyclic loadings.” J. of Geotech. Engg. Div. Vo. 105, No. GT6, pp. 715-726.
55. Rao, G. V., and Dutta, R. K. (2006). “Compressibility and strength behaviour of sand–tyre chip mixtures.” Geotech. Geol. Eng., 24(3), 711–724.
56. Reddy, B. S., Pradeep Kumar, D., and Murli Krishna, A. (2016). “Evaluation of the optimum mixing ratio of a sand-tire chips mixture for geoengineering applications.” J. Mater. Civ. Eng., 10.1061/(ASCE)MT.1943-5533.0001335.
57. Senetakis, K., Anastasiadis, A., and Pitilakis, K. (2012). “Dynamic properties of dry sand rubber (SRM) and gravel/rubber (GRM) mixtures in a wide range of shearing strain amplitudes.” Soil Dyn. Earthq. Eng., 33(1), 38–53.
58. Seed, H.B. and Lee, K.L. (1966). “Liquefaction of saturated sands during cyclic loading,” J. soil Mech. Found. Div., Vol. 92, No. SM6, pp. 105-134.
59. Seed, H.B., Idriss, I.M., Makdisi, F., and Banerjee, N. (1975). “Representation of irregular stress time histories by equivalent uniform stress series in liquefaction analysis,” EERC 75-29, Earthquake engineering research center, University of California, Berkeley.
60. Sheikh, M. N., Mashiri, M. S., Vinod, J. S., and Tsang, H. H. (2013). “Shear and compressibility behaviours of sand-tyre crumb mixtures.” J. Mater. Civ. Eng., 25(10), 1366–1374.
61. Sridharan, A., and Sivapullaiah, P. V. (2005). “Mini compaction test apparatus for fine grained soils.” Geotech. Test. J., 28(3), 240–246.
62. Taha, A., and Fall, M. (2013). “Shear behavior of sensitive marine clay-concrete interfaces.” J. Geotech. Geoenviron. Eng.,10.1061/(ASCE)GT.1943-5606.0000795.
63. Tatlisoz, N., Edil, T. B., and Benson, C. H. (1998). “Interaction between reinforcing geosynthetics and soil-tire chips mixtures.” J. Geotech. Geoenviron. Eng., 124(11), 1109-1119.

64. Tsang, H. H., Lo, S. H., Xu, X., and Sheikh, M. N. (2012). “Seismic isolation for low-to-medium-rise buildings using granulated rubber-soil mixtures: numerical study.” Earthq. Eng. and Str. Dyn., 41(14), 2009-2024.
65. Uchimura, T., Chi, N. A., Nirmalan, S., Sato, T., Meidani, M., and Towhata, I. (2007). “Shaking table tests on effect of tire chips and sand mixture in increasing liquefaction resistance and mitigating uplift of pipe.” Proc., Int. Workshop IW-TDGM 2007, Taylor and Francis, London, 179–186.
66. Umashankar, B. (2009). “Experimental study of the use of mixtures of sand and tire shreds as a geotechnical material.” Ph. D thesis, Purdue University, IN.
67. Umashankar, B., Yoon, S., Prezzi, M., and Salgado, R. (2014). “Pullout response of uniaxial geogrid in tire shred-sand mixtures.” Geotech. Geol. Eng., 32(2), 505–523.
68. Wood, D. M. (2009). Soil mechanics: A one-dimensional introduction, Cambridge University Press, USA.
69. Wu, J. T. H., Helwany, M. B., and Barrett, R.K. (1994). “Use of shredded tire as backfill for a new geosynthetic reinforced retaining wall system.” Proc., 5th Int. Conf. on Geotextiles, Geomembranes and Related Products, Singapore, 269–272.
70. Xiao, M., Ledezma, M., and Hartman, C. (2015). “Shear resistance of tirederived aggregate using large-scale direct shear tests.” J. Mater. Civil Eng., 10.1061/(ASCE)MT.1943-5533.0001007, 04014110.
71. Yoon, S., Prezzi, M., Siddiki, N. Z., and Kim, B. (2006). “Construction of a test embankment using a sand-tire shred mixture as fill material.” Waste Management 26 (9), 1033-1044.
72. Youwai, S., and Bergado, D. T. (2003). “Strength and deformation characteristics of shredded rubber tire-sand mixtures.” Can. Geotech. J., 40(2), 254–264.
73. Zornberg, J. G., Viratjandr, C., and Cabral, A. R. (2004). “Behaviour of tire shred-sand mixtures.” Can. Geotech. J., 41(2), 227–241.

LIST OF PUBLICATIONS

I REFEREED JOURNALS BASED ON THE THESIS

1. Senthen Amuthan, M., Boominathan, A., and Banerjee, S. 2018. "Density and shear strength of particulate rubber mixed with sand and fly ash." ASCE *Journal of Materials in Civil Engineering* http://dx.doi.org/10.1061/(ASCE)MT.1943-5533.0002322.
2. SenthenAmuthan, M., Boominathan, A., and Banerjee, S. "Concrete and sand interface behaviour of particulate rubber-sand-fly ash mixture." *International Journal of Geotechnical Engineering* (Accepted with minor revisions)
3. SenthenAmuthan, M., Boominathan, A., and Banerjee, S. "Post liquefaction and modeling the undarainedbehaviour of particulate rubber-sand mixtures." (Preparation for journal is in progress)

II PUBLICATIONS IN CONFERENCE PROCEEDINGS

1. Senthen Amuthan, M., Boominathan, A., and Banerjee, S. 2017. "Undrained shear strength of particulate rubber sand mixture (PRSM) mixed with fly ash." *In the proceedings of 3rd International conference on performance-based design in earthquake geotechnical engineering*, Vancouver, Canada; Paper No. 333.
2. Senthen Amuthan, M., Boominathan, A., and Banerjee, S. 2016 "Influence of Fly Ash on the Shear Strength and Volumetric Behaviour of Sand Rubber-tire Mixture (SRM)" *In the proceedings of International Geotechnical Engineering Conference on Sustainability in Geotechnical Engineering Practices and Related Urban Issues*, September 23-24, 2016, Mumbai.

CURRICULUM VITAE

1. **Name** **:** Senthen Amuthan M
2. **Date of birth** **:** 27-05-1991
3. **Educational qualifications**

2012 Bachelor of Engineering (B.E.)

Institution : Anna University, Chennai
Specialization : Civil Engineering

Master of Science (by Research)

Institution : Indian Institute of Technology, Madras
Specialization : Geotechnical Engineering
Registration date : 14-07-2015

GRADUATE TECHNICAL COMMITTEE

Chairperson: Dr. K Ramamurthy
Professor and Head
Civil Engineering

Guides: Dr. A Boominathan
Professor
Civil Engineering

Dr. Subhadeep Banerjee
Associate Professor
Civil Engineering

Members: Dr. S T G Raghukanth
Associate Professor
Civil Engineering

Dr. Srinivasan Chandrasekaran
Professor
Ocean Engineering